Characterization of
orthopox ankyrin repeat proteins in the
modified vaccinia virus Ankara background

Dissertation

**zur Erlangung des akademischen Grades
des Doktors der Naturwissenschaften
(Dr. rer. nat.)**

**eingereicht im Fachbereich Biologie, Chemie, Pharmazie
der Freien Universität Berlin**

vorgelegt von

Dipl.Biochem. Imme Sakwa

aus Eutin

2013

Die Promotion wurde am Institut für Virologie im Fachbereich Veterinärmedizin der Freien Universität Berlin unter der Leitung von Prof. Dr. Nikolaus Osterrieder von Mai 2009 bis September 2013 angefertigt.

1. Gutachter: Prof. Dr. Markus Wahl (FUB)
2. Gutachter: Prof. Dr. Nikolaus Osterrieder (FUB)

Disputation am 06.03.2014

List of contents

1. Introduction

1.1 Viruses in general

Viruses are defined as infectious and intracellular parasites. They show a wide variety in size as the diameter of circoviruses ranges from 12 to 26 nm, whereas poxviruses belong to the upper end of the size scale with up to 300 nm. The virus genome is composed of either RNA or DNA and is surrounded by a core or capsid. The core consists of proteins which are assembled from identical structural units. This leads to a characteristic helical or icosahedral symmetry. Nevertheless, the symmetry of poxviruses could not be classified to one of the two possibilities and is therefore termed as complex. Some viruses are surrounded by one or more membranes. These are termed as enveloped. The properties described are used for the virus classification by the International Committee on Taxonomy of Viruses.

A virus replication cycle starts with the attachment of the virus to the host cell, where in most cases a virus protein binds to a cell surface receptor. The virus can enter the host cell by different mechanisms for example via endocytosis in a caveolae or clathrin mediated manner. In the next step the genome is set free in a process known as uncoating (Flint et al., 2000). Thereby, the viral genome is released into the host cell and is used as template for viral protein production as well as genome replication. Progeny virions assemble and leave the cell either by budding from the cellular membrane (enveloped viruses) or lysis.

1.2 Poxviridae

The causative agent of smallpox *Variola major* is the best known poxvirus. Smallpox is one of the eldest reported infectious diseases as it can be backtracked to 2000 BC. It is assumed that the Egyptian pharaoh Ramses V died from smallpox. A rash of elevated "pustules" was revealed by the inspection of the mummy. Endemic diseases like smallpox need a sensitive crowd living close together. These circumstances were given after the progression of land farming and large settlements between 5 and 10 thousand years ago. Thereby the origin of *Variola virus* (VAV) is postulated between 1.9 and 10 thousand years ago (Babkin and Babkina, 2011).

1.2.1 Taxonomy of the poxviridae

The family of *Poxviridae* is subdivided into *Chordopoxvirinae* and *Entomopoxvirinae.* The agents of *Entomopoxvirinae* infect insects, whereas the members of the subfamily of *Chordopoxvirinae* cause infections in vertebrates and are classified into eight genera: *Avipoxvirus, Capripoxvirus, Leporipoxvirus, Mollusicpoxvirus, Orthopoxvirus, Parapoxvirus, Suipoxvirus* and *Yatapoxvirus.* The Orthopoxgenus illustrates the largest genus and harbours seven different species including the *vaccinia virus* (VACV) and VAV as well as the *cowpox virus* (CPXV) (Flint et al., 2000).

Poxviruses are DNA viruses and their double stranded DNA genome (dsDNA) encodes for about 200 proteins. The entire genome size ranges from about 135 kbp for *Orf virus* (*Parapoxvirus*) to 360 kbp for Canarypoxvirus. The genome size of the *Orthopoxvirus* CPXV is about 230kbp. Several strains belonging to the *Orthopoxvirinae* have been sequenced.

1.2.2 Structure of the poxvirus genome and virion

The brick-shaped or ovoid virus particles of poxviruses comprise some of the largest known virions and range from 220 to 450 nm long and 140 to 260 nm wide (Flint et al., 2000). The virus core is enveloped by at least one membrane. The core is biconcave in shape and associates with lateral bodies, which lie in the concavities of the core (Flint et al., 2000). Interestingly, the poxvirus core does not show any known symmetry as it is described for other viruses. For example, the capsid of *Tobacco mosaic virus* (TMV) has a helical symmetry. Within the poxvirus core the linear double stranded DNA genome is associated with DNA-binding proteins as well as proteins necessary for early gene transcription. Taken together, the core harbours roughly 200 proteins, making up almost half of the proteins encoded by the entire genome. At both termini the linear DNA double strand genome is enclosed by hairpin loops (Fig. 1). The DNA sequence localised in direct neighbourhood to the terminal hairpin at one end of the genome is also found at the other end, however in the opposite orientation. This led to the naming inverted terminal repeat (ITR). The ITR length varies from 0.7 kbp in VAV strains up to 10 kbp in VACV strains (Fig. 1). At the very end tandem repeats composed of two blocks of 70 bp sequences repeated 13 and 18 times are described (Pickup et al., 1982; Wittek and Moss, 1980). Poxvirus genes are densely packed and do not contain introns. The classical naming of the open readings frames (ORFs) of the, e.g., VACV genome is related to the cleavage of the DNA with HindIII. It results in 16 fragments, which are termed from A to P depending on their size. The ORFs in each fragment are numbered consecutively and their orientation is denoted with L for left or R for

right (Modrow et al., 2003). For example the ORF K1L maps to the fragment K, first ORF and a left reading orientation, whereas, the notation for CPXV and modified vaccinia virus Ankara (MVA) was done from the left end to the right end of the genome.
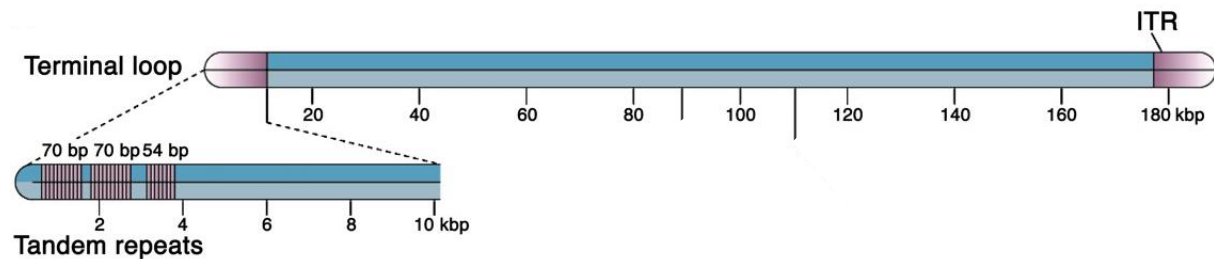
Fig. 1: Scheme of the *vaccina virus* genome
The double stranded DNA is enclosed by terminal hairpin loops. The ITRs are localised at both ends of the genome. The enlarged left ITR indicates the typical tandem repeats. Figure adapted from (principles of virology).

1.2.3 The poxvirus life cycle

Untypical for DNA viruses, poxviruses exclusively replicate in the cytoplasm (Minnigan and Moyer, 1985). Nevertheless, this is also proposed for the dsDNA Asfarviruses. Interestingly, two DNA virus families, *Iridoviridae* and *Phycoviridae,* belonging to the group of nucleo-cytoplasmic large DNA viruses, need both the cytoplasm and the nucleus for their efficient replication cycle.

The replication cycle starts with attachment described as the "contact between virus particle and host cell followed by the uptake or entry of the virus". The exact process for poxvirus attachment and entry is still unknown, as no specific cell receptors have been determined so far. Nevertheless, it has been shown that certain virus membrane proteins bind to glycosaminoglycans, chondroitin sulfate (Hsiao et al., 1999), heparan sulfate (Chung et al., 1998) and laminin at the host cell surface (Chiu et al., 2007). After virus entry and core release into the cytoplasm, the transcription of the virus genome starts immediately. The poxvirus transcription occurs in a cascade regulated fashion meaning it is subdivided into early, intermediate and late phases. Since early poxvirus transcription takes place in the still intact core it must contain all necessary proteins. The early mRNAs extrude through pores from the core into the cytoplasm (Kates and McAuslan, 1967; Munyon et al., 1967). They encode factors important for DNA-replication (Jones and Moss, 1985), host interaction (Kotwal et al., 1989) and intermediate transcription (Jones et al., 1987). The intermediate transcription proceeds and these transcripts encode factors necessary for DNA binding, packaging, late transcription and core-associated non-enzymatic proteins. In the late transcription phase early transcription factors, mature virion proteins together with proteins which play a role in the entry-fusion complex and the process of morphogenesis (Rosel and

Moss, 1985) are produced. Early expressed genes are especially localised to the ends of the linear DNA strand whereas intermediate and late expressed genes are predominantly found in the middle of the genome. Intermediate and late gene transcription is dependent on DNA-replication. If the process of DNA-replication is blocked by inhibitors, the transcription cascade is not able to proceed (Vos and Stunnenberg, 1988). The assembly of the virions occurs in special compartments within the cell named the viral factories. In these intracellular inclusions viral components are concentrated, leading to increased efficiency of replication and assembly. Two different infectious virus particles are produced by poxviruses. The particle naming is still under debate in the field. The termination to date is MVs for mature viruses and EVs for enveloped viruses. In older literature MVs are referred to internal mature viruses (IMVs), wrapped viruses (WVs) to internal enveloped viruses (IEVs) and extracellular EVs to external enveloped viruses (EEVs) or cell-associated enveloped virus (CEVs) (Moss, 2012). The MV is localised within the host cell whereas the EV is not. Nevertheless MVs are also released by the host cell. MVs and EVs differ from each other by their outer membrane, as EVs contain one additional membrane which is obtained during the process of exocytosis (Smith and Law, 2004) (Fig. 2).
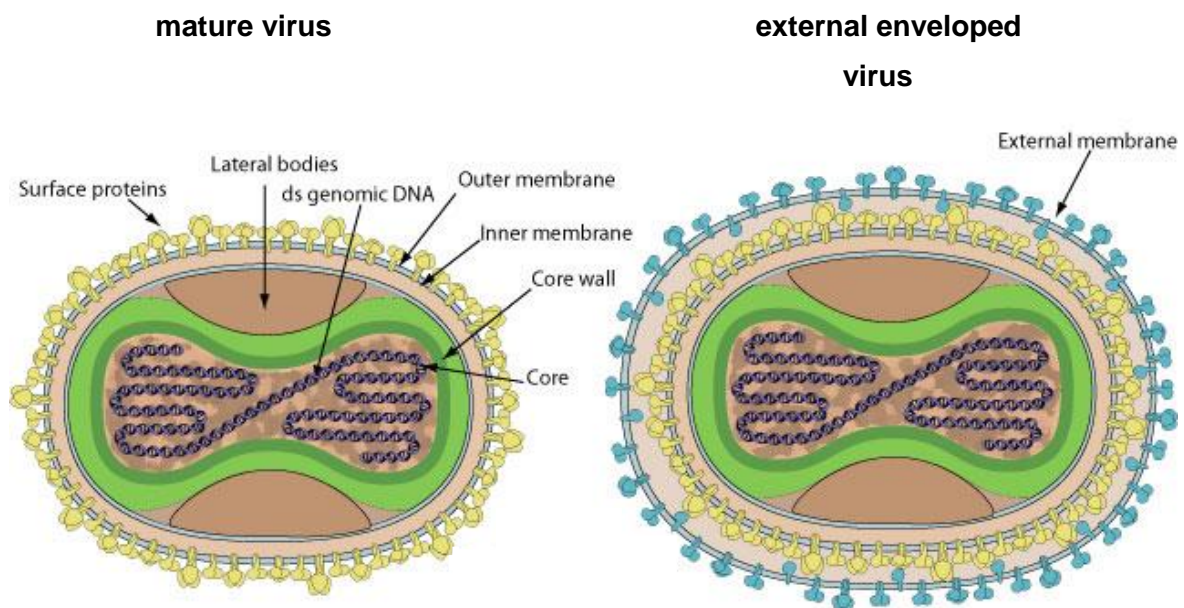
Fig. 2: Poxvirus infectious particles. Poxviruses produce two different infectious particles. The mature virus (left) has one membrane layer less than the external enveloped virus (right). It is shown that their cores are identical. The virions are called brick-shaped or ovoid. Figure adapted from (www.poxvirus.org).

The ways in which the viruses form their membranes are still the subject of controversial debate. The latest publication of Chlanda et al. showed the formation of cellular derived ruptured membrane material at scaffold proteins to crescent-shaped membranes (Chlanda et al., 2009). These crescents then build oval structures that take up enzymes as well as core

proteins. This particle is termed as immature virus particle (IV). After the viral DNA is packaged the oval structure closes completely. The structure of the IV matures into the brick-shaped MV including the complete reorganization of viral envelopes and the development of a core (Chichon et al., 2012). The newly built particles use cellular microtubules for their movement to the Golgi apparatus where they are wrapped and therefore termed WV (Chichon et al., 2012). Afterwards, again with the aid of microtubules (Hollinshead et al., 2001), the particles are transported to the cell membrane where they undergo exocytosis. In this state the virus is still externally attached to the host cell and termed EV (or formerly CEVs). EVs are driven to the neighbouring cells with the support of an actin-tail formation process. Beneath the bound virus particle actin-tails form a microvilli-like structure and direct the virion to the closest cell (Roper et al., 1998). This process is the most important for cell-to-cell virus spread (Blasco and Moss, 1992). If the virion is released from the cell, they were formerly termed EEV. This appropriately describes their location as the EEVs mediate the wide-reaching propagation of the virus (Fig. 3).
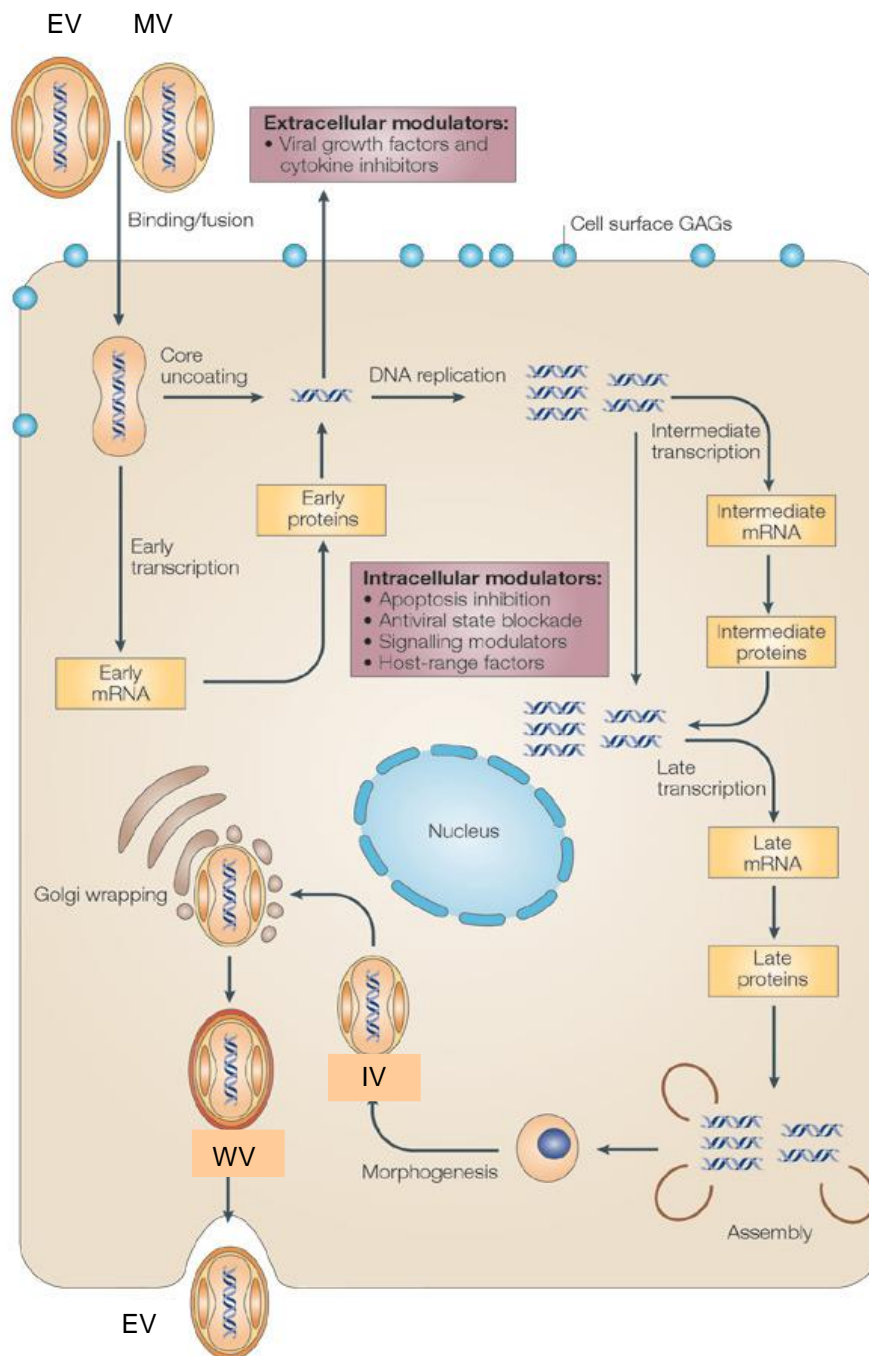
Fig. 3: Poxvirus replication cycle. After the entry of EV or MV, the core is released into the host cells cytoplasm. Within the core, the early gene expression starts immediately. In a process, which is also called uncoating the virus DNA is set free and DNA replication starts. As the DNA replication is the pre-requirement for intermediate and late transcription the cascade regulated transcription can proceed. The virus assembly begins with the formation of crescents. After DNA uptake the closed particle matures and is transported to the Golgi apparatus by microtubules. Following Golgi wrapping the WV is directed to the cell surface again mediated by microtubules. The particle fuses with the plasma membrane and is termed EV. Figure adapted from (McFadden, 2005).

1.2.4 The Cowpox virus (CPXV)

Wild rodents are widely accepted as the natural host for CPXV although the name suggests cattle as reservoir host. An argument against rats as natural reservoir host is the endemic appearance in contrast to the expected spreading all over the world via rats. Since the virus has a zoonotic potential the number of infections in humans increased over the years transmitted mostly from cats or domestic rats to human. In 2007, transmission from rat to elephant to humans was reported in Germany (Kurth et al., 2008). Interestingly, Chantrey et al. proposed bank voles and wood mice as the main hosts in Great Britain (Chantrey et al., 1999). The cowpox disease is endemic in Europe and Western Asia although surprisingly, Ireland shows complete absence of the CPXV. In immunocompetent humans the first signs of cowpox infection manifest after an incubation time of 8 to 12 days. Clinical symptoms include lesions on hands, face, as well as trunk which evolve in different stages as papules, vesicles, pustules, hemorrhagic ulcerations and lastly the healing in a scarring manner (Parrino and Graham, 2006).

CPXV has a long history since it was used by Edward Jenner as a vaccine against smallpox in the 1700's. He had documented that farm workers seemed to be immune against smallpox and therefore he concluded that a previous cowpox infection might be responsible for the immunity. For his first vaccination attempt he used material from a blister on the hand of a milk-maid, who suffered from cowpox and rubbed it into the skin of a healthy boy. Later on he challenged the boy with smallpox. The boy survived and did not develop smallpox (Smith and McFadden, 2002). This led to the naming vaccine, deriving from the latin *vacca* meaning cow (Riedel, 2005).

1.2.5 The Modified vaccinia virus Ankara (MVA)

Modified vaccinia virus Ankara (MVA) was generated by continuous passaging of the parental chorioallantois vaccinia virus Ankara (CVA) on chicken embryo fibroblast (CEF) cells for more than 500 passages (Mayr and Munz, 1964). The newly derived virus was tested concerning its safety and immunogenicity and it followed the assumption that after 570 passages on CEFs the virus was uniform and genetically stable. It showed a highly restricted host range in cell culture and was described as apathogenic *in vivo* (Mayr and Munz, 1964) In the process of passaging the parental CVA lost about 27 kbp of its DNA genome. A comparable restriction fragment length polymorphism (RFLP) revealed the loss could be divided into six major deletions (Meyer et al., 1991). Interestingly, it turned out that the deletion of the corresponding six genome areas of MVA into the parental VACV does not lead to an MVA-like phenotype (Meisinger-Henschel et al., 2010). The host range of MVA is

still controversially discussed. It was shown that MVA had impaired replication abilities in a variety of human cell lines, such as HeLa (Blanchard et al., 1998; Drexler et al., 1998; Wyatt et al., 1998) and HaCaT cells, whereas other groups reported a complete absence of replication ability in human cells (Carroll and Moss, 1997; Mayr and Munz, 1964; Meyer et al., 1991; Sutter and Moss, 1992). Nevertheless, the attenuated MVA is able to proceed through its full replication cycle in CEFs and baby hamster kidney (BHK) cells (Drexler et al., 1998).The question at which step in the replication cycle the MVA host restriction occurs was answered with the late stage of viral morphogenesis (Sutter and Moss, 1992). Hence, as a result immature virions accumulate within the cell. By comparing the strains MVA-572, MVA-1721 and MVA-BN, which are 100 % identical in their coding region nucleotide sequence, distinctions in their replication competence in different human cell lines were determined (Suter et al., 2009).

1.2.6 The Variola Virus (VAV)

The disease smallpox was life-threatening with a mortality of 30 % (Johnson et al., 2011) and even higher when the hemorrhagic form occurred. VAV had a higher mortality over the span of recorded disease history than all other infectious diseases taken together (McFadden, 2005). Patients infected with *variola major virus* developed the characteristic lesions in the mouth and on the skin of their extremities. In 1959 the WHO started a global smallpox eradication program. At that time smallpox was endemic in Brazil, India, Africa and Indonesia. Many different smallpox vaccines were used during this eradication program. The VACV strain EM-63 was used in the Soviet Union, the strain Temple of Heaven (Tian Tan) was used in China and in the United Kingdom the VACV strain Lister was used for vaccination (Fang et al., 2005; Kennedy et al., 2009; Parrino and Graham, 2006). In the late 70´s MVA was used as a prime vaccine followed by a booster vaccination with vaccinia strain Lister in Germany (Stickl et al., 1974). In contrast to Germany, the United States stopped the vaccination of the general public in 1972 (Parrino and Graham, 2006). About 20 years later from the start of the program in 1980 the WHO declared the world free of smallpox disease. One of the main reasons for the successful eradication of smallpox was the complete absence of an existing animal reservoir. Additionally, patients who suffered from smallpox either died or recovered completely without being infectious anymore. This means that they did not contribute to the virus spread after recovery. Hence, the virus is not known for the establishment of persistent or latent infections. Until now, VAV is stockpiled in Novosibirsk (Russia) and Atlanta (USA). The refusal of virus stock destruction provoked concerns about using this virus as a bioterroristic weapon. This led to the vaccination of members of the US

military and civilian healthcare workers with Dryvax in 2002 (Parrino and Graham, 2006). To date, Dryvax is the only licenced vaccine in the United States. For humans who have contraindications to the administration of Dryvax in terms of pregnancy, immunosuppression as well as cardiac disease the vaccination with MVA might be a safer alternative (McCurdy et al., 2004). Studies that compare Dryvax and MVA in a monkey model indicate equivalent T-cell response after injection of two doses of MVA, one dose of MVA followed by Dryvax or Dryvax alone (Earl et al., 2004). In case of Dryvax vaccination followed by a prime vaccination with MVA the vaccination derived lesions were smaller and healed more rapidly in contrast to Dryvax application alone (Earl et al., 2004).

1.2.7 The Rabbit fibroma virus (RFV)

Rabbit fibroma virus (RFV), formerly known as Shope fibroma virus (SFV), belongs together with myxoma virus (MYXV), hare fibroma virus (FIBV) and squirrel fibroma virus (SQFV) to the leporipox genus. RFV is host restricted to grey squirrels and lagomorphs resulting in the development of skin lesions and tumours in these animals after infection (Shope, 1932). It was the first DNA virus associated with transmissible tumours. The RFV strain Kasza is one of the two known RFV strains (Kasza and Boderlage) and was among the earliest poxvirus genomes to be completely sequenced. The genome is almost 160 kbp in length and encodes 160 genes. The RFV inverted terminal repeats span 12.4 kbp and encode for 11 ORFs (Willer et al., 1999). Surprisingly, the ITRs contain no repetitive DNA sequences at all. A genetic recombinant virus of RFV and MYXV named malignant rabbit fibroma virus (MRV) also belongs to this genus (Block et al., 1985). MRV has not been found in wild rabbits but causes a disease very similar to myxomatosis in laboratory rabbits and was used as a MYXV vaccine. In this study RFV was used as a helper virus for the MVA bacterial artificial chromosome (BAC) virus reconstitution.

1.2.8 Treatment of poxvirus infections

The treatment of poxvirus infections was successfully demonstrated for *molluscum contagiosum virus* and *orf virus* in immunosuppressed patients by usage of the acyclic nucleoside analogue cidofovir. Cidofovir was already known as an effective drug against DNA viruses, especially for its therapeutic administration in AIDS patients who suffer from cytomegalovirus that belongs to the *herpesviridae*. Cidofovir is not only used in poxvirus

infections, but also to treat vaccine-caused side effects in for example immunosuppressed patients (reviewed in (Andrei and Snoeck, 2010).

1.2.9 Poxviruses as therapeutics

Incidentally, oncolytic poxviruses are becoming more and more of central interest in the therapeutic field of cancer treatment. This can be attributed to their special abilities to replicate in tumour tissue and inefficient replication in normal tissue. For instance the replication of poxvirus strain JX-594 is dependent on an activated epidermal growth factor receptor (EGFR)/RAS pathway which is usually active in epithelial cancer cells (Parato et al., 2012). In a Phase I trial, where patients were treated with an intravenous infusion, it was shown that JX-594 replicates selectively in cancer tissue (Park et al., 2008). Based on this promising result further studies are needed to determine the poxvirus´ oncolytic potential. JX-594 was also used as a vaccinia virus vaccine during the World Health Organisation (WHO) smallpox eradication program.

1.3 Bacterial artificial chromosomes (BACs)

In contrast to yeast artificial chromosomes (YACs), which are able to maintain fragments up to 500 kbp, bacterial artificial chromosomes (BACs) allow cloning of fragments upwards of 300 kbp. BACs are based on the *Escherichia coli* (*E.coli*) F-factor. BAC-replication in *E.coli* is highly controlled by the F-plasmid (Shizuya et al., 1992). Hence, it is maintained one or two copies per bacteria cell. This low copy number is important on the one hand for the stability and on the other hand it minimizes the recombination potential between DNA fragments of interest sustained by the plasmid itself or/and bacterial chromosomal DNA. BACs were invented by Hiroaki Shizuya who cloned 300 kbp of human DNA in *E.coli* (Shizuya et al., 1992). By showing this new possibility, the Human Genome Program (HGP) started using BAC libraries for its purposes. The new opportunity of cloning large DNA fragments also led to the cloning of entire virus genomes as BACs. The first large DNA virus cloned and productively reconstituted, was the herpesvirus *mouse cytomegalovirus* (MCMV) with a genome size of around 230 kbp (Messerle et al., 1997). Subsequently, *human cytomegalovirus* (HCMV), *epstein barr virus* (EBV) and *human herpesvirus-8* (HHV-8) followed (Borst et al., 1999; Delecluse et al., 1998; Xu et al., 2006). Also the large DNA baculovirus, which infects exclusively invertebrates, was cloned as a BAC (Luckow et al., 1993). The first VACV BAC was generated by Domi and Moss in 2002, whereas the MVA BAC was produced by Cottingham and colleagues lately in 2008 (Cottingham et al., 2008;

Domi and Moss, 2002). Moreover, there are also BACs for RNA viruses available such as *yellow fever virus*, which is still a serious threat in Africa and South America (Rice et al., 1989). It was also possible to generate a stable cDNA based BAC of *SARS-coronavirus*, which harbours the biggest known RNA genome (Almazan et al., 2006).

The alteration of virus genes or genes in general is one of the pivotal procedures for their investigation. Thus a stable system in which DNA can be easily manipulated is of considerable advantage. In former times the generation of a special virus mutant could take many months. The BAC technology is a time saving tool as the genome can be manipulated more quickly and efficiently (Brune et al., 2000). Additionally the recombination procedures in *E.coli* are well understood. This led to the investigation of a Red system based method known as *en passant* mutagenesis for markerless generation of mutations in BACs (Tischer et al., 2010). The desired manipulations are often insertions, deletions, point mutations or sequence replacements in the gene of interest. In particular, the knowledge of single or families of viral genes is of major concern in investigating their role in immune modulation, pathogenesis as well as the establishment of infection. To date, BACs have proven useful in the development of vaccines, therapeutics and as mentioned above in the studies of viruses concerning their oncolytic potential. Plant genome BACs are also of interest with BAC libraries of *Arabidopsis thaliana* and of certain rice seeds already available (Song et al., 1997).

1.4 Ankyrin repeat proteins in general (structure of ankyrin repeat proteins)

Ankyrin repeat proteins (ARPs) are characterized by a repeating 33 amino acid residue motif (Sedgwick and Smerdon, 1999). This motif was first discovered in the yeast septin Cdc10p and the Notch receptor of *Drosophila melanogaster* (Breeden and Nasmyth, 1987). The mammalian cytoskeletal protein ankyrin is composed of 24 copies of the repeat which led to the name ankyrin for the motif (Lux et al., 1990). Each repeat consists of pairs of antiparallel α-helices followed by a β-hairpin (Fig. 4). The typical L-shaped domain, which occurs through stacking of consecutive repeats, allows insertion of additional non-conserved residues, thus leading to specific substrate binding (Michaely et al., 2002; Sedgwick and Smerdon, 1999). In fact, the ankyrin repeat is one of the most common amino acid sequences observed in protein-protein-interactions (Mohler et al., 2002; Mosavi et al., 2004; Sedgwick and Smerdon, 1999). In contrast to other protein motifs, ankyrin repeats do not prefer binding to a single class of protein targets. They play a role in many cellular functions such as modulation of the inflammatory response, signal transduction, cell cycle control, transcriptional regulation and inhibition or development of tumours (Bork, 1993; Michaely and Bennett, 1992; Mosavi et al.,

2004; Voronin and Kiseleva, 2007). Protein domains which strongly vary in their architecture are termed promiscuous or mobile domains (Basu et al., 2008). The functional variety of ARPs can be attributed to their domain promiscuity. However, only 12 different domain architectures are recognized in viral and bacterial genomes so far, whereas the PFAM database gives 425 unique domain architectures among ankyrin proteins in total (Al-Khodor et al., 2010). The binding of a suitable substrate needs contact to the exposed tip of the β-loop in addition to the surface opposite to the concave protein part, which is also known as ankyrin repeat groove (Becerra et al., 2004). The tertiary structure demonstrates a strong tendency to refold as deletion or prolongation of one repeat at a time does not affect the protein folding (Lee et al., 2006). Although ARPs are found in all superkingdoms, for example 733 ARPs in humans, 588 in mouse, 2901 in bacteria and 2908 in fungi (Al-Khodor et al., 2010), the ankyrin protein itself is missing in the yeast genome of *Saccharomyces cerevisiae* and in the plant *Arabidopsis thaliana*.

1.4.1 The Mammalian ankyrin repeat proteins

As mentioned above in contrast to other protein motifs, ARPs do not prefer the binding to a single class of protein targets. In mammalians ARPs play a pivotal role as adapters between the spectrin skeleton and a diversity of integral membrane proteins. Vertebrate ARPs are divided into three groups and each group harbours different spliced versions: ankyrins-B (B for broadly expressed), ankyrins-G (G for giant size and general expression) and ankyrins-R (R for restricted distribution) (Mohler et al., 2002)(Fig. 4).
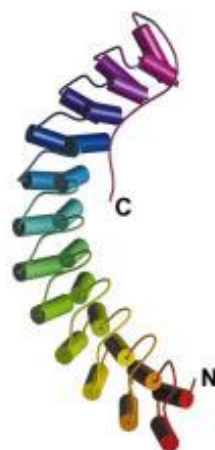
Fig. 4: crystal structure of a 12 ankyrin repeat stack from human ankyrinR. AnkyrinR possesses 24 ankyrin repeats in total. The knowledge of the crystal structure of its half has been used for modelling the entire ankyrin part. The individual repeats are rainbow colored (Michaely et al., 2002)

These proteins are ubiquitously expressed and one can find cell types which express all three members mentioned above. Nevertheless, they show tissue-dependent and

development regulated expression. Conserved domains of ankyrinR include the spectrin-binding domain, the death domain as well as the membrane-binding domain, which is built up from 24 copies of the 33 amino acid (aa) residues and functions in protein recognition (Lux et al., 1990). The 24 ankyrin repeats fold into six subdomains each with specific binding properties, such as the interaction with clathrin and tubulin (Michaely et al., 1999). The death domain was first described as functioning in the apoptosis protein Fas and the tumour necrosis factor receptor. Due to alternative splicing and alternate exon usage many ankyrin isoforms were identified. For example small ankyrins, which lose several domains, are associated with intracellular compartments like lysosomes, Golgi apparatus or the sarcoplasmic reticulum. On the other hand giant ankyrins have insertions between their spectrin and the death domain and these isoforms are found in unmyelinated axons or nodes of ranvier.

This class of proteins is able to exist solely by being built up of ankyrin repeats or combined with other structural motifs such as SOCS-box (suppressor of cytokine signaling), zf-DHHC domain (Zn-finger domain) or an F-box motif described later on.

1.4.2 The Poxvirus ankyrin repeat proteins

The *Poxviridae* possesses a huge repertoire of ARPs. Nowadays, the detection of ARRs in *Polydnaviridae*, *Iridoviridae, Phycodnaviridae* and *Mimiviridae* shows that they are no longer unique for poxviruses. The ORFs encoding ankyrin proteins are predominantly localised at the ends of the poxvirus genome. Phylogenetic analyses from Sonnberg and colleagues showed that, apart from ankyrin genes duplicated in the ITRs, no orthologue group encode for two full-length ankyrin genes in the same virus species (Sonnberg et al., 2011). In the genome of *canarypox virus* 51 ORFs encode for ankyrin repeat proteins what is about 21 % of the virus genome (Tulman et al., 2004). Thus, this virus shows the largest amount of these proteins in the P*oxviridae*. The widely accepted description of CPXV as the most closely related ancestor of *orthopoxvirus* was also confirmed by Sonnberg et al. as CPXV encodes the largest set of ankyrin proteins (Sonnberg et al., 2011). Based on whole genome sequencing the CPXV-GRI 90 strain was proposed as a separate species from CPXV-GER and CPXV BR (Hendrickson et al., 2010). Investigating the ankyrin repeat proteins of these three strains confirmed this hypothesis (Sonnberg et al., 2011). But contrary to these findings and with the knowledge that ECTV separated at first from all the other orthopoxviruses (OPV)s it is proposed that the ARP BR019 was duplicated from BR016. This event happened potentially after the separation of ECTV but before the evolution of the other OPVs (Babkin and Babkina, 2011).

Concerning the repeat number, six or less repeats are the most common number per protein. In contradiction to mammalian ARPs, poxvirus ankyrins proteins only show their ankyrin repeat motifs at the N-termini. In addition some have a conversed F-box motif at the C-terminus known for guiding them to the cellular SCF (Skp-1, cullin-1, F-box) ubiquitin ligase complex. This motif is termed after the mammalian cyclin-F (Bai et al., 1996). The F-box consensus sequence is 50 aa in length and contrary to cellular F-box proteins, with the virus versions being truncated. Additionally, the C-terminal location is also special to this set of proteins. The F-box motif recruits target proteins to the SCF-complex which leads to their polyubiquitination followed by proteasomal degradation. In doing so this motif functions in cell cycle regulation, DNA repair as well as in innate immunity. Besides the F-box protein, which binds to the linker protein Skp1, the RING finger ubiquitin ligase Roc1 and the scaffold protein cullin-1 assemble into the highly conserved SCF complex.

Recently, the poxvirus F-box like motif was termed PRANC (pox protein repeats of ankyrin C-terminus) and interestingly, it is also found in *Rickettsia*, bacteria which are intracellular parasites as well (Sonnberg et al., 2008). The shortest F-box motif with only 13 amino acids shows the CPXV encoded protein CP77. This may display the minimal sequence needed for Skp1 interaction. In opposition to *leporipoxviruses*, OPVs show the lowest F-box frequency (55 %). It was found for ankyrin repeat proteins lacking an F-box motif that they give evidence for gene fragmentation as indicated by taking together three ORFs of the *horsepoxvirus* which lead to an ankyrin orthologue in o*rthopoxvirus* (Sonnberg et al., 2011).

MVA has only one ankyrin repeat protein left (Genbank U94848.1). The deletion of this ORF causes a lack of viral transcription in NIH 3T3 and HaCaT cells with the most effect at viral intermediate and late gene transcripts (Sperling et al., 2009). This leads to a negative impact on viral late protein synthesis in these cell lines. Furthermore, the virus is unable to amplify its DNA in both NIH 3T3 and HaCaT cells (Sperling et al., 2009). This observation is in line with the known dependence on intermediate/late gene transcription and virus DNA replication. Additionally, a time lag for the shut off of host protein synthesis was observed.

1.4.3 Poxvirus ankyrin repeat proteins and viral tropism

Viral tropism can be subdivided into three levels: cellular, tissue and host tropism. If a virus infects and replicates productively in BHK cells but not in other cell types, it is noted as a virus with cellular tropism limited to BHK cells. An example for tissue tropism is influenza virus which has the ability to infect lung tissue but not brain tissue (McFadden et al., 2009). MYXV is known for host tropism in rabbits as the virus infects *Sylvilagus* rabbits but not *Oryctolagus* rabbits or humans. This fact made it possible to specifically eradicate feral

rabbits in Australia (Fenner and Radcliffe, 1965). Interestingly, among poxviruses, *myxoma virus* also shows differences concerning the *in vitro* host-cell specificity and the *in vivo* host-range as the virus is normally restricted to rabbit cells but can replicate in select primate and human tumour cells (McFadden, 2005). VAV and *molluscum contagiosum* virus are further examples of limited host tropism due to the fact that they infect exclusively humans (McFadden, 2005).

One special poxvirus host range gene K1L was found by an 18 kbp deletion in VACV (Drillien et al., 1981; Gillard et al., 1985; Gillard et al., 1986). This deletion mutant is unable to complete its replication cycle in rabbit kidney cells but this limitation can be rescued by the stable expression of the K1L gene in rabbit cells (Sutter et al., 1994). Interestingly, the cowpox ankyrin protein CP77 can also neutralize the effect of K1L deletion in rabbit kidney cells (Ramsey-Ewing and Moss, 1996). For CP77 it was shown previously that it enables vaccinia and ectromelia virus to grow on chinese hamster ovary cells (Chen et al., 1992; Ramsey-Ewing and Moss, 1995; Spehner et al., 1988). A vaccinia virus K1L and C7L double knock-out mutant resulted in the abortive replication in most human cell lines. For HeLa cells the replication inhibition was detected at the intermediate translation stage (Hsiao et al., 2004). Surprisingly, the growth defect of the double mutant can be reversed by K1L, C7L and CP77 in human cells but only K1L and CP77 have the capacity to do this in RK13 cells (Perkus et al., 1990; Ramsey-Ewing and Moss, 1996).

1.5 NF-κB signaling

NF-κB is a key player in the host immune defence, inflammatory response as well as apoptosis. The NF-κB family includes five different members: RelA (p65), RelB, c-Rel, NF-κB1 (p105/p50) and NF-κB2 (p100/p52), which form homo- and heterodimers in various combinations (Hayden and Ghosh, 2008). In unstimulated cells the interaction of NF-κB inhibitory proteins, termed IκBs keep NF-κB in the cytoplasm (Mohamed and McFadden, 2009). In the so called canonical pathway NF-κB is activated by the proteasomal degradation of IκB, which is mediated by the phosphorylation of IκB via the IκB kinase (IKK) complex made up of IKKα and IKKβ (Hayden and Ghosh, 2008). In the non-canonical pathway p100 becomes phosphorylated. This leads to its partial proteolysis and thus releases p52 which then translocates to the nucleus especially bound to RelB (Beinke and Ley, 2004). In the nucleus, the NF-κB complex acts as a transcription factor and binds to DNA leading to the transcription of several rather diverse target genes including adhesion molecules, immunregulatory surface molecules, inflammatory cytokines, chemokines as well as inhibitors of apoptosis.

1.5.1 Poxvirus ankyrin repeat proteins as NF-κB modulators

Potential inhibition of the host NF-κB pathway was shown for the gene product of ORF150 termed MNF (myxoma nuclear factor) protein of *myxoma virus* (Camus-Bouclainville et al., 2004). MNF contains nine ankyrin repeats and the eighth has a very high similarity to the ankyrin repeats in IκB which itself harbours an ankyrin motif. The ability of MNF to localize to the nucleus was lost by removing the eighth anyrin repeat (Camus-Bouclainville et al., 2004). If cells are treated with tumour necrosis factor alpha (TNF-α) MNF colocalizes together with NF-κB in the nucleus (Camus-Bouclainville et al., 2004). *In vivo* studies of an almost apathogenic MNF knockout virus proposed MNF as a critical virulence factor (Camus-Bouclainville et al., 2004). The cowpox ankyrin protein CP77, also known as host range factor for Chinese hamster ovary (CHO) cells, binds via its ankyrin domain to NF-κB/p65 and with its already mentioned very short F-box like motif to Skp1 and cullin1 of the SCF complex (Chang et al., 2009). Although it is not related to its host range function, both the ankyrin repeat and F-box like motif of CP77 are necessary for inhibition of NF-κB activation (Chang et al., 2009). Studies of a cowpox knockout mutant of the ARP encoded by the ORF 006 show high level secretion of NF-κB controlled cytokines such as TNF-α, IL-1β and IL-6 in THP1 cells, a human acute monocytic leukaemia cell line (Mohamed et al., 2009b). The knockout virus was also found to be attenuated in mice. The VACV ankyrin protein K1L, mentioned above for its host range function in RK13 cells, is known for the inhibition of IκB degradation and the subsequent block of host NF-κB activation (Shisler and Jin, 2004). Beside secreted poxvirus ligand inhibitors poxviruses express intracellular NF-κB inhibitors like the cowpox protein CrmA which interferes with the caspase1-mediated pathway (Ray et al., 1992). Additionally, the *Iridoviridae* ankyrin repeat protein ORF124L, encoded by the *infectious spleen and kidney necrosis virus* (ISKNV), contains four ARPs in total and is known for its interaction with IKKβ and the attenuation of TNF-α induced activity in NF-κB (Guo et al., 2011).

1.6 Apoptosis

Dependent on the stimulus, cell death can occur in two different ways. On the one hand cells can undergo necrosis, described as uncontrolled cell death, where neighbouring cells are damaged, fast loss of membrane integrity happens and cellular contents are released into the extracellular space. On the other hand they can undergo apoptosis, described as controlled or programmed cell death. Apoptosis does not only help the organism to control

tissue size and cell numbers in both the developed state and in the process of developing, it also plays a role in the disposal of damaged and infected cells. Hallmarks of this controlled cell destruction include the hydrolysis of nuclear DNA, the condensation and fragmentation of the nucleus, the Golgi apparatus, the endoplasmic reticulum and the mitochondrial network (Kerr et al., 1972; Taylor et al., 2008). These mechanisms are triggered by enzymes called caspases named for an essential Cys residue in their active site and the requirement for an Asp residue in the cleavage site in the chosen substrate (Nicholson, 1999). Most components of the cytoskeleton, such as actin, intermediate filaments and microtubular proteins, are all substrates for caspases. The proteolysis of cytoskeletal proteins results in the typical retraction and rounding of cells in early stages of apoptosis, while neighbouring cells remain unaffected. This is followed by plasma membrane blebbing which seems to require a slightly intact cytoskeleton.

Caspases act in a cascade like manner. Normally, they patrol in the cytoplasm in an inactivate precursor state and become activated by other caspases upstream in the cascade or by one of the three following pathways. Activation by the extrinsic pathway is caused by the binding of extracellular ligands, for instance TNF-α or FasL to the transmembrane death receptor TNFR for example. In the granzyme B-pathway this protease is delivered into the target cell by granules coming from cytotoxic T lymphocytes (CTL) or natural killer (NK) cells. In the intrinsic route proteins belonging to the BH3-only protein family become activated. This leads to the formation of Bak and Bax "channels" within mitochondrial outer membranes (Letai et al., 2002). Through these channels cytochome *c* and other mitochondrial intermembrane space proteins are released into the cytoplasm (Adrain and Martin, 2001). To date, caspases are not thought to play a role in mitochondrial fragmentation, but they do contribute to the shut down of mitochondrial function during apoptosis (Taylor et al., 2008).

1.6.1 Apoptosis mediated by poxvirus proteins

Several poxvirus encoded proteins play a role in the inhibition of apoptosis. The VACV protein F1L inhibits the activation of Bax by inhibiting the formation of Bax oligomers thus blocking the N-terminal activation of Bax (Wasilenko et al., 2005). Additionally F1L inhibits the cellular relocation of Bax to the mitochondria as well as the subsequent insertion into the outer membrane (Taylor et al., 2006).

In contrast to other host range proteins, the VACV host range protein K1L does not lead to an increase of apoptosis in RK13 cells infected with a K1L virus knockout mutant (Chung et al., 1997).

1.7 Aim of the thesis

ARPs encoded by poxviruses are well known as host range factors and immune modulators. Therefore, the deletion of ARP encoding ORFs one after the other will be made in a MVA BAC to obtain a complete ARP free virus. The resulting viruses should be characterized concerning their replication efficiency by performing growth kinetics, plaque size assays and monitoring the phenotype on infected CAMs of embryonated chicken eggs.

As CPXV harbours a large number of ARPs in comparison to other poxviruses, those virus ARPs were chosen for the characterization in the MVA background.

To circumvent the effect of compensation, the above generated deletion mutants should be used for the insertion of CPXV ARPs. The introduction of individual CPXV ARPs into the ankyrin negative MVA mutants will allow the functional characterization of single ARPs in the viral context. The ORFs for knock-in mutant construction were chosen according to the phylogenetic relation to each other, the presence of homologous genes in other OPVs and published data from the literature.

The generated ankyrin knock-in virus mutants should be evaluated with respect to their host range function. As MVA is host restricted to BHK and CEF cells, it is a suitable tool to study enhanced host range function of different proteins. For this purpose, different cell lines will be used for determination of replication efficiency and to identify important host range factors.

NF-κB as a key player in immune response is known to be affected by the ability of viruses to circumvent the host´s cells defence mechanisms. Therefore, single ARP virus mutants will be monitored and analyzed respecting their impact on the NF-κB pathway.

As it is still under discussion, if there is any correlation between host range function and apoptosis, identified host range mutants should be verified concerning potential influence on apoptosis. Histopathological analysis of pocks and eventual shifting of cell type composition in embryonic chicken CAMs due to virus infection will be studied using embryonated chicken eggs infected with different MVA mutants.

2. Materials and Methods

2.1 Materials

2.1.1 Consumables

Consumables were taken from VWR, Hartenstein, TPP, Whatman, Flexam and Roth.

2.1.2 Equipment

equipment	manufacturer
Bunsen burner, Typ 1020	Usbeck, Radevormwald
Cell incubator, Excella ECO-1	New Brunswick Scientific, Hamburg
Centrifuges, Type 5424/ 5804	Eppendorf, Hamburg
Cryo storage container, Cryo 1°C	Thermo Scientific, Langenselbold
Electroporator, GenePulser Xcell	Bio-Rad, München
Elisa reader, Tristar LB941	Berthold technologies, Bad Wildbach
Fluorescence microscope Axiowert M1	Zeiss, Oberkochen
Fluorescence microscope Axiowert S100	Zeiss, Oberkochen
Fluorescence microscope camera, Axiocam Mrm	Zeiss, Oberkochen
Gel electrophoresis chamber, big	peqlab, Erlangen
Gel electrophoresis chamber, small 100-230V	VWR, Darmstadt
Ice machine, AF100	Scotsman, Sprockhövel
Immunblot detection system, Chemismart 5100	Peqlab, Erlangen
Inverse light Microscope, MOTIC AE20	Ehlert & Partner, Niederkassel-Rheidt
Laminar flow	Bleymehl, Inden
Microwave	Bosch, Stuttgart
Nanodrop spectrophoto-meter, ND-1000	Peqlab, Erlangen
Nitrogen tank	Air liquide, Düsseldorf
PCR cycler, TGradient	Biometra, Göttingen
pH-meter	Hanna Instruments, Kehl am Rhein
Pipettes	VWR, Darmstadt
Pipettor, Accu jet pro	Brand, Wertheim
Power supply, 300V	VWR, Darmstadt
Real time, 7500 Fast Real-Time PCR system	Applied Biosystems, Darmstadt
Thermomixer comfort	Eppendorf, Hamburg
UV detection system, Biovision 3026	Peqlab, Erlangen
Vortexer	Hartenstein, Würzburg
Water bath	Julabo, Seelbach

2.1.3 Chemicals, enzymes and transfection reagents

chemicals, enzymes and transfection reagents	manufacturer
Acetic Acid	Applichem, Darmstadt
Acetone	Applichem, Darmstadt
Agarose	Lonza, Köln
Antartic phosphatase	NEB, Frankfurt am Main
L-Arabinose	Alfa Aesar, Karlsruhe
$CaCl_2$	Roth, Karlsruhe
Colenterazin	P.J.K., Kleinblittersdorf
DMSO	Roth, Karlsruhe
dNTPs	Bioline, Luckenwalde
EDTA	Sigmal-Aldrich, München
EGTA	Sigma-Aldrich, München
Ethanol	Applichem, Darmstadt
Ethidium bromide	Roth, Karlsruhe
Formaldehyde	Merck, Darmstadt
Fugene	Roche, Penzberg
Gene ruler 1kb plus DNA ladder	Fermentas, St. Leon-Rot
Glycerol	Applichem, Darmstadt
HCl	Roth, Karlsruhe
Isopropanol	Applichem, Darmstadt
K_2HPO_4	Applichem, Darmstadt
KCl	Merck, Darmstadt
KH_2PO_4	Applichem, Darmstadt
Luciferin	P.J.K., Kleinblittersdorf
Methanol	Applichem, Darmstadt
Methylcellulose	Sigmal-Aldrich, München
$MgSO_4$	Merck, Darmstadt
$Na_2EDTAx2H_2O$	Merck, Darmstadt
NaCl	Applichem, Darmstadt
Na_2HPO_4	Merck, Darmstadt
Natriumazide	PAA, Pasching
Page ruler Plus Prestained protein ladder	Fermentas, St. Leon-Rot
PermaFluor mounting medium	Thermo Scientific, Langenselbold
Phusion-polymerase	Thermo Scientific, Langenselbold
Phusion-polymerase buffer (5x)	Thermo Scientific, Langenselbold
Quick-ligase	NEB, Frankfurt am Main
Restriction enzymes	NEB, Frankfurt am Main, Fermentas, St. Leon-Rot
RNase A	Applichem, Darmstadt
SDS	Sigmal-Aldrich, München
T4-ligase	NEB, Frankfurt am Main
Taq-polymerase	Peqlab, Erlangen
Taq-polymerase buffer (10x)	Peqlab, Erlangen
Tris-base	Applichem, Darmstadt
Triton	Merck, Darmstadt
Trypsin	GIBCO, Darmstadt
Tween-20	Sigmal-Aldrich, München
XtremeGENE HP	Roche, Penzberg
Coomassie blue G 250	Serva, Heidelberg

Ponceau S	Serva, Heidelberg
Bromphenol blue	Alfa Aesar, Karlsruhe
Bacto-tryptone	Merck, Darmstadt
Bacto-yeast extract	Merck, Darmstadt
DTT	Sigmal-Aldrich, München
Nonident P-40	Merck, Darmstadt
Na-desoxycholate	Merck, Darmstadt

2.1.4 Buffers, media and solutions

buffers, media and solutions	composition
4x sample buffer (10 ml)	2.4 ml 1M Tris, pH 6.8 8 % (w/v) SDS 40 % (v/v) glycerol 0.2 % (w/v) bromphenol blue 1 ml β-mercaptoethanol 2.8 ml ddHO
Buffer I (for virus DNA preparation)	1.5 ml 2 M NaCl 400 µl 1M Tris, pH 8.0 400 µl 0.5 M EDTA 17.7 ml ddH$_2$O
Buffer II (for virus DNA preparation)	400 µl 1 M Tris, pH 8.0 400 µl 0.5 M EDTA 1.5 ml SDS 10 % (w/v) 650 µl protein kinase K 20 mg/ml 17.05 ml ddH$_2$O
CE buffer (immunoblot)	10 mM HEPES 10 mM KCl 0.1 mM EDTA, pH 8.0 0.1 mM EGTA 1 mM DTT 1x complete EDTA-free proteinase inhibitor cocktail (Roche)
Coomassie blue destain	0.5 % (w/v) coomassie blue G-250 50 % (v/v) methanol
Coomassie blue stain	10 % (v/v) acetic acid 40 % (v/v) methanol 10 % (v/v) acetic acid
LB medium	1 % (w/v) bacto-tryptone 0.5 % (w/v) bacto-yeast extract 0.5 % (w/v) NaCl
P1 (plasmid and BAC DNA purification)	50 mM Tris, pH 8.0 10 mM EDTA, pH 8.0
P2 (plasmid and BAC DNA purification)	0.2 N NaOH 1 % (w/v) SDS
P3 (plasmid and BAC DNA purification)	3 M KAcetate, pH 5.5
PBS	137 mM NaCL 2.7 mM KCl 10 mM Na$_2$HPO$_4$ 2 mM KH$_2$PO$_4$
PBS-T (for immunoblot)	PBS 0.1 % (v/v) Tween-20

Ponceau S stain	0.2 % (w/v) ponceau S powder 3 % (v/v) trichloracetic acid
RIPA (protein sample preparation)	20 mM Tris-HCl, pH 7.5 150 mM NaCl 1 % (v/v) Nonident P-40 0.5 % (w/v) Na-desoxycholate 0.1 % (w/v) SDS 1x complete EDTA-free proteinase inhibitor cocktail (Roche)
SDS running buffer (10x)	250 mM Tris-base 1.92 M glycine 1 % (w/v) SDS
TAE (pH 8.0)	50 mM Tris-base 2.5 mM $Na_2EDTAx2H_2O$ 25 mM Acetic acid 99 % (v/v)
TE (pH 7.5)	10 mM Tris-base 1 mM $Na_2EDTAx2H_2O$
Transfer buffer (for immunoblot)	25 mM Tris-base 250 mM glycine 20 % (v/v) methanol

2.1.5 Inhibitors, immunostimulants and cytokines

inhibitors, immunostimulants and cytokines	manufacturer
AraC	Sigmal-Aldrich, München
Cycloheximide	Sigmal-Aldrich, München
Polyinosinic:polycytidylic acid	Invivogen, Toulouse
rATP	Applichem, Darmstadt
TNF-α	Applichem, Darmstadt
1x complete EDTA-free proteinase inhibitor cocktail	Roche, Penzberg

2.1.6 Kits

kit	manufacturer
ECL Plus Detection Kit	GE Healthcare, München
Hi Yield Gel/PCR DNA Fragments Extraction Kit;	SLG, Gauting
Invisorb Spin Tissue Mini Kit	Stratatec, Berlin
Plasmid Mini Kit I	GE Healthcare, München
QUICK Clean II Gel extraction Kit	Genscript, Germany
TOPO TA Cloning Kit	Invitrogen, Darmstadt

2.1.7 Cell culture media and supplements

cell culture media and supplements	manufacturer
Dulbecco´s Modified Eagles Medium (DMEM)	Biochrom AG, Berlin

Fetal bovine serum	GIBCO, Darmstadt
Medium 199 Earls´	Biochrom AG, Berlin
Minimal Essential Medium (MEM)	Biochrom AG, Berlin
OptiMEM	GIBCO, Darmstadt

2.1.8 Antibiotics

antibiotics	final concentration	manufactorer
Ampicillin	100 µg/ml	Roth, Karlsruhe
Chlorampenicol	30 µg/ml	Roth, Karlsruhe
Kanamycin	50 µg/ml	Roth, Karlsruhe
Penicillin	100 U/ml	Fisher Scientific, Schwerte
Streptomycin	100 U/ml	Applied Biosystems, Darmstadt

2.1.9 Antibodies

2.1.9.1 Primary antibodies

primary antibodies	host	dilution	mancufactorer
anti-actin	rabbit	1:2000 PBS-T, 2.5 %(w/v) milkpowder	cell signaling, Frankfurt am Main
anti-L1R	rabbit	1:1000 PBS-T, 3 % (w/v) BSA	gift from RKI, Berlin
anti-E3L	mouse	1:1000 PBS-T, 3 % (w/v) BSA; 1:50, TBS, 5 (w/v) % FCS	(Weaver et al., 2007)
anti-vaccinia virus (Lister strain)	rabbit	1:50, TBS, 5 (w/v) % FCS	Acris antibodies, Herford
anti-IkappaB-alpha	mouse	1:1000 PBS-T, 3 % (w/v) BSA	cell signaling, Frankfurt am Main
anti-PARP	rabbit	1:1000 PBS-T, 3 % (w/v) BSA	cell signaling, Frankfurt am Main
anti-eIF2alpha	mouse	1:1000 PBS-T, 3 % (w/v) BSA	santa cruz technology, Heidelberg
anti-p-eIF2alpha	rabbit	1:1000 PBS-T, 3 % (w/v) BSA	epitomics, Hamburg

2.1.9.2 Secondary antibodies

secundary antibodies	host	dilution	manufactorer
anti-rabbit-HRP	goat	1:10000 PBS-T, 5 (w/v) % milkpowder	southern biotech, Eching
anti-mouse-HRP	goat	1:10000 PBS-T, 5 (w/v) % milkpowder	Sigmal-Aldrich, München
anti-mouse Alex fluor 568	goat	1:1000, PBS, 1 (w/v) % FCS	Invitrogen, Darmstadt

2.1.10 Oligonucleotides

oligonucleotide	sequence
#015_T7	TAATACGACTCACTATAGGG
#018_BGH	TAGAAGGCACAGTCGAGG

#192_MVA Test R fwM	AACTGATACAATCTCTTATCATGTGGGT
#194_MVA Test R rvM	CATGCCAGTACGATATATTGTTTCATG
#199_MVA_186_del_F	AACAATTATATGAGGACTTTTACCACAAAGCATCATAAAATTG TATTTTTCTCATGCGATTAGGGATAACAGGGTAATCGATTT
#200_MVA_186_del_R	ATATCAGTTTTTTTACACACATCGCATGAGAAAAATACAATTTT ATGATGCTTTGTGGTAGCCAGTGTTACAACCAATTAACC
#203_MVAfl186inR	CAACTCGAGGACACTTTGCGCTGAATGGCTCT
#204_MVAfl186inF	TGGACTAGTGATAAACTATCGTTATATCTG
#205_MVA186MCSR	GTCCTAGGCGGCCGCATCGCATGAGAAAAATACAATTTTATG
#206_MVA186MCSF	GCCTAGGACGCGTGTGTAAAAAAACTGATATTATATAAATA TTTTAG
#207_MVA186kanR	CTGGCGCGCCTTAGGGATAACAGGGTAATCGATTT
#208_MVA186kanF	GGACGCGTGTGTAAAAAAACTGATATTATATAAATATTTTAGT GCCGTATAATGAAGAGCCAGTGTTACAACCAATTAACC
#298_211inMVA F	ATGCGGCCGCTGAAAAATGGATTACAAGGATGACGATGACAA GAGTCGTCGTCTGATTTATGTTTTAAAT
#299_211inMVA R	TTCCTAGGCTATACTTTGGTAGGTGGATATGATATATT
#300_220inMVAF	GATGCGGCCGCTGAAAAATGGATTACAAGGATGACGATGACA AGCTATGCGATTATGATACAAAGATGTTT
#301_220inMVAR	GTCCTAGGCTAGTTAAATTTATAATAATGTTTTAGATGGTTAC
#302_225inMVAF	TGCGGCCGCTGAAAAATGGATTACAAGGATGACGARGACAAG TCAACCATTACTAAAAAAATATATTGTTCTG
#303_225inMVAR	GTCCTAGGCTAGTATGGATAATGTTTGTAATGGTTCTT
#312_BR006inF1	TGATGGAATCTATTTCATCGAATG
#313_BR006inF2	TCCTCGTATCGGCTCCTCTAG
#322_BR220inF1	AACATATCATCATCCATGCTCATG
#323_BR220inF2	TTCTGATAGTATAGATAGCTTTAGCGAA
#324_BR220inF3	CGATGAATACTATAATGACAATTACACC
#329_pCeu3F	GAAACTAGTGAATGTTACTCGAGTTCGCTACCTTAGGACCGT TATAGTTACGTCACTGG
#330_pCeu3R	TTCACTAGTTTCGCTACCTTAGGACCGTTATAGTTACGAGTA ATC
#349_RFV1 fw	AAAGATGCGTACATTGGACCC
#350_RFV1 rv	GTTCGAGACTAGAAAAGCGCC
#372_pcFL_BR016_F	AAGCGGCCGCATCAAAATGGACTACAAAGACGACGACGACA AAGCATCATTAACCGAACACGCTATAGT
#373_pc_BR016_R	TTCCTAGGTCACGCTTCATCAGTAAGTCGAGCA
#376_pcFL_BR019_F	AAGCGGCCGCCTTACCATGGACTACAAAGACGACGACGACA AAAACTCATTAATCGAAAATTCTGTACTCCA
#377_pc_BR019_R	TTCCTAGGTTAATTCAGATGATTTAATGTCGGCAATAT
#379_pcFL_BR027_F	AAGCGGCCGCACGATCATGGACTACAAAGACGACGACGACA AAATTAACGATAAGATACTCTATGATAGTTGTAA
#380_pc_BR027_R	TTCCTAGGTTATAGGAACGCGTACGAGAAAATC
#382_pc_BR041_R	ATCCTAGGTTAGTTTTTCCGCGCATAATTGACG
#384_pc_BR213_R	ATCCTAGGTCATGTCTGTGTAGAAACAGACCTCGT
#387_pcFL_BR041_F	AAGCGGCCGCTAAGACATGGACTACAAAGACGACGACGACA AAGATCTGTCACGAATTAATACTTGGAAGTC
#389_pcFL_BR213_F	AAGCGGCCGCACAATAATGGACTACAAAGACGACGACGACA AAGACGAAGATAAGATACGACTATCTAAGTAT
#390_MVAD171/2F	AATTGAAAAGGGATAACATGTTACAGAATATAAATTATATAGAT ACGGTAAACATCCTTCTAGGGATAACAGGGTAATCGATTT
#391_MVAd171/2R	GACTAGTGCACTTCACGAAAGAAGGATGTTTACCGTATCTAT

	ATAATTTATATTCTGTAAGCCAGTGTTACAACCAATTAACC
#396_BR016seqF1	CGGTATCCTACACGCGTATCTCG
#397_BR016seqF2	CAGAAACCGATAACGATATAAGACTAGATG
#401_BR027seqF1	GACGATTACGATTACGACTACACCACT
#402_BR027seqF2	ATTTGACAATAGGGATCCTAAAGTTG
#406_BR213seqF1	CGGGATATATGGCAAGAACATAATG
#407_BR213seqF2	GTATAACGGAAATGATATAAACGCA
#433_M186PLfw	CGATGCGGCCGCCTTAGCTAGCTTACCTAGGTTTACGCG TGTGT
#434_M186PLrv	ACACACGCGTAAACCTAGGTAAGCTAGCTAAGGCGGCCGC ATCG

Underlined bps indicate cleavage sites.

2.1.11 Plasmids

plasmid name	description	source
pcDNA3.1 BR027	insertion of the CPXV ORF CPXV027 (NC_003663.2)	this thesis
pcDNA3.1 BR041	insertion of the CPXV ORF CPXV041 (NC_003663.2)	this thesis
pcDNA3.1/V5-His-Topo BR006	insertion of the CPXV ORF CPXV006 (NC_003663.2)	this thesis
pcDNA3.1/V5-His-Topo BR016	insertion of the CPXV ORF CPXV016 (NC_003663.2)	this thesis
pcDNA3.1/V5-His-Topo BR019	insertion of the CPXV ORF CPXV019 (NC_003663.2)	this thesis
pcDNA3.1/V5-His-Topo BR213	insertion of the CPXV ORF CPXV213 (NC_003663.2)	this thesis
pcDNA3.1/V5-His-Topo BR220	insertion of the CPXV ORF CPXV220 (NC_003663.2)	this thesis
pEP-kanS	plasmid harbouring kan cassette	
pCeu2	harbouring two I-Ceu cleaveage sites	(Tischer et al., 2007)
pCeu3	pCeu2 with SpeI	this thesis
pCeu3-Flank	pCeu3 with MVA flanks	this thesis
pCeu3-MCS	pCeu3-Flank with MCS	this thesis
pEPtrans	pCeu3-MCS with kanamycin cassette	this thesis
pEP-trans-BR006	pEPtrans with BR006	this thesis
pEP-trans-BR016	pEPtrans with BR016	this thesis
pEP-trans-BR019	pEPtrans with BR019	this thesis
pEP-trans-BR027	pEPtrans with BR027	this thesis
pEP-trans-BR041	pEPtrans with BR041	this thesis
pEP-trans-BR213	pEPtrans with BR213	this thesis

2.1.12 BACs

BAC name	description	source
pBRf	CPXV-BR genome cloned as a BAC	(Roth et al., 2011)
pMVA	MVA genome cloned as a BAC	(Cottingham et

		al., 2008)
pMd-co	pMVA co-integrate for ORF186 deletion	this thesis
pMd	pMVA with ORF186 deletion	this thesis
pMdd-co	pMVA-d186 co-integrate for ORF171 deletion	this thesis
pMdd	pMVA-d186 with ORF171 deletion	this thesis
pMd-BR027 co	pMVA-d186 co-integrate for BR027 insertion	this thesis
pMd-BR027	pMVA-d186 with BR027 insertion	this thesis
pMd-BR041 co	pMVA-d186 co-integrate for BR041 insertion	this thesis
pMd-BR041	pMVA-d186 with BR041 insertion	this thesis
pMd-BR213 co	pMVA-d186d171 co-integrate for BR213 insertion	this thesis
pMd-BR213	pMVA-d186 with BR213 insertion	this thesis
pMdd-BR006 co	pMVA-d186d171 co-integrate for BR006 insertion	this thesis
pMdd-BR006	pMVA-d186d171 with BR006 insertion	this thesis
pMdd-BR016 co	pMVA-d186d171 co-integrate for BR016 insertion	this thesis
pMdd-BR016	pMVA-d186d171 with BR016 insertion	this thesis
pMdd-BR019 co	pMVA-d186d171 co-integrate for BR019 insertion	this thesis
pMdd-BR019	pMVA-d186d171 with BR019 insertion	this thesis
pMdd-BR027 co	pMVA-d186d171 co-integrate for BR027 insertion	this thesis
pMdd-BR027	pMVA-d186d171 with BR027 insertion	this thesis
pMdd-BR041 co	pMVA-d186d171 co-integrate for BR041 insertion	this thesis
pMdd-BR041	pMVA-d186d171 with BR041 insertion	this thesis
pMdd-BR213 co	pMVA-d186 co-integrate for BR213 insertion	this thesis
pMdd-BR213	pMVA-d186d171 with BR 213 insertion	this thesis

2.1.13 Viruses

virus name	description	source
vMVA	reconstituted from pMVA	this thesis
vMd	reconstituted from pMVA-d186	this thesis
vMdd	reconstituted from pMVA-d186d171	this thesis
vMd-BR027	reconstituted from pMVA-d186-BR027	this thesis
vMd-BR041	reconstituted from pMVA-d186-BR041	this thesis
vMd-BR213	reconstituted from pMVA-d186-BR213	this thesis
vMd-BR220	reconstituted from pMVA-d186-BR220	this thesis
vMddBR006	reconstituted from pMVA-d186d171-BR006	this thesis
vMddBR016	reconstituted from pMVA-d186d171-BR016	this thesis
vMddBR019	reconstituted from pMVA-d186d171-BR019	this thesis
vMdd-BR027	reconstituted from pMVA-d186d171-BR027	this thesis
vMdd-BR041	reconstituted from pMVA-d186d171-BR041	this thesis
vMdd-BR213	reconstituted from pMVA-d186d171-BR213	this thesis

2.2 Molecular biology methods

2.2.1 Polymerase chain reaction (PCR)

The polymerase chain reaction (PCR) is one of the most important techniques used in modern molecular biology. This method is an easy and fast way for the amplification of DNA fragments. One requirement for the development of this technique was the discovery and isolation of heat-stable enzymes.

For amplification of DNA fragments the following reaction mix and cycling program were used:

PCR reaction mix (50 µl):

forward oligonucleotide (10 µM)	1.0 µl
reverse oligonucleotide (10 µM)	1.0 µl
dNTPs (10 mM)	1.0 µl
Phusion polymerase (1U/l)	1.0 µl
Phusion polymerase buffer HF (5x)	10.0 µl
template DNA	1.0 µl
ddH$_2$0	35.0 µl

PCR-cycling program:

step	temperature	time	description
1)	98 °C	5 min	initial denaturation of double stranded (ds)DNA
2)	98 °C	2 min	denaturation of (ds)DNA, time variable
3)	50 °C	30 sec	oligonucleotide annealing
4)	72 °C	1 min	elongation time, variable
10 cycles from step 2) to 4)			
5)	98 °C	30 sec	denaturation of (ds)DNA, time variable
6)	60 °C	20 sec	oligonucleotide annealing, temperature variable
7)	72 °C	1 min	elongation, time variable
8)	72 °C	7 min	final elongation
9)	4 °C	∞	storage
20 cycles from step 5) to 8)			

The time required for the denaturation of the first 10 cycles was dependent on the template used. BAC DNA needs 2 min for denaturation, whereas plasmid DNA needs only 30 sec to 1 min for heat denaturation. The oligonucleotide annealing temperature did depend on the ordered oligonucleotide sequence. The elongation time did depend on the expected fragment size that was supposed to be amplified. The polymerases Phusion and Taq were required to perform the PCR reaction. The protocol and program were modified upon the manufacturer´s instructions.

2.2.2 Restriction fragment length polymorphism (RFLP)

The RFLP was used for the confirmation of generated plasmids, BACs and DNA from reconstituted viruses. The DNA was cleaved by an appropriate enzyme in a 20 µl reaction.

mixture (20 µl):
plasmid DNA	1 µl
or BAC/virus DNA	10 µl
buffer (10 x)	2 µl
enzyme	1 µl
add to 20 µl with ddH$_2$O	x µl

2.2.3 Agarose gel electrophoresis

For the verification of PCRs and cleavage of plasmids agarose gel electrophoresis was performed. For this, 1 % (w/v) agarose gels were prepared in 0.5x TAE buffer. DNA samples were mixed with 6x loading dye and loaded in the gel slots. The gels were run at constant 100 V for at least 30 min. In contrast, cleaved BAC and virus DNA was exposed to 70 V for 20 h or more in an ethidium bromide free 0.8 % (w/v) gel, prepared in 1.0x TAE. These gels were stained afterwards in an ethidium bromide bath for 20 min to 30 min and rinsed with water for destaining. In both gel types the DNA was detected with 260 nm UV light. If a DNA fragment should be excised from the gel, 360 nm were used for the prevention of DNA damage.

2.2.4 DNA fragment purification

Both PCR amplified and cleaved DNA fragments were excised from agarose gels. They were then either purified with the Hi Yield Gel/PCR DNA Fragments Extraction Kit (SLG) or with the QuickClean II Gel Extraction Kit (Genscript) according to the manufacturer´s instructions.

2.2.5 Ligation

The primary function of a ligation reaction is the connection between DNA fragments and the secondary function of DNA ligases is to catalyze the formation of phosphodiester bonds

between juxtaposed 5´phosphate and 3´hydroxyl termini in duplex DNA. Normally they repair fractionated single DNA strands in an ATP-dependent manner, where diphosphate is set free as a by-product.

For the generation of plasmids containing specific inserts, the cleaved and purified insert DNA as well as the vector backbone were ligated in different vector/insert ratios ranging from 5:1 to 1:5 in a total volume of 10 µl. The respective ligase buffer systems were either T4-ligase or Quick-ligase. The mix was incubated between 5 min to 30 min at room temperature depending on recommended instructions.

If the TOPO TA cloning Kit was used, the ligation reaction was mixed as recommend by the manufacturer.

2.2.6 Sequencing

For the determination of the correct nucleotide sequence of plasmids or BACs, the entire plasmid or PCR amplified fragments from BAC or virus DNA were sent to the sequencing facility StarSEQ or LGC Genomics. For this purpose, the sample DNA was column purified and the concentration was measured with the nanodrop according to the standard operating procedures. An appropriate amount of DNA was then mixed with the oligonucleotide needed for successful sequencing and filled up to 7 µl or 14 µl with water. The derived sequences were analysed for their correctness with the alignment tool of VectorNTI (Life Technologies Corporation, Darmstadt).

2.2.7 Preparation of chemocompetent *E.coli*

Different *E.coli* strains are needed for different purposes. For this thesis, the *E.coli* strain MDS42 was appropriate. For the preparation of chemically competent *E.coli* a 4 ml overnight culture was added to 400 ml fresh LB medium and incubated at 37 °C and 220 rpm. The cells grew until they reached an optical density (OD_{600}) of 0.5 to 0.6. The cell suspension was transferred in falcon tubes, centrifuged for 10 min at 5000 rpm before removing the supernatant. The cells were kept strictly on ice during the entire procedure. The cell pellet was resuspended in 10 ml prechilled 100 mM $MgCl_2$ and further incubated for 20 min to 30 min on ice. After an additional centrifugation step at 4 °C for 10 min at 4000 rpm, the supernatant was removed and the pellet resuspended in 2 ml prechilled 100 mM $CaCl_2$/15 %

(v/v) glycerol solution. This solution was divided into 100 µl aliquots and the cells were stored at -70 °C.

2.2.8 Transformation of chemocompetent *E.coli*

Introduction of artificial DNA into *E.coli* is commonly used for the multiplication and isolation of DNA for further experiments and usage. After the ligation, a part or the entire ligation mix was added to chemically competent MDS42 *E.coli* and the mixture was incubated 30 min on ice. A heat shock for 45 sec at 42 °C in a water bath followed by addition of 1ml of prewarmed LB-medium and the mixture was incubated for 1h at 37 °C and shaking. The transformation mixtures were plated on LB-plates containing the desired antibiotics and incubated at 37 °C overnight.

2.2.9 Plasmid and BAC DNA preparation

Overnight cultures of 5 ml LB-medium were either grown at 37 °C for simple plasmids or at 32 °C for BAC clones in the *E.coli* strain GS1783. Then each culture was centrifuged at 4500 x g for 5 min and the supernatant was discarded before resuspending the cell pellet in 300 µl of solution P1. The cells were lysed by adding 300 µl of solution P2. The mixture was left to stand for 5 min at room temperature before the precipitation of the proteins was achieved. The proteins were precipitated by adding 300 µl of the neutralizing solution P3, followed by a centrifugation for 10 min at maximum speed (20.000 x g). For DNA precipitation the supernatant was transferred into a fresh vial together with the same volume of isopropanol was added. The tube was inverted several times before the mixture was centrifuged for 15 min at maximum speed (20.000 x g). The DNA pellet was washed once with 70 % (v/v) ethanol and dried afterwards. 30 µl of TE buffer containing RNase A (40 µg/ml) was added to dissolve the DNA. The prepared plasmid DNA was stored at -20 °C and BAC DNA at 4 °C.

2.2.10 *En passant* mutagenesis

The two-step *en passant* mutagenesis is a markerless BAC manipulation method, in which the Red recombination system, encoded by the special bacteria strain GS1783 and the expression of the homing endonuclease I-SceI play an essential role. It is based on the ability of homologous sequences to recombine. As an example the generation of a deletion BAC mutant is shown in Fig. 5. *En passant* mutagenesis is only possible if a positive selection

marker, a I-Scel cleavage site and the presence of duplicated sequences, which are localized next to the sequence to be altered, are present. These sequences allow the homolog recombination in the first recombination step as well as the excision of the positive selection marker in the second recombination step. During the first recombination (Fig. 5a) a linearized DNA fragment (Fig.5 b), harbouring the positive selection marker flanked by the I-Scel cleavage site and duplication sequences, is inserted into the parental BAC (Fig. 5c). The resulting product is termed a co-integrate (Fig. 5d). In the second recombination (Fig. 5f) event, the I-Scel endonuclease expression (Fig. 5e) is induced by L-Arabinose. The I-Scel endonuclease activitity produces free dsDNA ends. This allows the homolog recombination between the duplicated sequences with the excision of the positive marker sequence as a consequence and finishes with the generation of a deletion BAC mutant (Fig. 5g) (Jamsai et al., 2003; Tischer et al., 2010).

Larger sequences, such as ARP encoding ORFs, can be inserted using the generation of a transfer construct, which harbours flanking regions with duplications for the homologous recombination events, the I-Scel cleavage site, the selection marker and the sequence, which has to be inserted.
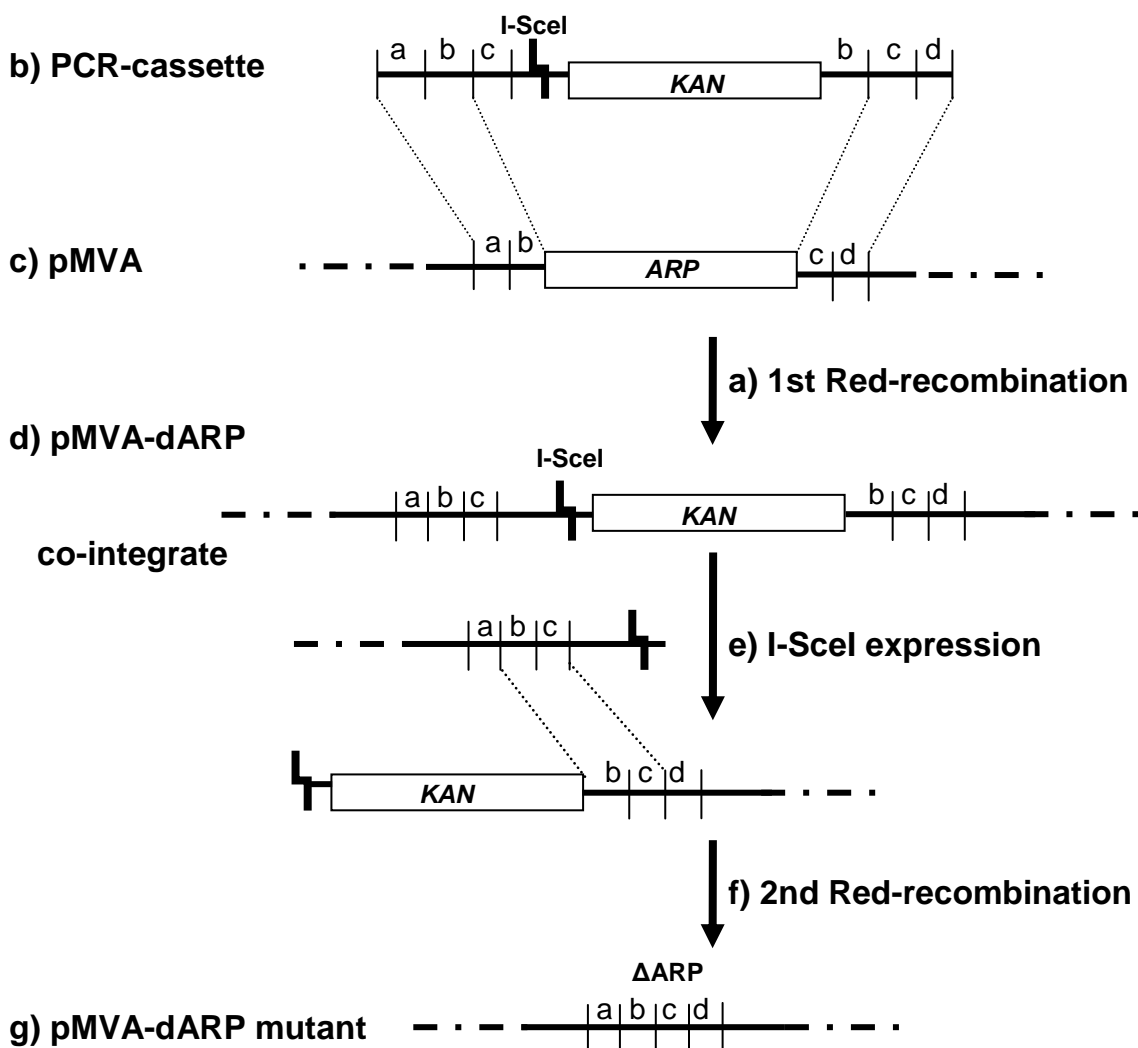
Fig. 5: Generation of a deletion BAC mutant by *en passant* mutagenesis. The marker cassette amplified with extensions b) is used in the 1st Red recombination b) to generate a co-integrate d). After induction of I-Scel expression e) the second Red recombination f) occurs, where the marker cassette is excised and the BAC mutant of interest g) is generated. Figure adapted from (Tischer et al., 2010).

2.2.10.1 Preparation of electrocompetent *E.coli*

The *E.coli* strain GS1783 was used to perform *en passant* mutagenesis in this thesis. An overnight culture containing the desired parental BAC clone was grown in chloramphenicol containing LB medium at 32 °C. This culture was used for the inoculation at a 1:50 ratio of 5 ml fresh chloramphenicol containing LB medium. Under shaking conditions at 32 °C this culture was grown to an OD$_{600}$ of 0.5 to 0.7. Then the Red recombination system was induced by transferring the culture to 42 °C for 15 min. An incubation time of 20 min on ice followed, before the bacteria were pelleted for 10 min by centrifugation at 4500 x g. The supernatant was discarded and the pellet was resuspended in 5 ml of 10 % (v/v) ice-cold glycerol or ddH$_2$O before a second centrifugation step followed. In the final washing step 1 ml of 10 % (v/v) ice-cold glycerol or ddH$_2$O was added to resolve the bacteria. After a last centrifugation, 50 µl 10 % (v/v) ice-cold glycerol or ddH$_2$O was added for resolving the bacteria pellet and the tube was placed on ice or stored at -70 °C until electroporation.

2.2.10.2 1st Red recombination

A *Dpn*I digested PCR product or a cleaved and purified fragment of a transfer plasmid was used for the first recombination step. 1 µl of the PCR product or 1 to 5 µl of the gel purified transfer plasmid fragment were added to the ice-cold electrocompetent *E.coli* and transferred into a 1mm electroporation cuvette. Electroporation was carried out at 25 µF and 200 Ω. Afterwards the bacteria were left to recover in antibiotic free media for 1 h at 32 °C with shaking. Then they were streaked out on chloramphenicol and kanamycin containing plates and incubated for 1-2 days at 32 °C.

2.2.10.3 2nd Red recombination or resolution of co-integrates

For the resolution of co-integrates the desired bacterial clones were grown for 1-2 h at 32 °C in 1 ml chloramphenicol containing LB medium under shaking conditions until the culture became faintly cloudy. The I-Scel cleavage site was induced by the addition of 1 ml pre-warmed LB medium containing chloramphenicol and 2 % (w/v) L-Arabinose. The cultures

were grown for an additional 1h under shaking conditions. The Red recombination system was induced by heat activation for 30 min at 42 °C. After two additional hours of shaking incubation at 32 °C, 5-10 µl of a 1:100 and 1:1000 dilutions were plated on chloramphenicol and 1 % (w/v) L-Arabinose containing LB-plates. The plates were incubated for 1-2 days at 32 °C. Material from grown colonies was transferred to kanamycin and chloramphenicol containing replica plates to exclude false positive colonies. Putative positive clones were inoculated in an overnight culture. After BAC-DNA preparation their correctness were confirmed by RFLP.

2.2.11 Glycerol storage of bacterial strains

For a bacterial glycerol stock preparation, 800 µl of grown bacterial culture and 800 µl of 75 % (v/v) glycerol were mixed. The glycerol stock was stored at -70 °C for long-term storage.

2.3 Proteinbiochemical based methods

2.3.1 SDS (sodium dodecyl sulphate) polyacrylamide gel electrophoresis (PAGE)

The SDS PAGE is commonly used for the separation of proteins in a gel matrix. Through the excess of SDS, the proteins become negatively charged, proportional to their molecular weight. Thereby, they can be separated independently of their own charge but in relation to their molecular weight.

A SDS gel consists of a separation gel with a stacking gel on top. Different compositions for various separation gels and stacking gels are shown below.

composition of various separation gels:

for 1 gel	6 %	8 %	10 %	12 %	15 %
ddH$_2$O	2.6 ml	2.3 ml	1.9 ml	1.6 ml	1.1 ml
1.5 M Tris pH 8.8	1.3 ml	1.3 ml	1.3 ml	1.3 ml	1.3 ml
30 % (v/v) acrylamide	1.0 ml	1.3 ml	1.7 ml	2.0 ml	2.5 ml
10 % (w/v) SDS	50 µl	50 µl	50 µl	50 µl	50 µl
10 % (w/v) APS	50 µl	50 µl	50 µl	50 µl	50 µl
TEMED	4 µl	3 µl	2 µl	2 µl	2 µl

composition of stacking gels:

5 % gel	1 gel	2 gels
ddH$_2$O	21.4 ml	2.7 ml
1 M Tris pH 6.8	250 µl	500 µl
30 % (v/v) acrylamide	330 µl	670 µl
10 % (w/v) SDS	20 µl	40 µl
10 % (w/v) APS	20 µl	40 µl
TEMED	2 µl	4 µl

2.3.2 Preparation of protein samples for immunoblot

To analyze cellular or viral proteins, cells were washed once with PBS. After scraping they were pelleted in a centrifugation step for 5 min at maximum speed. After removing the supernatant, the pellet was resuspended in RIPA or CE buffer. If RIPA buffer was used the samples were incubated for 30 min on ice. In contrast, lysis with CE buffer was carried out in 5 min. Large amounts of viral DNA in protein samples can influence the running abilities of the sample in the gel, thus if cells were infected with a high MOI, 0.5 µl of the enzyme benzonase, an enzyme randomly cleaving single and double stranded RNA and DNA, was added for the cleavage of virus DNA. After the incubation on ice the samples were centrifuged for 5 min at maximum speed and the supernatant was transferred to a new vial, which was stored at -20 °C until further usage for immunoblot. The protein samples were mixed with 4 x sample buffer and boiled for 5 min at 95 °C before loading on a SDS gel. The separation was achieved by using constant 100 V for 15 min followed by an increased voltage of up to 180 V for at least 45 min.

2.3.3 Immunoblot

The immunoblot uses specific antibodies to detect individual proteins that have been adsorbed onto membranes. After proteins are separated by SDS PAGE, the proteins are further transferred to a membrane using an electric current. Commonly used membranes are made of nitrocellulose or PVDF, which were moistened in transfer buffer together with whatman paper for 5 min, before the semidry blotting chamber was assembled as follows: anode, 3x whatman paper, membrane, gel, 3x whatman paper, cathode. The proteins were transferred out of the gel and onto the membrane using the semi-dry transfer system at 100 to 180 mA for 30 min. The transfer was verified by ponceau S staining of the membrane for 1 min. Afterwards the membranes were blocked for 1 h at room temperature either with 3 %

(v/v) BSA in PBS 0.1 % (v/v) Tween20 or in 5 % (w/v) milkpowder in PBS 0.1 % (v/v) Tween. The first antibody diluted in the used blocking buffer was incubated over night at 4 °C. Afterwards the membrane was washed three times for 10 min in PBS 0.1 % (w/v) Tween, before the secondary antibody was added to the membrane for 1 h at room temperature, followed by another washing step. For the detection the membrane was incubated for 5 min in ECL reagent following the manufacturer´s instructions.

2.3.4 BCA Protein Assay Kit

For comparable immunoblot analysis the protein sample concentration was measured with the Pierce BCA Protein Assay Kit. If samples were prepared with CE buffer, they had to be dialysed in advance to the measurement, because of interfering substances with the BCA working reagent in the buffer. The BCA working reagent was prepared by adding BCA reagent B to BCA reagent A in a 1:50 ratio. The assay was performed in replicates where 10 µl of sample were mixed with 200 µl working reagent in a microplate well. After incubation at 37 °C for 30 min the absorbance was measured at 560 nm with a plate reader.

2.4 Cell culture based methods

2.4.1 Maintenance of cell cultures

The mammalian cell lines listed below, were grown in cell culture flasks or plates and incubated at 37 °C at a 5 % CO_2 environment in a humidified atmosphere. The maintenance of the different cell lines were done by removing the media and washing them once with PBS. 0.25 % (v/v) trypsin was added and the cells were incubated under the conditions mentioned above until complete cell detachment. The cells were then divided in a 1:2 to 1:10 ratio depending on the planned usage. The following table shows the different cell lines together with their appropriate medium.

cell line	origin	medium
MDBK	bovine	MEM, 5 % (v/v) FCS, 1x P/S
KEN-R	bovine	MEM, 5 % (v/v) FCS, 1x P/S
CRFK	cat	MEM, 5 % (v/v) FCS, 1x P/S
NBL-6	equine	MEM, 10 % (v/v) FCS, 1x P/S
Vero	green monkey	MEM, 5 % (v/v) FCS, 1x P/S

BHK	hamster	MEM, 5 % (v/v) FCS, 1x P/S
HaCaT	human	DMEM, 10 % (v/v) FCS, 1x P/S
NIH 3T3	human	DMEM, 10 % (v/v) FCS, 1x P/S
HeLa	human	MEM, 5 % (v/v) FCS, 1x P/S
A549	human	DMEM/HAMS 12, 5 % (v/v) FCS, 1x P/S
Nie168	mouse	Earl´s 199, 5 % (v/v) FCS, 1x P/S
RK13	rabbit	MEM, 5 % (v/v) FCS, 1x P/S

2.4.2 Cryoconservation of eukaryotic cells

For the long term storage of eukaryotic cells, the medium was removed and the cells washed once with PBS. Then 0.25 % (v/v) trypsin was added followed by the incubation for cell detachment at 37 °C with 5 % CO_2 atmosphere. Instead of dividing cells, they were frozen in growth medium containing 7 % (v/v) DMSO. The mixture was aliquoted into cryovials and stored in cryoconservation containers, which cool down 1 °C per minute overnight. The cells were then transferred to liquid nitrogen containers to maintain a temperature of -196 °C.

To revive cells, vials were thawed quickly and diluted before seeding in a cell culture flask with recommended medium. After cell setting, the medium was changed to remove residual DMSO from the cells.

2.5 Virus based methods

2.5.1 Virus reconstitution

For virus reconstitution 10 µl of freshly prepared mutant BAC DNA was added to 86 µl OptiMEM. After addition of 4 µl transfection reagent (Fugene or XtremeGENE HP) the mixture was rocked and incubated for 20 min at room temperature. Afterwards, the transfection mix was added dropwise to seeded BHK cells. The BAC DNA used for virus reconstitution encodes for GFP under a late 4b fowlpox promoter. Thereby, single cell infection and plaque formation could be monitored by fluorescence microscopy. Additionally, titer determination was performed by counting fluorescent plaques formed by GFP expressing viruses by fluorescence microscopy.

The rabbit fibroma virus or helpervirus, necessary for the efficient start of the early transcription from the BAC DNA was added to the cells 1 h post transfection. Successful replication was monitored after 24 h. If newly transfected cells showed a high number of GFP expressing cells, the material was transferred to CEF cells after two freezing and thawing

cycles. This was necessary to eliminate the prior added helpervirus, as rabbit fibroma virus is unable to complete its replication cycle in CEF cells. Passaging of the newly generated virus was repeated at least three times. Afterwards the newly generated virus was tested for the absence of rabbit fibroma DNA by PCR.

2.5.2 Virus stock preparation

Poxviruses do not release a high amount of virions into the medium. Therefore, it is necessary to disrupt the cells mechanically for the preparation of applicable virus stocks. Virus stocks used for the infection in the different experiments were prepared by the infection of confluent cell monolayers grown in flasks or plates. The virus infection rate was monitored by the percentage of GFP expressing cells as the generated viruses express GFP under a late 4b fowlpox promoter. At an infection rate of 80 % to 100 %, the cell medium was removed except for 10 ml. The cells were scraped and transferred in a 50 ml reaction tube containing glass beads in a volume to glass bead ratio of 5:1. The mixture was vortexed for 30 sec before freezing at -70 °C. The vortex step in the presence of the glass beads disrupts the cell membranes. After complete freezing the cell suspension was thawed and vortexed again for 1 min, before cells were frozen once again at -70 °C. Then the cell suspension was thawed for the last time and was finally vortexed for 2 min. The glass beads and cell debris were pelleted by the centrifugation for 10 min at 3000 x g. The resulting supernatant was aliquoted in 1.5 ml reaction tubes and stored at -70 °C until further usage.

Alternatively, virus stock preparation was prepared using a syringe-based method. After complete infection of the cells, they were scraped and pelleted by centrifugation for 5 min at 4500 x g. The supernatant was discarded and the pellet washed once with PBS. Afterwards the pellet was resuspended in 1 ml 10 mM Tris pH 9.0 and incubated for 30 min on ice. The high pH should swell the cell membranes. After the incubation on ice, the mixture was transferred into a syringe with a 22 gauge needle and passaged 10 times up and down for mechanical cell disruption. A sonification step for 3x 30 sec followed, before the mixture was centrifuged to pellet the cell debris (5 min, 1800 x g). The supernatant was diluted to 10 ml in fresh medium and aliquoted in 1.5 ml reaction tubes and stored at -70 °C until further usage.

2.5.3 Virus titration

To determine the exact virus titer of prepared virus stocks, the aliquoted virus mixture was titrated. For that purpose, cells were seeded in 24 well plates to reach a confluent density 24

h later. One vial of the virus stock to be titrated was thawed and on used for a 10 fold dilution series. 100 µl of each dilution step was used for the infection of the seeded cells in duplicates. 1 h post infection at 37 °C in a 5 % CO_2 environment the medium was removed and methocel was added to prevent the infection of cells by virions released into the medium. Therefore, in cell monolayers overlayed with methocel the virus can only spread from one cell to the neighbouring cell and thereby forms a virus plaque. A virus plaque consists of three or more infected cells close to each other, which are not derived through cell cycle division. After 48 h the GFP expressing virus plaques were counted under a fluorescence microscope. The virus titer was given in plaque forming units (PFU) per ml.

2.5.4 Virus DNA preparation

Dependent on the required amount of DNA, cells seeded in six well or 12 well plates were infected. The cells were harvested by scraping in PBS buffer and transferred to a reaction tube. After centrifugation (10 min, 20000 x g) the cell pellet was washed once with PBS before it was resuspended in 300 µl buffer 1. Afterwards the proteinase K containing buffer 2 was added (750 µl) and the mixture was incubated at 55 °C for at least 4-5 h with shaking conditions. Then 300 µl supersaturated NaCl (6 M) was added and the tube was inverted several times. For DNA precipitation 900 µl isopropanol was added and after inverting the tube, the mixture was centrifuged 10 min at maximum speed. The precipitated DNA was washed once with 70 % (v/v) ethanol and after drying dissolved in 30-100 µl TE containing RNaseA (40 µg/ml).

buffer 1 (20 ml):
1.5 ml 2 M NaCl
400 µl 1 MTris pH 8.0
400 µl 0.5 M EDTA
17.7 ml ddH$_2$O

buffer 2 (20 ml):
400 µl 1 M Tris pH 8.0
400 µl 0.5 EDTA
1.5 ml 10 % (w/v) SDS
650 µl proteinase K (20mg/ml)
17.05 ml ddH$_2$O

For special purposes (real time experiment) the virus DNA was isolated with the Invisorb Spin Tissue Mini Kit from Stratatec. The procedure was carried out by using the manufacturer´s instructions.

2.5.5 Growth kinetics

Cells were seeded in 24 well plates 24 h before infection and incubated at 37 °C in a 5 % CO_2 environment. The virus was diluted to the indicated multiplicity of infection (MOI) in

medium and 1 ml was added for infection. After 1 h post infection the medium was discarded and the cells were washed twice with PBS. Fresh medium (1 ml) was added and the point of time T_0 was taken immediately by removing the media and centrifugation for 5 min at 1800 x g. The supernatant was transferred into a new tube and stored at -70 °C. 1 ml medium was given to the remaining cells on the plate and the plate was stored at -70 °C. The following samples were taken in the same procedure at the indicated points of time.

For titration, the vials and plates were frozen and thawed two times. The cells in the 24 well plates were scraped and mixed by pipetting up and down before 10 fold dilution series were prepared. The supernatant material in the vials was used directly after thawing and freezing procedure for preparation of the 10 fold dilution series. After adding 100 µl of each prepared virus dilution step to cells, which were seeded in 24 well plates 24 h before, the infected cells were incubated for 1 h under the described conditions. The infection of the cells was done in duplicates for each dilution step. The medium was removed and methocel was added to the cells. After 48 h the virus plaques expressing GFP were counted by fluorescence microscopy.

2.5.6 Plaque size assay

The size of a virus plaque gives information about the ability of a virus to spread from cell to cell. Cells were seeded in six well plates 24 h before infection with a virus dilution containing 100 PFU. After 1h the medium was removed and the cells were overlayed with methocel. The plates were incubated for another 48 h and before 50 pictures were taken from each virus. The total number of plaques per well must have not differ in more than 10 %. The area of the plaques was determined by the program ImageJ.

2.5.7 Poxvirus infection of the chorion allantoic membrane (CAM)

Embryonated chicken eggs were incubated under rotating conditions for 11 days. To locate the embryo, the air sac and the veins in the chorion allantoic membrane (CAM), the eggs were exposed to a strong light. The air sac and a vein free area were marked on the egg shell. The infection took place under a sterile working bench and the outer egg shell was sterilized with 80 % (v/v) ethanol. With the help of a rotating carborundum disc a hole was drilled carefully into the formerly "vein-free" marked area in the egg shell without disrupting the shell membrane. Complete removal of the egg shell was confirmed by dropping PBS on the area. If the calciferous layer was completely removed the shell membrane became visibly

transparent after PBS application. A sterile stick was used to form a hole in the thin shell membrane. Afterwards, another small hole was drilled at the side of the air sac and the air was sucked out and thus removed. A 200 µl virus dilution with indicated PFU was inoculated through the shell membrane directly on the CAM. Liquid paraffin wax was used for closing the holes in the eggs. The eggs were then incubated under non-rotating conditions for additional 5 days. Before CAM harvest, the eggs were stored 30 min at -20 °C. After egg opening the chick head was immediately severed. The CAM was prepared and washed with PBS three times. For histological studies the CAMs were fixed in 4 % (v/v) buffered formalin.

2.6 Immunfluorescence staining

Immunostaining was used to visualize the expression of early and late virus proteins in cells. The cells were seeded on cover slips in 24 well plates to a density of 60 % to 70 %. The next day the cells were infected with a multiplicity of infection (MOI) of 0.01. The multiplicity of infection describes the ratio between virus particle and cell count. If an infection with a MOI of 3 is used in an experiment, a dilution with 3 infectious virus units per cell is given to the cell monolayer. The virus infected cells were overlayed with methocel after 1 h post infection. The fixation took place in 90 % (v/v) ice cold acetone or a methanol/acetone (50:50) mixture for 15 min at -20 °C or 4 % (v/v) formaldehyde for 15 min at room temperature. Afterwards, the fixative was removed and the cells were dried and rehydrated in PBS for 5 min with shaking conditions. For blocking reasons, 250 µl blocking buffer was added to the cells for 45 min. The first antibody diluted in TBS buffer containing 5 % (v/v) FCS was added afterwards for another 45 min. Then the cells were washed three times for 10 min in TBS before adding the secondary antibody for additional 45 min. The third antibody was added after completing the incubation of the secondary and the following three washing steps of 10 min each. This last antibody was left on the cells for 45 min and the unbound antibodies were removed by a final washing procedure. The cover slips were embedded upside down in permafluor mounting medium on a glass slide. The stained cells were examined under the Zeiss Axio Imager M1.

blocking buffer:
1 x TBS
5 % (v/v) FCS
0.3 % (v/v) Triton X-100

2.7 Real time qPCR experiments

In the real time experiments twofold DyNAmo SYBR Green qPCR buffer from Fermentas was used. The oligonucleotides were added to a 200 nM final concentration each. The real time program started with an initial denaturation step at 95 °C for 7 min. The 40 cycles were set up as followed: 95 °C 10 sec, 55 °C 15 sec, 72 °C 30 sec. The signal measurement took place after the elongation step (72 °C 30 sec) in each cycle. The virus DNA was prepared with Invisorb Spin Tissue Mini Kit and diluted 1:1000 in ddH_2O. As a standard, BAC DNA was used in different dilution steps. The BAC DNA was diluted in Lambda DNA (1 ng/µl).

2.8 Firefly-Luciferase and Renilla Assay

The luciferase assay method is used for reporter gene quantitation. It has a wide application range as it is also used to study environmental monitoring, virus propagation and the functionality of receptors. The effect of virus infection on the NF-κB pathway can be studied by the usage of an NF-κB response element localised upstream from the promotor of a luciferase expressing plasmid. Luciferases catalyze the oxidation of substrates upon light emission. As different luciferases with distinct substrate specificities exist, one can easily combine two different luciferases in one reaction. The following scheme represents the oxidation of D-Luciferin to oxyluciferin by the firefly luciferase.

luciferase reaction mechanism:

$$ATP + D\text{-luciferin} + O_2 \xrightarrow{\underline{luciferase}} AMP + PP_i + oxyluciferin + CO_2 + light$$

BHK and RK13 stable cell lines, harbouring pGL4.32 expressing luciferase and pCRL expressing Renilla luciferase were generated in this lab and used for the luciferase assay experiments. The pGL4.32 harbours the firefly luciferase gene under the control of an NF-κB response element. Thereby, the expression of the luciferase reporter gene is proportional to the amount of free NF-κB. Additionally, the Renilla gene is constitutively expressed in the generated cell lines and thus used to compare the experimental normalization. The assay was performed in a 24 well format. Infected cells were treated with or without 10 ng/ml TNF-α and polyinosinic:polycytidylic acid (polyIC) 4h post infection for additional 4 h. Afterwards, the medium was removed and the cells were washed twice with PBS before 200 µl lysis buffer (0.5 % (v/v) TritonX100 in PBS) was added and the plate was frozen at -70. After thawing and pipetting up and down, 25 µl of the solution was transferred to a 96 well-plate. For the measurement, 50 µl of luciferin measuring solution or 50 µl Renilla measuring solution were added. The mixture was shaken for 5 sec, before the luciferin and Renilla emission were measured for 1 sec in Tristar LB941.

rATP stock solution: 100 mM
200 mg rATP
205 ml ddH$_2$O
600 µl 1M Tris pH 8.8
store at -20 °C

1 M K$_x$PO$_4$ solutions:
solution 1: 1 M KH$_2$PO$_4$ pH 4.3
solution 2 : 1 M K$_2$HPO$_4$ pH 9.1

kaliumphosphate buffer (K$_x$PO):
10 ml solution 1
150 ml solution 2
adjust pH to 5.1 by adding solution 1 or 2

500x D-luciferin stock solution:
10.51 mg D-luciferin in 1 ml luciferin assay buffer

luciferin assay buffer (pH 8.0):
3.303 g glycylglycin
15 ml KPO$_4$-buffer pH 7.8
1.521 g EGTA
15 ml 1 M MgSO$_4$
ad 970 ml ddH$_2$O

luciferin measuring solution (10 ml):
200 µl 100 mM rATP
100 µl 0.1 M DTT
20 µl D-luciferin (500x)
ad 10 ml ddH$_2$O

Renilla assay buffer (100 ml)
6.43 g NaCL
0.082 g Na$_2$EDTA
22 ml 0.22 M K$_x$PO$_4$
ad 100 ml ddH$_2$O

colenterazin stock (500x)
1 mg colenteraizn in 3300 µl ddH$_2$O/50 % (v/v) EtOH
store at -20°C

Renilla measuring solution
add 2 µl colenterazin (500x) per ml Renilla assay buffer

3. Results

ARPs in Poxviruses are known to play a pivotal role in virus tropism and as NF-κB modulators. Due to continuously passaging procedures of MVA only two ARP encoding ORFs are left in the MVA virus genome. To study the function of those MVA ARPs, the corresponding ORFs were deleted in an MVA-BAC via *en passant* mutagenesis.

3.1 Generation of MVA *ORF186* BAC deletion mutant

For the deletion of *ORF186* in the MVA-BAC, oligonucleotides for *en passant* mutagenesis were generated as follows. The forward oligonucleotide contains sequences which match 40 bp upstream and 20 bp downstream of the MVA *ORF186*, described in part 2.2.10 (Fig. 5). Within the described sequence a 40 bp duplication which is needed for the release of the kanamycin resistance gene cassette in the resolution step is present.

The amplification of the marker cassette was realized by adding around 24 bp of the kanamycin sequence to the oligonucleotides. In more detail, the sequence of the reverse oligonucleotide starts with 23 bp matching to the kanamycin resistance gene cassette, in the 60 bp afterwards, the first 20 bp anneal perfectly to the area upstream of the MVA *ORF186*. The remaining 40 bp anneal downstream of *ORF 186*. Those oligonucleotides were used for the amplification of the *aphAI*-I-SceI cassette from pEPkan-S. The generated PCR product was used in the procedure described in part (2.2.10). The correctness of the generated deletion mutant, termed pMd, was verified by restriction fragment length polymorphism (RFLP).

3.2 Generation of MVA *ORF171* BAC deletion mutant

Apart from published annotations of the genome sequence, we identified one additional potential ARP encoding ORF at position 171 in MVA. The *ORF171* was deleted in the same manner as described for *ORF186* in the parental BAC and also in pMd. The resulting BACs were termed pMd171 and pMdd, for the double deletion mutant. The pMdd does not harbour any ARP encoding sequences which could lead to the expression of a functional protein. Therefore, virus reconstitution of pMdd led to a complete ARP free virus. A typical BAC DNA restriction pattern upon cleavage with PvuI is shown in Fig. 6.
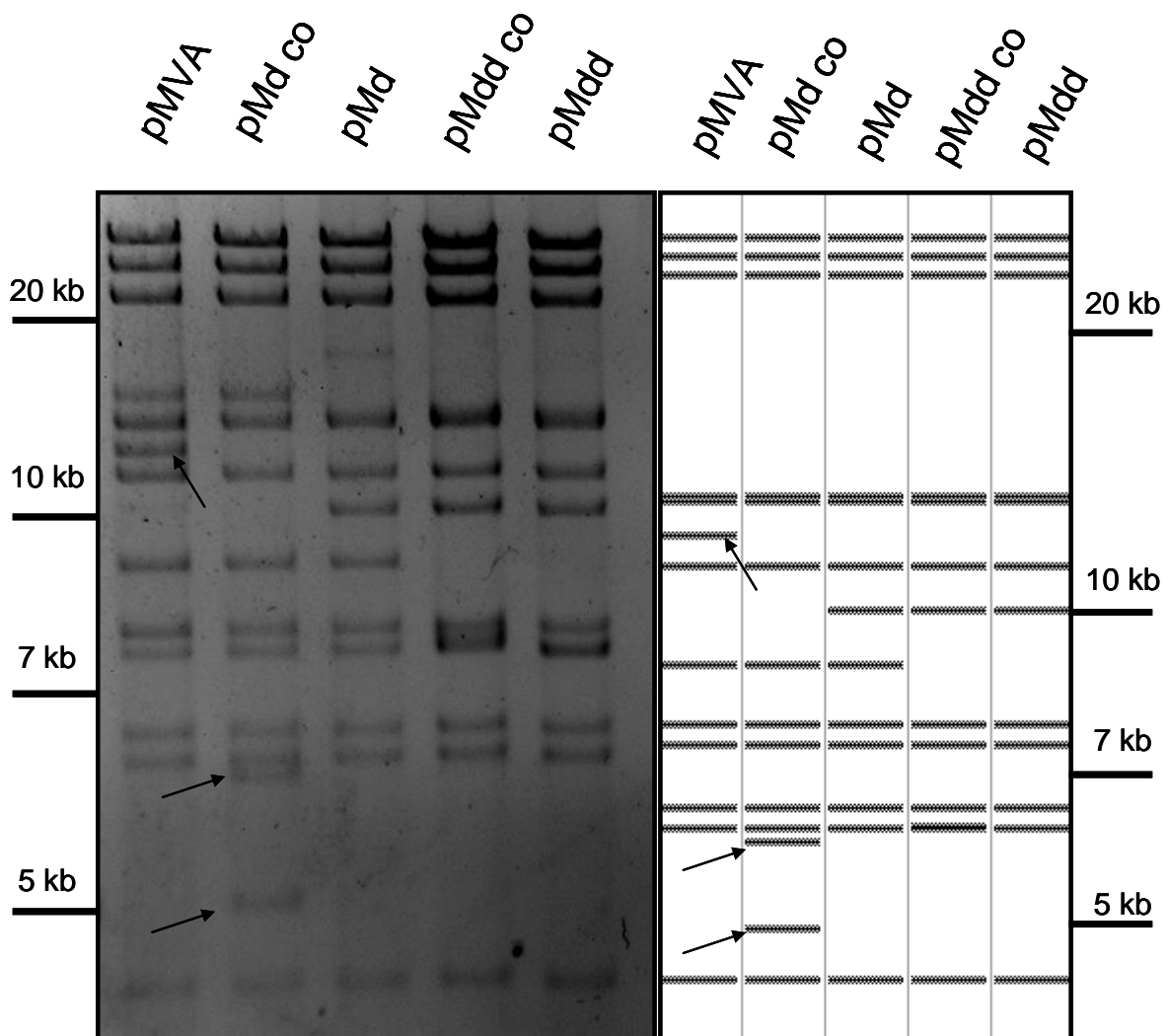
Fig. 6: RFLP of BAC DNA. BAC DNA of pMVA, pMd co, pMd, pMdd co and pMdd was prepared and cleaved with PvuI. The predicted patterns are shown on the right. Arrows indicate shifted bands during the process of BAC mutant generation. 'Co' indicates the intermediate constructs in *en passant* mutagenesis termed co-integrates.

After virus reconstitution (see 2.5.1) the deletion was verified by sequencing of the mutated area and also by cleavage of virus genomic DNA (Fig. 7). Furthermore, the virus stocks were passaged on CEF cells until no more helpervirus DNA was detectable by PCR. As mentioned above, the reconstituted viruses express GFP under a late 4b fowlpox promoter. This is a convenient tool to determine virus titers and follow late gene expression in several different cell lines.
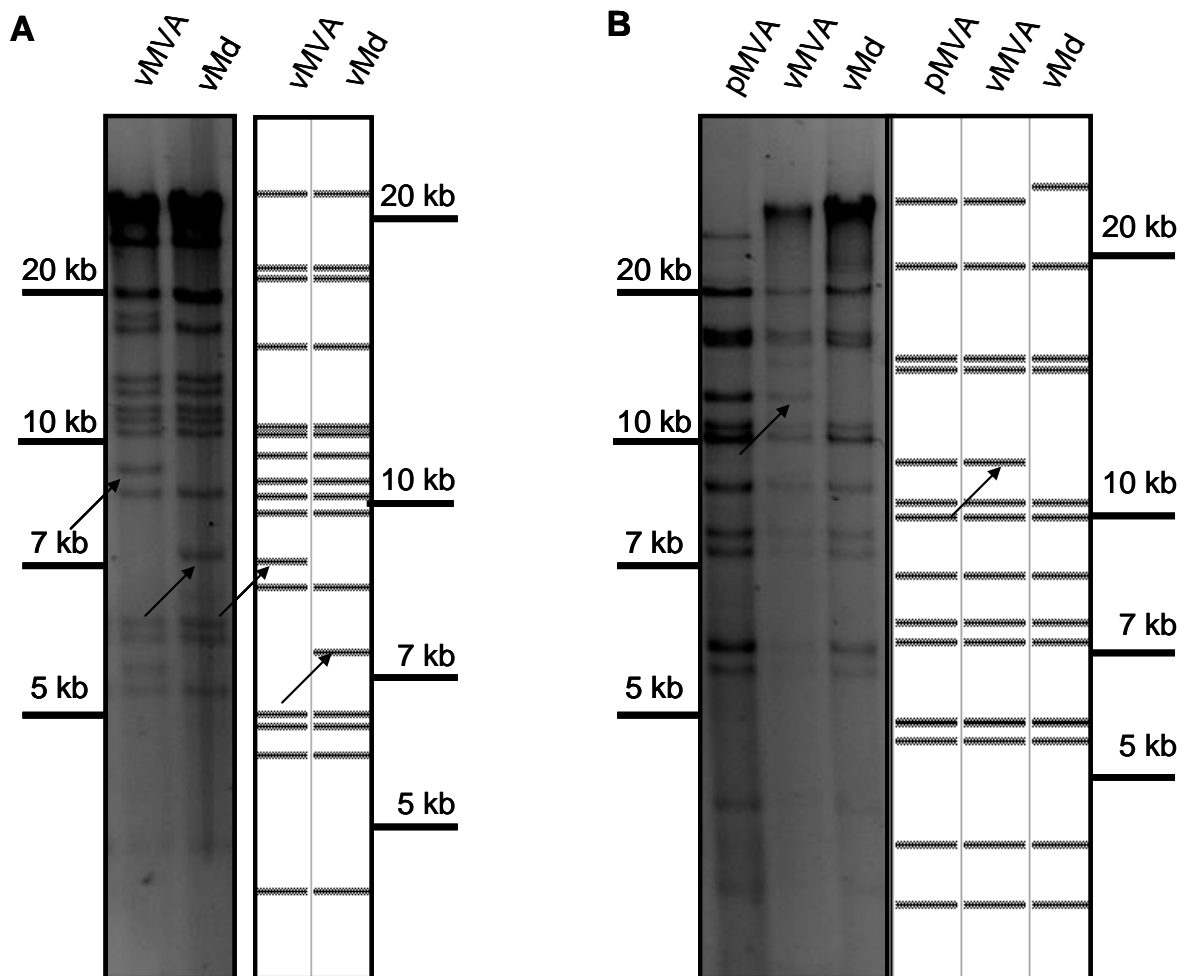
Fig. 7: RFLP of BAC and virus DNA with two different enzymes. BAC DNA (pMVA) and virus DNA (vMVA, vMd) were isolated and cleaved with NruI (A) and MluI (B). Arrows indicate shifted bands in the process of BAC generation. Prediction of banding patterns is given on the right.

3.3 Characterization of vMd and vMdd

3.3.1 Multiple-step growth analysis

The replication efficiency is one of the main critical parts for a virus to maintain the ability of spreading and therefore ongoing infection. To compare the replication abilities of the parental vMVA and deletion mutants vMd and vMdd, multiple-step growth analyses were performed. BHK cell monolayers were infected at an MOI of 0.01 and at indicated points of time supernatants and cells were harvested separately. The determined virus titers were similar for vMVA, vMd and vMdd in the supernatant and were also comparable in infected cells (Fig. 8).
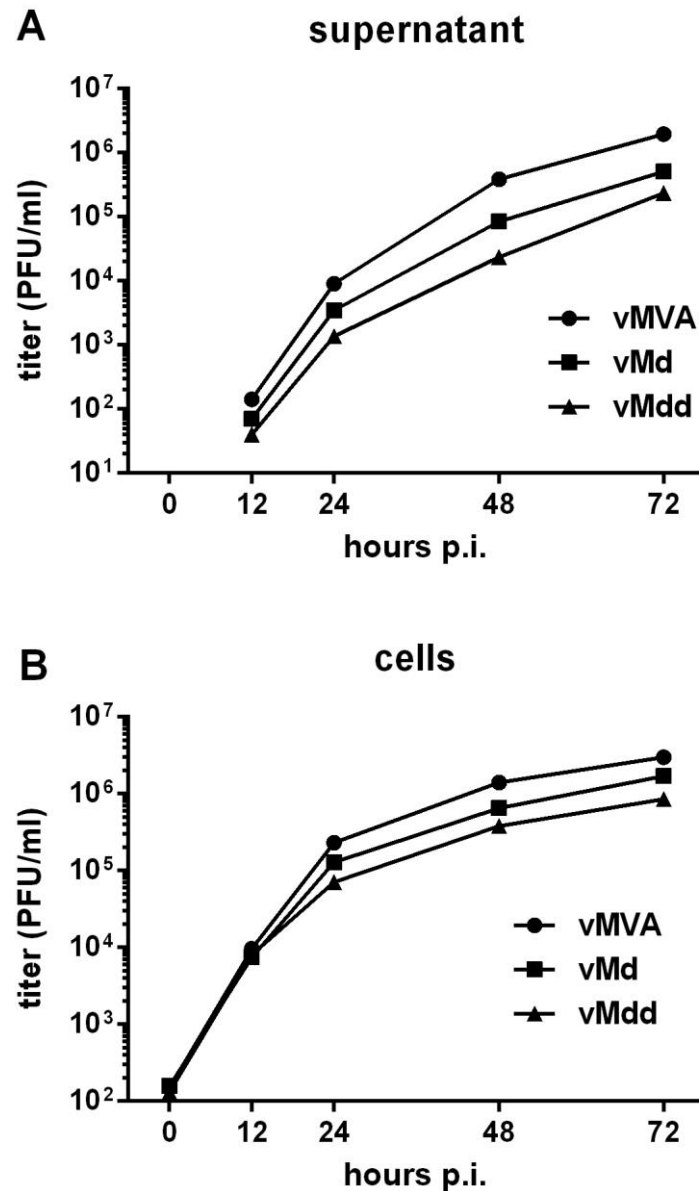
Fig. 8: Virus growth analyses of vMVA, vMd and vMdd in BHK cells. Cells were infected with an MOI of 0.01 for multiple-step kinetics. Virus from supernatant (A) and infected cells (B) was titrated independently. Growth curves are representative of two independent experiments with double titrations.

Therefore, it could be shown that the deletion mutants, however, with tendencies to slower replication, replicate with comparative efficiencies to each other and to the parental vMVA in BHK cells.

3.3.2 Early virus protein expression in BHK and HaCaT cells

In poxviruses protein expression takes place in a cascade dependent manner. The early protein expression starts almost directly after infection followed by intermediate and late protein expression. To characterize the virus protein expression at early states of infection, permissive BHK and non-permissive HaCaT cells were infected with vMVA, vMd and vMdd at an MOI of 0.3. Whole cell lysates were prepared 4 h post infection. The expression of the early expressed virus protein E3L after 4h of infection in BHK and HaCaT cells is shown in (Fig. 9).
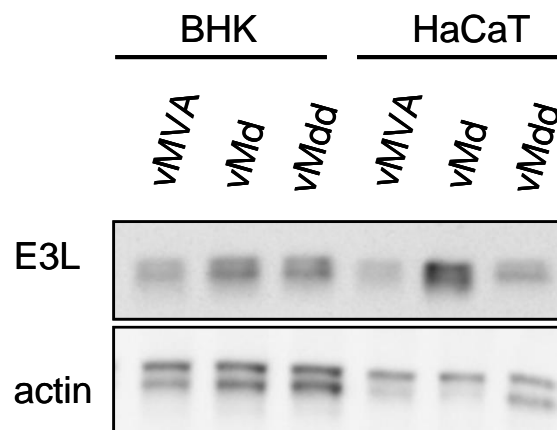
Fig. 9: Comparison of E3L protein levels in BHK and HaCaT cells. BHK cells and HaCaT cells were infected with vMVA, vMd and vMdd at an MOI of 0.3. Whole cell lysates were prepared 4 h post infection. After protein separation by SDS-PAGE and transfer to nitrocellulose membrane E3L (early expressed virus protein) and actin were detected.

The expression level of E3L in BHK and HaCaT cells infected with vMVA, vMd and vMdd is comparable between the distinct viruses. This indicates that the onset of virus replication is not affected in the mutant viruses in comparison to the parental vMVA.

3.3.3 Late virus protein expression in BHK and HaCaT cells

The early virus protein expression does not seem to be affected by the deletion of ARP encoding ORFs in MVA. Consequently, the late protein expression was analyzed to figure out if the gene deletion may have an impact in later stages of infection. For this purpose, BHK and HaCaT cell monolayers were infected with vMVA, vMd and vMdd at an MOI of 0.3 for 24h, before whole cell lysates were prepared. The expression levels of the late virus protein L1R in BHK (A) and HaCaT (B) cells are shown in (Fig. 10).
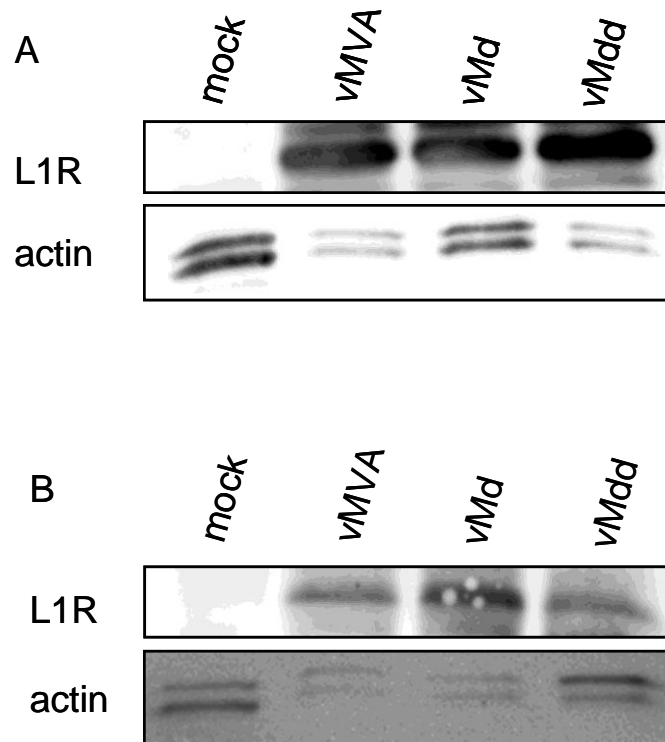
Fig. 10: Comparison of L1R protein levels in infected BHK and HaCaT cells. BHK cells (A) and HaCaT cells (B) were infected with vMVA, vMd and vMdd at an MOI of 0.3. Whole cell lysates were prepared 24 h post infection. After protein separation by SDS-PAGE and transfer to nitrocellulose membrane L1R (late virus protein) and actin were detected.

The amount of L1R protein does not differ between the various virus mutants in BHK cells as well as in HaCaT cells. This result is in contrast to Sperling et al.(Sperling et al., 2009). They published that a MVA-Δ68k-ank virus mutant, which corresponds genetically to vMd, shows decreased late virus protein expression in NIH and HaCaT cells (Sperling et al., 2009).

3.3.4 Early and late virus protein expression in NIH cells

To verify the contrasting result found in HaCaT cells, another non-permissive cell line was also tested for late as well as early protein expression. Non-permissive NIH cells were infected with vMVA, vMd and vMdd at an MOI of 0.3. For early E3L virus protein expression whole cell lysates were prepared 2 and 4 h post infection. The lysates for late L1R virus protein expression were prepared 6 and 24 h post infection. E3L and L1R protein levels were detected by western blotting (Fig. 11).
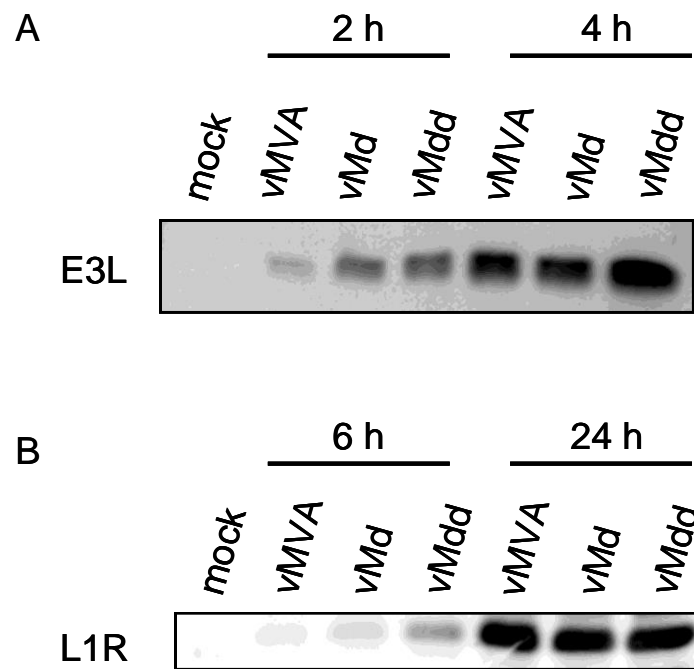
Fig. 11: Comparison of E3L and L1R protein levels in NIH cells. NIH cells were infected with vMVA, vMd and vMdd with a MOI of 0.3. Whole cell lysates were prepared 2, 4, 6 and 24 h post infection. After protein separation by SDS-PAGE and transfer to nitrocellulose membrane E3L (early virus protein) and L1R (late virus protein) were detected.

At 2 h after virus infection with vMVA, vMd and vMdd comparable protein amounts of E3L were detectable in NIH cells. At 4 h after infection the E3L protein amounts were indistinguishable between the parental and the single and double knockout mutants. As expected the protein amount in total was higher in comparison to the level at 2 h. The detection of late protein L1R was faintly at 6 h, in comparison to the strong detection at 24 h. Nevertheless, the expressed proteins in vMVA, vMd and vMdd infected NIH cells were comparable to each other. This result concerning the late protein expression is again in contrast to the published data form Sperling et al. (Sperling et al., 2009).

3.3.5 Determination of plaques areas on BHK cells

The measurement of plaque sizes gives information about the ability of a virus to spread from cell-to-cell. For a plaque size assay, monolayers of BHK cells were infected with 100 PFU for 1 h before cells were overlayed with methocel. Fluorescence pictures of plaques were taken at 48 h post infection and plaque sizes were determined by imageJ software. Diameters were calculated by taking the square root of absolute plaque area values. Relative plaque diameters were defined to parental normalized plaque diameter. Statistical analysis

was done by one-way ANOVA. It could be shown that infection with both vMd and vMdd lead to significantly reduced plaque sizes in BHK cells (Fig. 12).
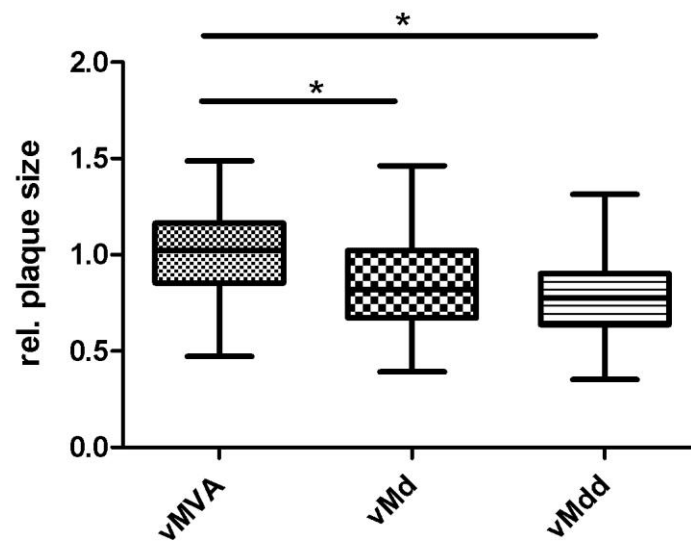

Fig. 12: Comparative plaque size analysis of vMVA, vMd and vMdd on BHK cells. Cells were infected with 100 PFU of parental and mutant viruses. Bars show data from two independent experiments with 50 pictures of each virus infection. Statistical analysis was by done one-way ANOVA. A probability P value of less than 0.05 was considered significant. Asterisks mark significant differences.

In comparison to the parental vMVA, vMd and vMdd produced significant smaller plaques. Considering that vMd is the parental virus of vMdd and between those two mutants no significant differences could be determined, it could be concluded that the effect is mainly due to the deletion of *ORF186* in MVA.

3.4 Macroscopic description of infected CAMs

Poxvirus proteins are known for the ability to modify pock morphology on infected CAMs. Consequently, it was analyzed whether the deletion of ARPs in MVA leads to a modification in pock formation on CAMs. To answer this question, the generated deletions mutants were used for the inoculation of 11 days old embryonated chicken eggs. The CAMs were infected with 25 PFU on day 11 and harvested 5 days post infection. The macroscopical investigation of CAMs infected with vMVA, vMd and vMdd showed pock formation to varying extents (Fig. 13). The parental vMVA developed one prominent pock (d) and a number of smaller secondary pocks (g). The prominent pock showed strong cell proliferation up to 7 mm in height. In contrast vMd and vMdd revealed only a number of smaller pocks (e, f) which were

comparable in size to the secondary pocks of vMVA. The characteristic pock development could also be confirmed in inoculation experiments with 10 PFU (data not shown).
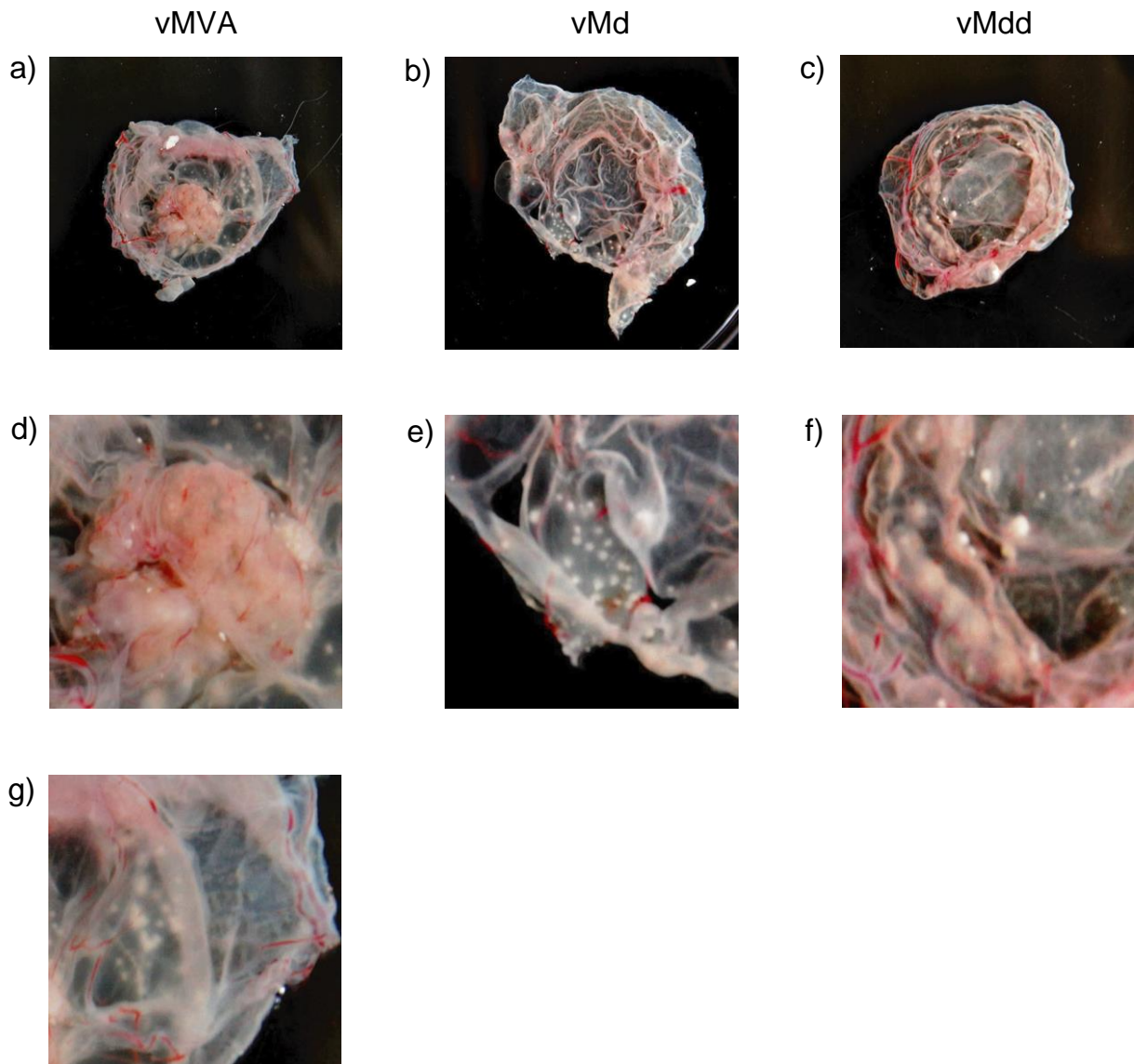
vMVA	vMd	vMdd

Fig. 13. Macroscopic comparison of pock phenotype on CAMs infected with vMVA, vMd and vMdd. The CAMs were infected with 25 PFU and harvested 5 days post infection. The PFU in the inocula were confirmed by back titration.

3.5 Generation of the transfer plasmid pEPtrans

Conversely to others, it was shown in this study that the deletion of ARPs in MVA did not have a strong impact in alternation of viral protein expression. Nevertheless, effects in plaque size and pock formation were observed. This led to the hypothesis that the insertion of single CPXV ARPs in an otherwise complete free ARP virus background may result in modified plaque sizes, pock formation and host range in general. To test this hypothesis a transfer plasmid had to be constructed for the insertion of the CPXV ARP coding sequences into the

ankyrin deletion mutants, pMd and pMdd. This plasmid should be used for the introduction of CPXV ARPs via *en passant* mutagenesis in the ARP deletion mutants. The pMd mutant served as PCR template for the amplification of flanking regions starting 249 bp upstream (flank A) and terminating 269 bp downstream (flank B) of the formerly deleted *ORF186*. The flanks were amplified by PCR (oligonucleotides #203 and #204, see 2.1.10) and subcloned into TOPO pcDNA3.1 for sequencing purposes. The cleavage sites SpeI and XhoI were added to the PCR product. Using those cleavage sites the flanks should be placed between the two inverse I-CeuI recognition sites of pCeu2 (Tischer et al., 2007), which served as backbone. The I-CeuI sites are used for the release of the entire starting fragment for *en passant* mutagenesis. Unfortunately, the insertion of this fragment into the compatible cleavage sites in pCeu2 was reproducibly unsuccessful. Therefore, the entire pCeu2 vector was amplified by oligonucleotides #329 and #330 (see 2.1.10) to exchange the XbaI site into SpeI cleavage site (Fig. 14a). This vector was termed pCeu3. Thereafter, the flanks (PCR 186del, green) were inserted (Fig. 14b) in pCeu3 resulting in pCeu3-flank.
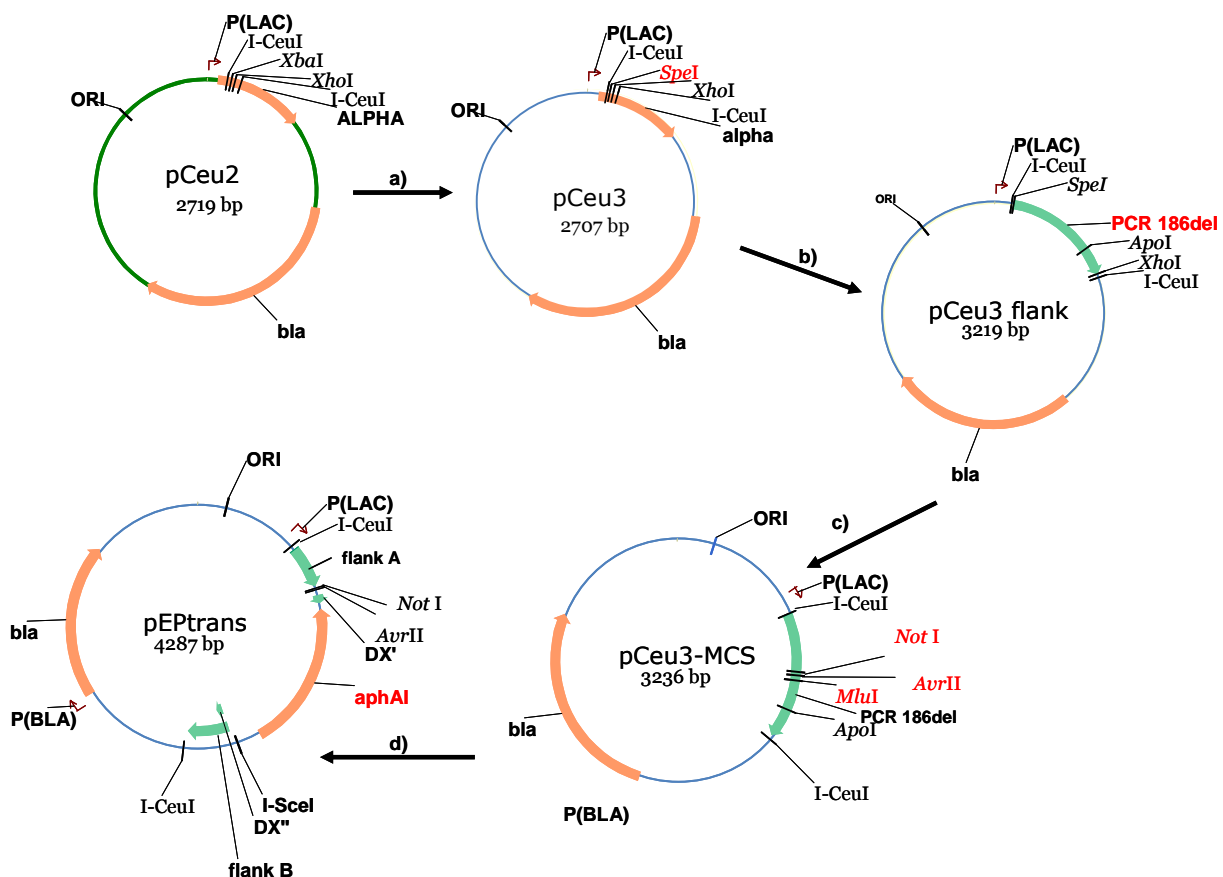

Fig. 14: Schematical transferplasmid cloning procedure.

To add NotI and AvrII recognition sites, which were needed for the insertion of the CPXV ARP coding sequences, together with a MluI recognition site, for insertion of the kanamycin resistance gene sequence (*aphAI*), an inverse (Fig. 14c) PCR with oligonucleotides #205 and #206 (see 2.1.10) was performed. In addition, *Avr*II was used for re-ligation of the linear

PCR fragment resulting in pCeu3-MCS. In the final cloning step, the *aph*A*I* sequence with adjoining 50 bp duplication and a I-SceI recognition site was introduced via *Apo*I and *Mlu*I into pCeu3-MCS (Fig. 13d). For that purpose, the kanamycin resistance gene of pEPkanS was amplified with oligonucleotides #207 and #208 (see 2.1.10) (not shown). The introduced duplicate sequences are needed for the resolution of co-integrates in the second step of *en passant* mutagenesis. The final transfer plasmid was termed pEPtrans. After insertion of respective ARP coding sequences using NotI and AvrII sites the plasmids were termed respectively to the chosen ORF. The pEPtrans-BR006 for example contains the coding sequence for BR006.

3.6 Generation of knock-in mutants

The question arose if single CPXV ARPs may have an effect on virus behaviour. To answer this question, CPXV ARPs should be introduced in the ARP deletion MVA mutants pMd and pMdd. The knock-in mutants were generated using construct pEPtrans as backbone for insertion of desired CPXV ARP coding sequences, which were first amplified by PCR from pBRf. The pBRf harbours the genome of the CPXV isolate Brighton Red (BR). The amplification product was extended with a NotI restriction site upstream and an AvrII site downstream of the respective ORF. Additionally, a Flag-tag sequence was placed directly after the start codon. Those amplicates were inserted into TOPO-TA or TOPO pCRII, sequenced and cloned into pEPtrans via the NotI and AvrII sites. For *en passant* mutagenesis, the pEPtrans vector harbouring the CPXV ARP coding sequence was cleaved with I-CeuI. Released fragments were gel purified and used for *en passant* mutagenesis. Derived co-integrates were confirmed by RFLP before going on with the second step, the resolution. Loss of kanamycin resistance marker was also confirmed by RFLP. The newly generated mutant BAC clones (Table1) were used for virus reconstitution on BHK cells (see 3.5.1). The appropriate viruses express GFP under the late 4b fowlpox promoter. Loss of helpervirus was carried out by transferring derived virus mutants to CEF cells. After three passages on CEF cells, presence of RFV was monitored by PCR. If necessary the passaging was continued until produced virus stocks were free from any detectable RFV genome sequences. DNA of newly generated virus mutants was prepared and integrity of virus genomes and mutant loci was confirmed by RFLP. Additionally, the altered sequence regions were analyzed by sequencing. For this, the regions of interest were amplified by PCR from the virus DNA and sent for sequencing.

The inserted ORFs were chosen regarding to their homologous relation and published data. Phylogenetic analyses of CPXV ARPs showed that some of them group and some do not.

Especially, CPXV-BR041, the homolog of the known VACV host range factor K1L does not belong to any group.

As an example for the generated mutants the RFLP of pMdd-BR041 is shown in Fig. 15. BAC DNA was prepared and cleaved with PvuI.
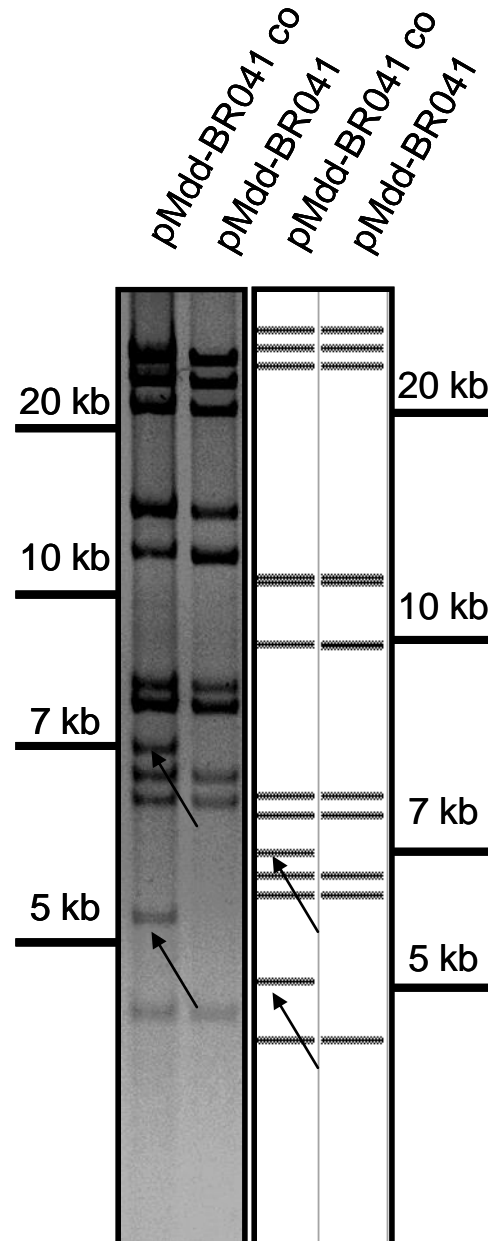

Fig. 15: RFLP of pMdd-BR041. PMdd-BR041 co and pMdd-BR041 BAC DNA was prepared and cleaved with PvuI. Theoretical banding patterns are shown on the right. Arrows indicate shifted bands during the process of BAC mutant generation. Co indicates the intermediate construct in the process of mutant generation via *en passant* mutagenesis.

The other known ARPs can be subdivided in four groups. At least one ORF of each group was chosen virus knock-in generation. Group A consists of BR008, BR017, BR025 and BR027. For BR025 a host range function on CHO cells was published (Spehner et al., 1988). BR027 is phylogenetically close to BR025. Therefore, this ORF was chosen from this group. Group B consists of BR006, BR211 and BR220. For BR006 an influence on the NF-κB

pathway was published (Mohamed et al., 2009b). Consequently, this ORF was chosen. Group C consists of two members only and nothing is known about their function in other poxviruses. Hence, both ORFs were chosen for the insertion into MVA double deletion mutant vMdd. Group D consists also of two members BR011 and BR213. Here BR213 was taken, because it has more known homologs in other poxviruses. Additionally, it is phylogenetically closer to VARV and *camelpox virus* (CMLV) which posses a narrow host range in comparison to other poxviruses. An overview of generated BAC knock-in mutants is given in Table 1.

	pMd	pMdd
BR006	-	+
BR016	-	+
BR019	-	+
BR027	+	+
BR041	+	+
BR213	+	+

Table 1: Overview of generated knock-in mutants. + indicates ARP ORF insertion, where – indicates no insertion in parental ARP deletion mutants.

For the revertant of pMd-BR041 termed pMd-BR041-rev the "empty" transferplasmid pEPtrans was used. The procedure for virus revertant generation was the same as for the knock-in mutants. Generation of pMd-BR041 and pMd-BR041-rev is shown in Fig. 16.
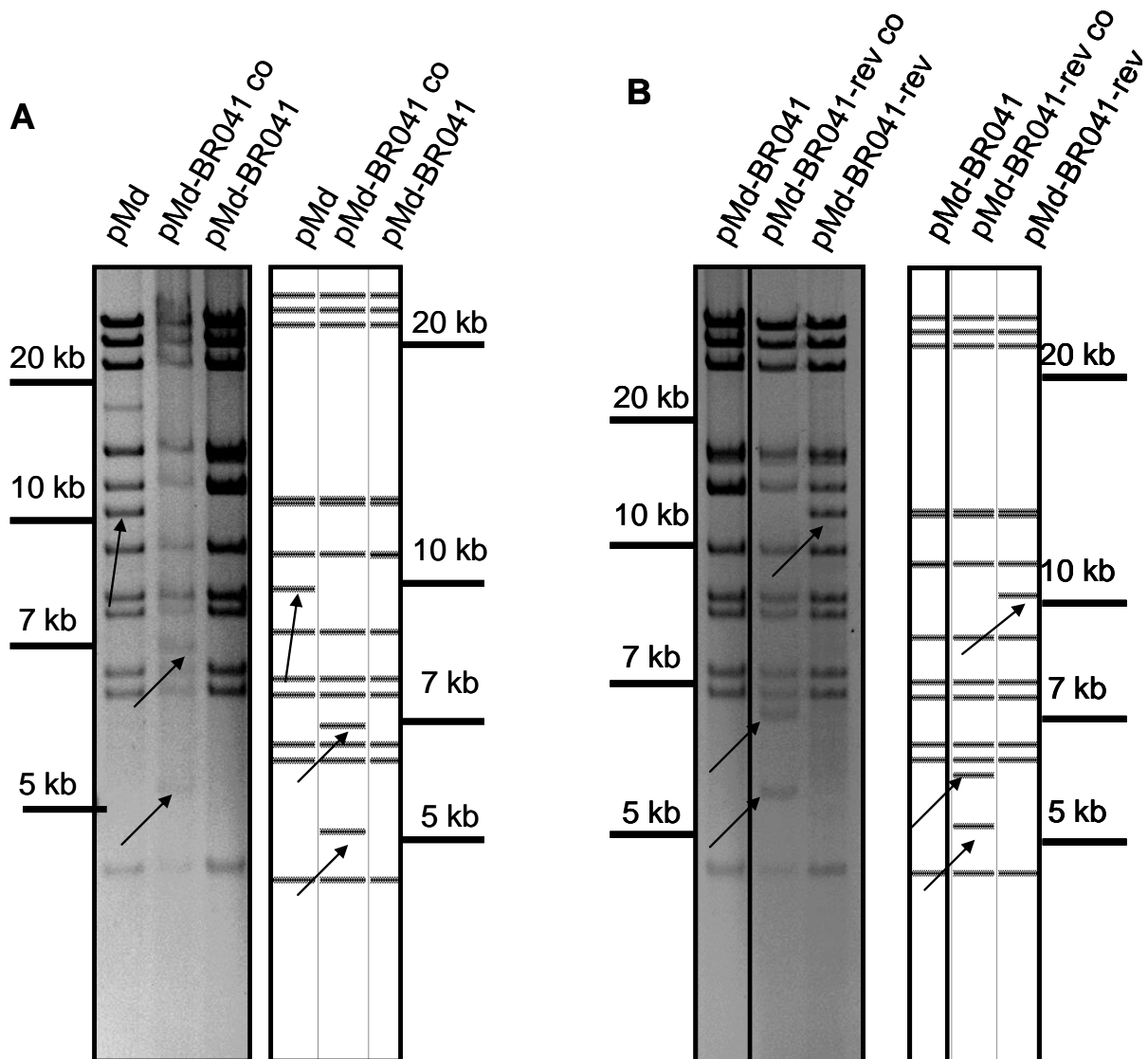
Fig. 16: RFLP of pMd-BR041 and pMd-BR041-rev. BAC DNA of pMd, pMd-BR041 co and pMd-BR041 (A) was prepared and cleaved with PvuI. For generation of revertants pMd-BR041, pMd-BR041-rev co and pMd-BR041-rev were prepared and digested with PvuI (B). Co indicates the intermediate step during the process of BAC mutant generation. Theoretical restriction banding patterns are shown on the right.

3.7 Host range determination

To investigate the host range functionality of single CPXV ARPs, distinct cell lines were infected with different reconstituted GFP expressing knock-in virus mutants at an MOI of 0.1. After virus adsorption for 1 h, cells were washed twice with PBS and 1 ml fresh medium was added before cells were incubated for 48 h before harvest. Virus titer determination for each cell line was performed. Virus multiplication (fold increase in virus titer) was determined as ratio by dividing determined virus titer at 48 h and back titrated input titer. Titers were

determined on BHK cells. Cell lines with virus growth ratio below 1 were defined as non-permissive, while a ratio of 1 to 25 was defined as semi-permissive and a replication of more than 25-fold corresponds to a fully-permissive cell line (Carroll and Moss, 1997). Seven cell lines (CRFK, MDBK, HaCaT, A549, NIH 3T3, HeLa, CHO) could be categorized as non-permissive for infections with MVA mutants, similar to vMVA (Fig. 17). Three more cell lines (Nie168, NRB, Ken-R) could be newly defined as non-permissive for infections with vMVA and derivative MVA mutants. RK13 cells were non-permissive for mutant MVA with the exception of vMd-BR-041 and vMdd-BR-041. For both vMd-BR-041 and vMdd-BR-041, RK13 cells were determined as fully-permissive with a virus multiplication ratio greater than 25. The VACV homolog of BR041 (K1L) is known as host range factor for RK13 cells.
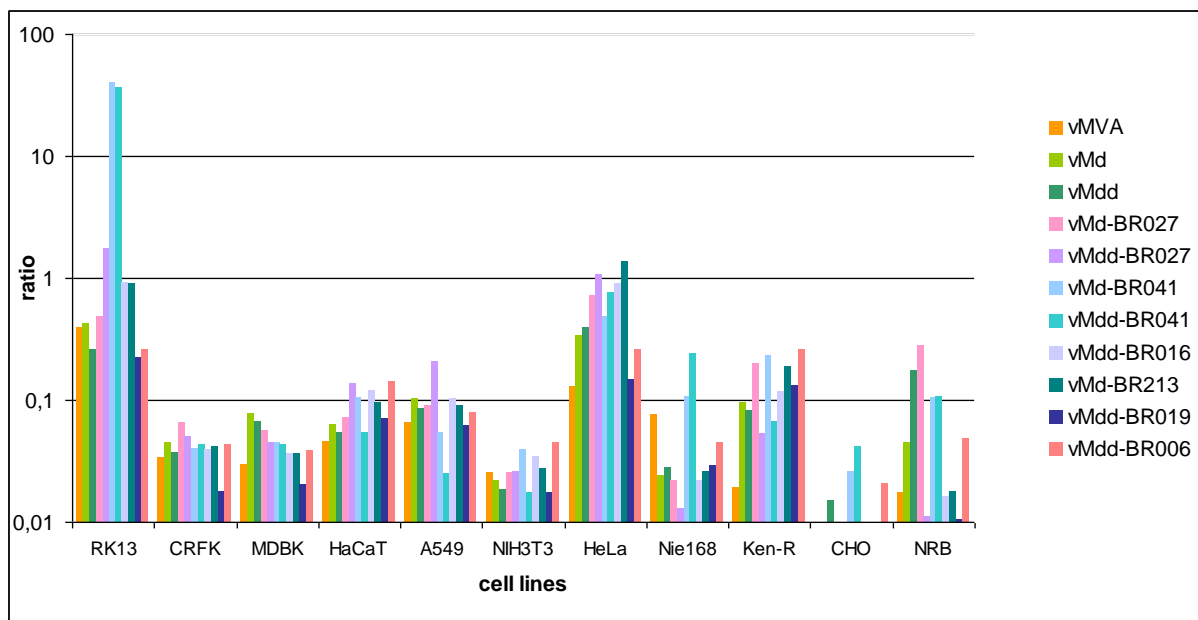

Fig. 17: MVA mutant virus replication in different cell lines. Cells were infected with vMVA, VMd, vMdd, vMd-BR027, vMdd-BR027, vMd-BR041, vMdd-BR041, vMdd-BR016, vMd-BR213, vMdd-BR019 and vMdd-BR006 at an MOI of 0.1. Cells were harvested 48 h post infection and virus was titrated on BHK cells in duplicate. Ratios were calculated by dividing output titer at 48 h by backtitrated input titer.

The cell lines BHK, DF-1 and CEF could be confirmed as permissive (Fig. 18).
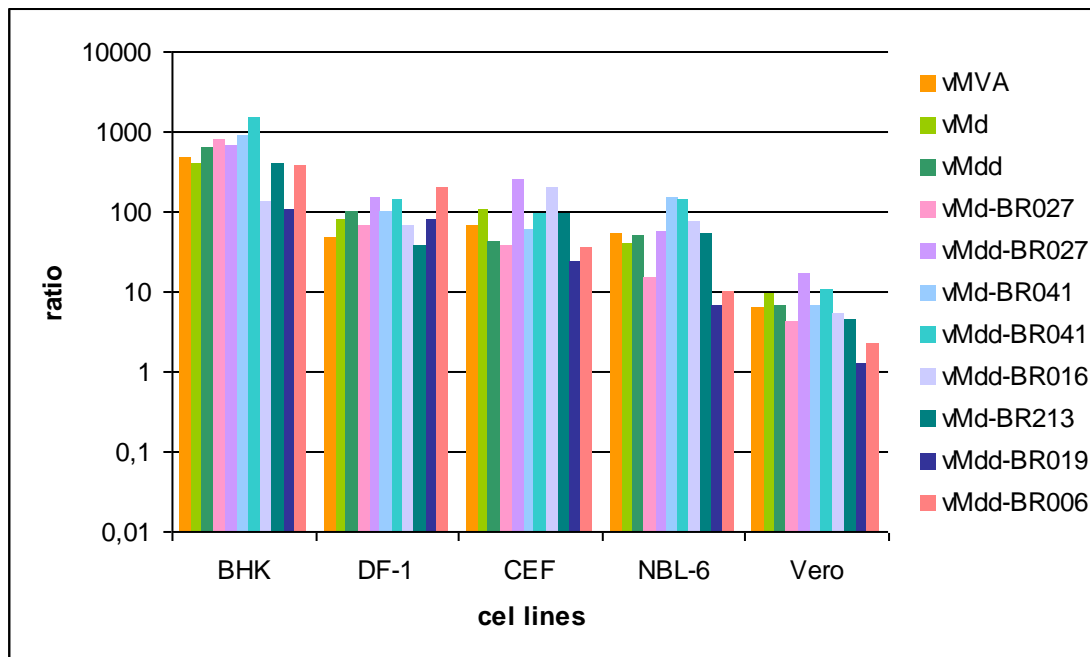
Fig. 18: Virus replication in BHK, DF-1, CEF, NBL-6 and Vero cells. Cells were infected with vMVA, vMd, vMdd, vMd-BR027, vMdd-BR027, vMd-BR041, vMdd-BR041, vMdd-BR016, vMd-BR213, vMdd-BR019 and vMdd-BR006 at an MOI of 0.1. Virus progeny was harvested 48 h post infection and titrated on BHK cells in duplicate. Ratios were calculated by dividing output titer at 48 h by input titers.

Furthermore, the equine cell line NBL-6 could newly be classified as permissive for recombinant derived MVA infections. Nevertheless, vMd-BR027, vMdd-BR019 and vMdd-BR006 reached only virus replication ratios determined as semi-permissive. Although, DF-1, CEF and NBL-6 cells did not reach the same values of virus multiplication compared to BHK cells, they fulfilled the requirement for permissive with replication ratios higher than 25. Replication abilities of different mutant MVA were comparable within the same cell line. Vero cells were confirmed as semi-permissive for vMVA, but none of the MVA mutants led to an enhanced virus multiplication as they all showed replication efficiencies comparable to vMVA. Summarized, NBL-6 cells could be determined as permissive for recombinant MVA. On RK13 cells both vMd-BR041 and vMdd-BR041 showed full replication capabilities and BR041 could be identified as host range factor for this cell line. Three cell lines (Nie168, Ken-R, NRB) were newly identified as non-permissive for MVA. Except for RK13 cells, all ankyrin knock-in mutants showed replication efficiencies comparable to parental vMVA in the entire set of tested cell lines. This result was independent from the state of permissiveness.

3.8 Determination of vMd and vMdd knock-in mutant plaques areas on BHK cells

As measurement of plaque sizes can show an enhanced or delayed ability of virus replication, all generated knock-in mutants were analyzed for cell-to-cell spread on BHK cells. Although, the deletion mutants vMd and vMdd showed replication abilities comparable to the parental vMVA in growth kinetics, they developed significant smaller plaque areas. Consequently, plaques areas from knock-in mutants were compared to appropriate parental virus. One-way ANOVA was used to assess significant differences in plaque size. For knock-in mutants based on vMd significant differences could not be determined. The insertion of BR027, BR041 and BR213 in vMd does not affect the development of plaque areas (Fig. 19).
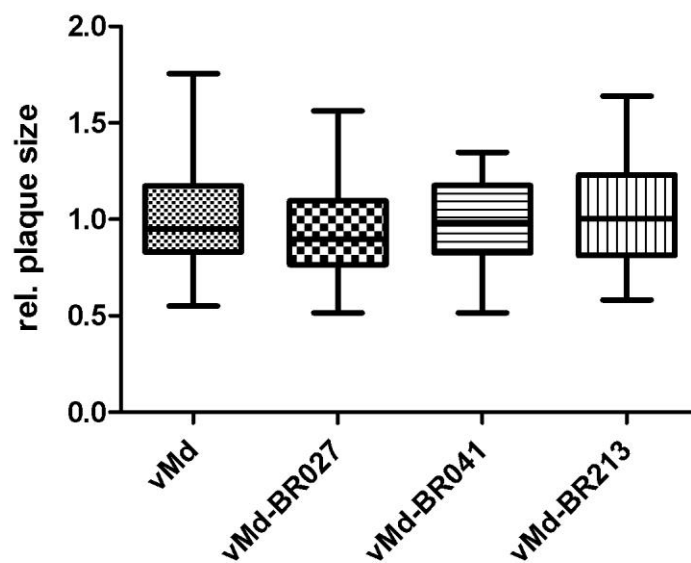

Fig. 19: Comparative plaque size analyses of vMd, vMd-BR027, vMd-BR041 and vMd-BR213 on BHK cells. Cells were infected with 100 PFU of the indicated virus and overlayed with methocel 1 h post infection. Bars show data from one experiment with 50 pictures of each mutant. Data were normally distributed and statistical analysis was performed with one-way ANOVA. A probability P value of less than 0.05 was considered significant. Differences were not statistically significant.

For knock-in mutants based on vMdd the plaque size characterization was performed in the same way (Fig. 20). The Kruskal-Wallis-test was used to evaluate significant differences.
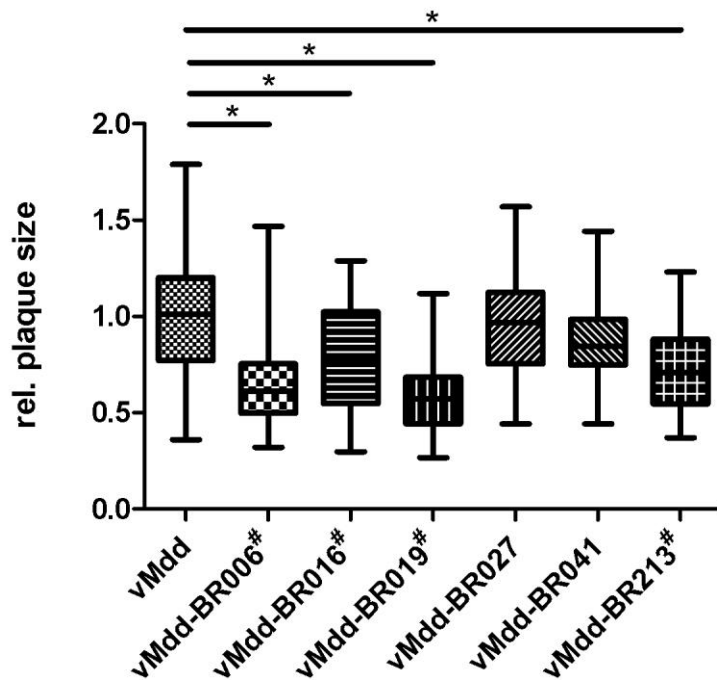

Fig. 20: Comparative plaque size analysis of vMdd, vMdd-BR006, vMdd-BR016, vMdd-BR019, vMdd-BR027, vMdd-BR041 and vMdd-BR213 on BHK cells. Data from at least two independent experiments with 50 pictures of each mutant are shown. Statistical analysis was done by one-way Kruskal-Wallis-test. P < 0.05 was considered to indicate statistically significant differences, which were marked by asterisks. # indicates not normally distributed data.

For vMdd-BR006, vMdd-BR016, vMdd-BR019 and vMdd-BR213 a significant reduction in plaque size area was shown. In contrast a significant influence by insertion of BR027 and BR041 could not be determined. In summary, the insertions of BR006, BR016, BR019 and BR213 in vMdd seem to influence the development of plaque areas on BHK cells, whereas the insertion of BR027 and BR041 in vMd or vMdd does not, as well as the insertion of BR213 in vMd.

3.9 Histologic characterization of infected CAMs

Smaller pock formation on CAMs was shown for vMd and vMdd. Additionally, to this macroscopic observation, a selection of different virus infected CAMs was histologically examined. It should be investigated whether the deletion or insertion of ARPs causes modifications in the cellular composition. For this purpose, CAMs from 16 days old sacrificed embryonated chicken eggs were prepared on day 5 post infection with the indicated viruses (Fig. 21). After removal of the egg shell the CAMs were washed three times in PBS 10 min

each and fixed in 4 % buffered formalin. For histopathological analysis the tissue was embedded in paraffin and prepared sections were stained with hematoxylin-eosin (Fig. 21).

a) mock infected
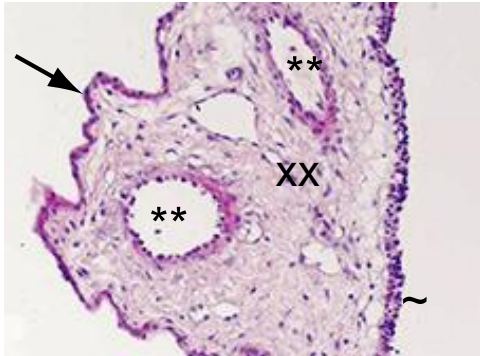
chorion membrane ➝
mesenchyme (xx)
blood vessel (**)
allantoic membrane (~)

b) non-recombinant MVA
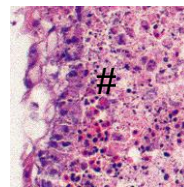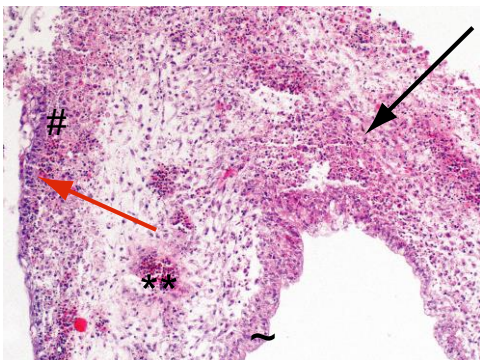
infiltration (black arrow)
epithelial proliferation (red arrow)
blood vessel (**), necrosis (#)
broadened allantoic membrane (~)

c) vMVA
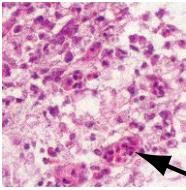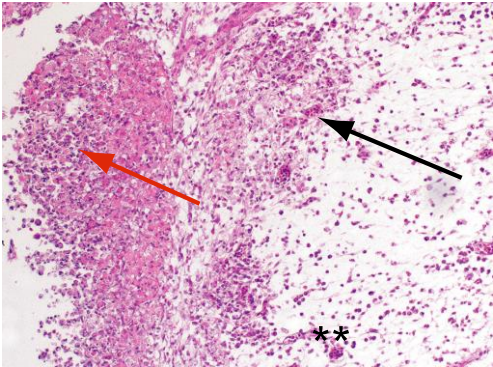
infiltration (black arrow)
epithelial proliferation (red arrow)
blood vessel (**)

d) vMd
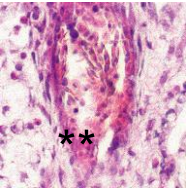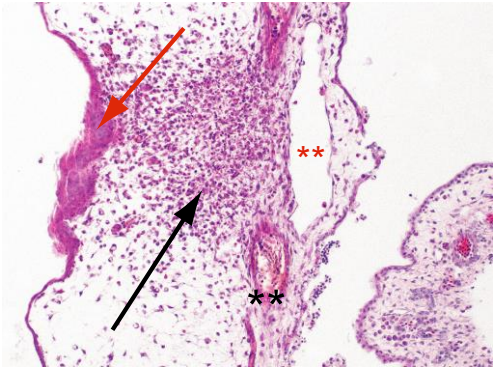
infiltration (black arrow)
lymph vessel (**)
epithelial proliferation (red arrow)
blood vessel (**)

e) vMdd
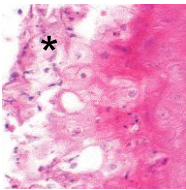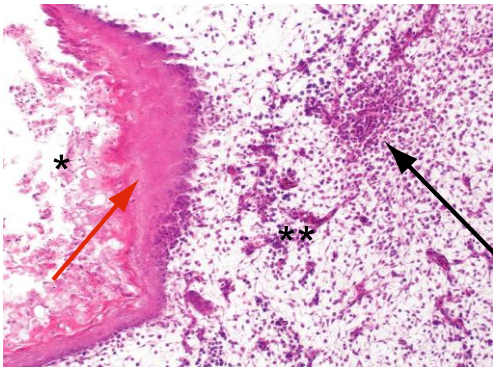
infiltration (black arrow)
epithelial proliferation (red arrow)
blood vessel (**)
balloon cells (*)

f) vMd171
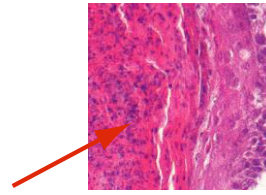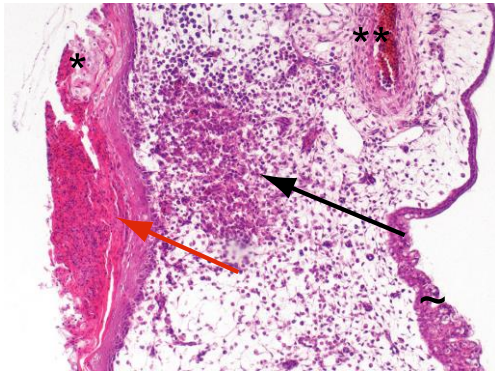
infiltration (black arrow)
epithelial proliferation and superficial
hyperkeratosis (red arrow)
blood vessel (**), balloon cells (*)
broadened allantoic membrane(~)

g) vMd-BR041
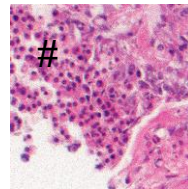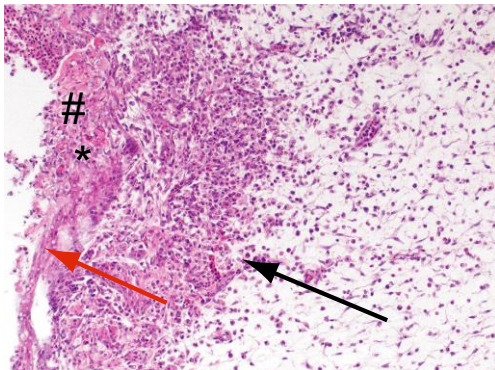
infiltration (black arrow)
epithelial proliferation (red arrow)
necrosis (#)
balloon cells (*)

h) vMd-BR027
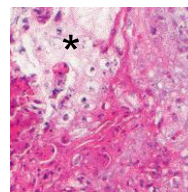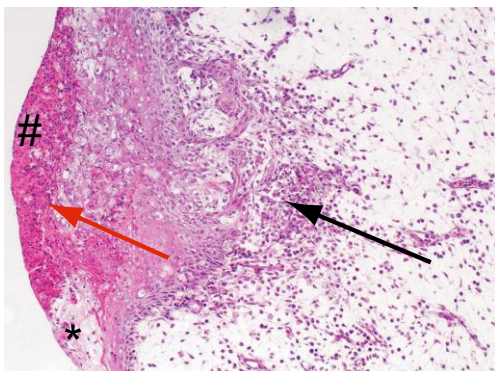

infiltration (black arrow)
epithelial proliferation (red arrow)
necrosis (#)
balloon cells (*)

i) vMdd-BR006
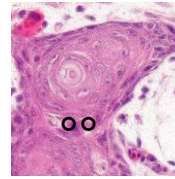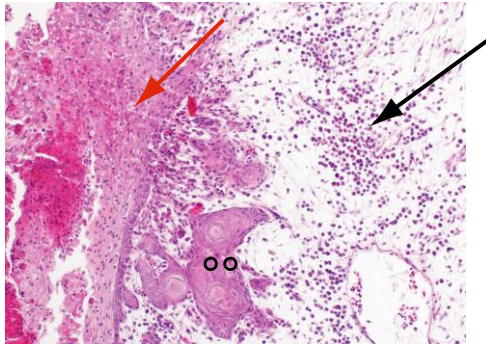
infiltration (black arrow)
epithelial proliferation (red arrow)
cornification (°°)

Fig. 21: Hematoxylin-eosin stained histological sections of CAMs infected with non-recombinant MVA, vMVA, vMd, vMdd, vMd171, vMd-BR041, vMd-BR027 and vMd-BR006. A mock infected CAM served as control.

Histopathologic analyses of infected CAMs confirmed epithelial proliferation in the chorion membrane. In addition, necrosis was present at late stage of pock developments. The strongest autolysis and necrosis was observed for the non-recombinant MVA (Fig. 21b), where necrotic cells were present in the major part of the tissue samples. Dependent on the status of epithelial proliferation, a complete loss of the basal lamina below the pock could be observed. Below the developed pocks, infiltration of heterophilic granulocytes and macrophages was present in all samples. The non-recombinant virus, vMVA, vMd171, vMd-BR041 and vMd-BR027 showed a higher presence of heterophils than macrophages in the area of infiltration, whereas the amount of both cell types was equal in vMd, vMdd and vMdd-BR006 infected CAMs (Fig. 21b-i). Additionally, the allantoic membrane, which is facing the embryo, was broadened in non-recombinant MVA and vMd171 (Fig. 21b and f). Most of the virus infections, except the ones with non-recombinant MVA, vMd and vMd-BR027, lead to cornification, where epithelia cells grow in circles into the mesenchyme with the appearance of a cornified perl-like structure in the middle of the tissue (Fig. 21b, d and h). Most clearly seen is this aspect in vMdd-BR006 (Fig. 21i). Furthermore, the ones that developed cornification showed epithelial cell proliferation in a cone forming manner into the mesenchyme. Besides to epithelia proliferation, mesenchymal proliferation was also monitored to different extents. The observation of blood vessels in the section determined most of them as hyperaemic shown by the accumulation of blood cells within the vessel. CAM endothelia cells were not infected by any MVA virus mutant applied. Nevertheless, the vascular walls were not even intact after infection with non-recombinant MVA (Fig. 21b). Balloon cells, characterized by a perinuclear vacuole, could be determined in vMdd, vMd-BR041 and vMd-BR027 (Fig. 21e, g and h). Interestingly none of the infected CAMs

developed inclusion bodies as it was described for CPXV infected CAMs. A mock infected CAM served as control (Fig. 21a).The results are summarized in Table 2.

virus (25 PFU)	epithelial proliferation	cornification	epithelial cones	infiltration	mesenchymal proliferation	inclusion bodies
non-recombinant MVA	+	/	/	H>M	+	/
vMVA	+++	+++	+++	H>M	+++	/
vMd *	+	/	/	H=M	+	/
vMdd	+++	++	++	H=M	+++	/
vMd171	++	++	++	H>M	+++	/
vMd-BR041	++	++	++	H>M	+++	/
vMd-BR027	++	/	/	H>M,Ly	+	/
vMd-BR006	+++	+++	+++	H=M	+++	/

Table 2: Comparison of the histopathogic lesions in CAMs infected with non recombinant MVA, vMVA, vMd, vMdd, vMd171, vMd-BR041, vMd-BR027 and vMdd-BR006. H: heterophilic granulocytes, M: macrophages, Ly: lymphocytes, *: less pocks, /: not detectable, >: more than, =: equal amounts, +: weak appearance, +++: strong appearance.

3.10 Characterization of vMd-BR041 and vMdd-BR041 on RK13 cells

Results from host range experiments consequently led to characterization of both vMd-BR041 and vMdd-BR041 in more detail. At first virus encoded GFP expression was monitored in RK13 cells.

3.10.1 Monitoring of virus-encoded GFP expression in RK13 cells

RK13 cell monolayers were infected with vMVA, vMd, vMdd, vMd-BR-041, vMd-BR-041 and vMd-BR041-rev at an MOI of 0.01 and overlayed after 1h post infection with semisolid medium to ensure that the virus spreads from cell to cell only (Fig. 22). Virus infection could be monitored by late virus-encoded GFP expression. Pictures of infected cells were taken 48 h post infection. In contrast to infection with vMVA, vMd, vMdd and vMd-BR041-rev, where

only infected single cells could be observed, virus spreading from cell to cell was observed after infection with vMd-BR041 and vMdd-BR041 by plaque formation.

vMVA   vMd   vMdd

vMd-BR041   vMd-BR041-rev   vMdd-BR041
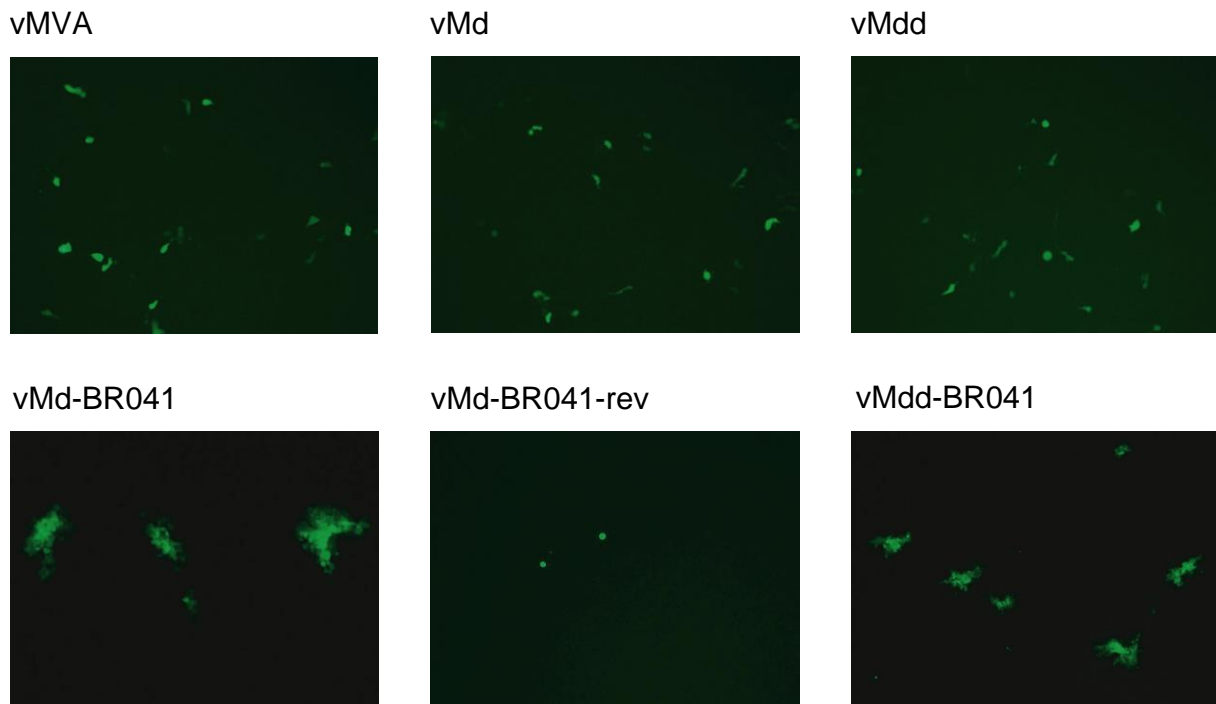
Fig. 22: Presentation of virus-encoded GFP expression in RK13 after infection with vMVA, vMd, vMdd, vMd-BR-041, vMd-BR041-rev and vMdd-BR041. Cells were infected with an MOI of 0.01 and overlayed with methocel medium 1 h post infection. Pictures were taken after 48 h of incubation. Infected single cells are detectable in vMVA, vMd, vMdd and vMd-BR041-rev infected cells. Plaque formation could be detected in cells infected with vMd-BR041 and vMdd-BR041.

3.10.2 Multiple step growth kinetics in RK13 cells

As the results from the host range experiment gave only information about the endpoint titers after 48h, the replication capacity of BR041 knock-in mutants were studied in more detail by multiple step growth kinetics. RK13 cells were infected with vMVA, vMd, vMdd, vMd-BR-041, vMdd-BR-041 and vMd-BR-041-rev at an MOI of 0.1. Supernatant (A) and cells (B) were harvested at the indicated points of time and titrated separately (Fig. 23).
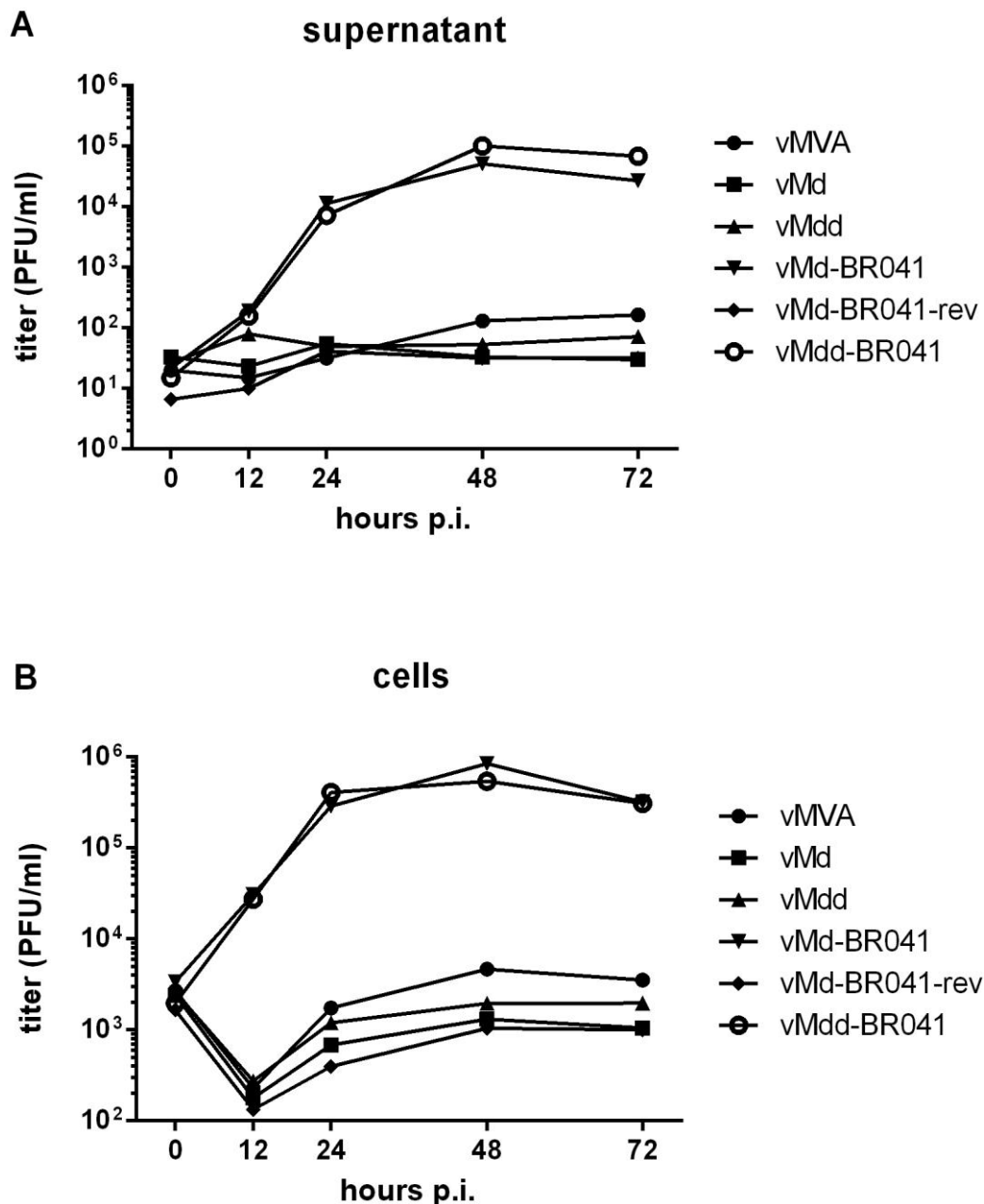
Fig. 23: Growth kinetics with low MOI with vMVA, vMd, vMdd, vMd-BR-041, vMd-BR041-rev and vMdd-BR041 in RK13 cells. Cells were infected with a MOI of 0.1 for multiple-step growth kinetics. Supernatant (A) and cells (B) were titrated separately. Growth curves are representative of three independent experiments titrated in duplicate.

The replication of vMd-BR-041 and vMdd-BR-041 was clearly increased by about two orders of magnitude at 24 h post infection in the supernatant (Fig. 23A). At 48 h respectively 72 h post infection the difference in magnitude increased to three orders in the supernatant (Fig. 23A). Interestingly, the titers determined for intracellular viruses dropped at 12 h post infection for vMVA, vMd, vMdd and vMd-BR041-rev (Fig. 23B). Furthermore, the growth kinetics revealed a two fold increase in virus production from 12 h post infection onwards in cells for vMd-BR041 and vMdd-BR041. Infection with the revertant virus vMd-BR-041-rev led

to virus titers comparable to the parental vMVA, vMd and vMdd (A and B). These results confirm the effect found in the host range and the immunofluorescence experiments.

3.10.3 RK13 endpoint titrations

Additionally, endpoint titers were also obtained from infection of RK13 cells with MOIs ranging from 0.1 to 5. For that purpose, cells and supernatants were harvested 48 h post infection and titrated together. Fig. 24 depicts data of two independent experiments titrated in duplicate.
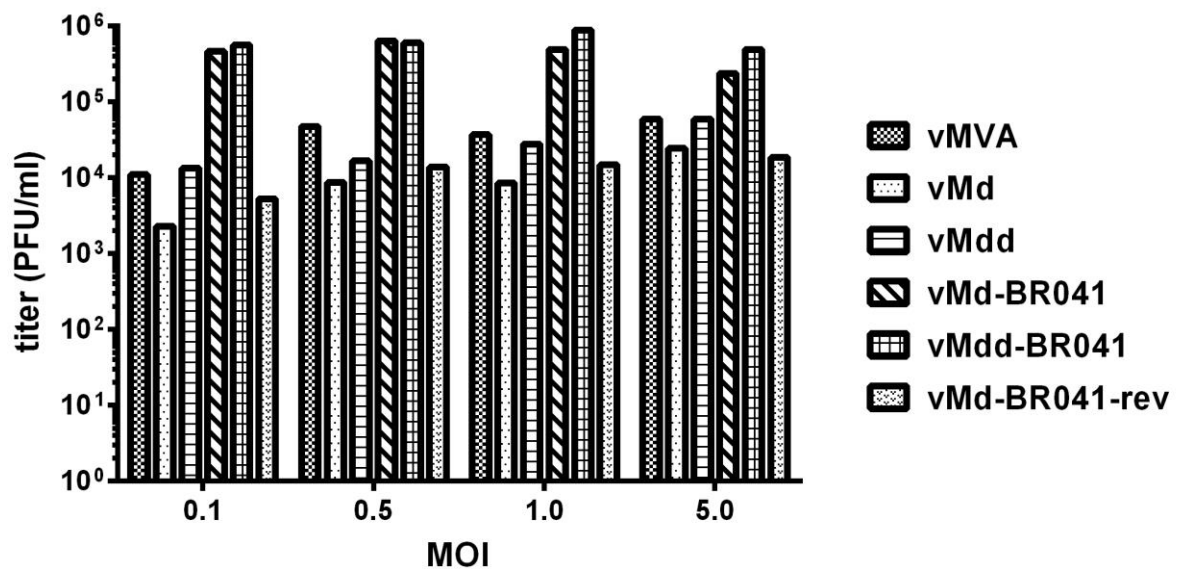
Fig. 24: Comparative virus replication of vMVA, vMd, vMdd, vMd-BR-041, vMd-BR041-rev and vMdd-BR041 in RK13 cells. Cells were infected with different MOIs ranging from 0.1 to 5.0 and harvested 48 h post infection. Cells and supernatant were titrated together. Bars represent two independent experiments titrated in duplicate.

It could be verified that the virus titers were about two orders of magnitude higher in cells infected with vMd-BR-041 and vMdd-BR-041 compared to infection with vMVA, vMd, vMdd and vMd-BR041-rev by usage of a MOI of 0.1, 0.5 or 1.0. Nevertheless, difference was less prominent in cells infected with a MOI of 5.0 than with lower MOI.

3.10.4 Comparison of virus genome replication in RK13 cells

From kinetic experiments, the question arose if a change in virus genome copy number could be detected. Therefore, absolute virus genome copy numbers were compared by real time quantitative PCR. RK13 cells were infected for 8 h with vMVA, vMd, vMdd, vMd-BR041,

vMdd-BR041 and vMdd-BR027 at an MOI of 3. Cells were harvested and virus DNA was prepared before the virus DNA was quantified by real time PCR (Fig. 25). The PCR was performed with oligonucleotides #195 and #194 (see. 2.1.10) and SYBR Green was used as double-stranded DNA-binding dye. Results were analysed by Applied Biosystems 7500 Fast Real-Time software and the ratio of viral DNA replication was calculated relative to vMVA virus DNA copy number. For determination of absolute copy numbers defined pMVA was used as a standard.
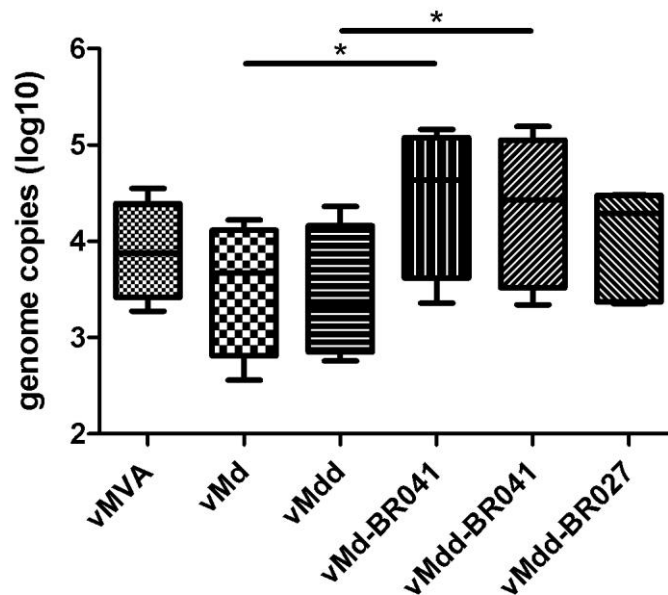
Fig. 25: Comparison of genome copy number on RK13 cells. RK13 cells were infected with vMVA, vMd, vMdd, vMd-BR041, vMdd-BR041 and vMdd-BR027 for 8 h before cells were harvested and virus DNA was prepared. Data are representative of at least three independent experiments measured in duplicate. *$p<0.05$, one-way ANOVA.

Significant differences in genome copy number were determined between vMd and vMd-BR041 as well as for vMdd and vMdd-BR041. Both vMd-BR041 and vMdd-BR041 showed significant higher amounts of DNA in comparison to their parental viruses. In contrast vMdd-BR027 did not show any significant results to its parental virus vMdd. The determination of genome copy number underlines the findings above and BR041 could be listed as host range factor for RK13 cells.

3.10.5 Immunofluorescence staining of early and late virus proteins in infected RK13 and HeLa cells

To investigate the effect of BR041 knock-in mutants on early and late virus protein expression in permissive and non-permissive cell lines, RK13 as well as HeLa cells were infected with vMVA, vMd, vMdd and vMd-BR-041 at an MOI of 0.01 and overlayed with methocel 1 h post infection. After 48 h cells were fixed and stained with antibodies against

late vaccinia virus proteins and against the early expressed protein E3L. Results of the staining are depicted in Fig. 26.

A   late protein   E3L   merge

vMVA

vMd
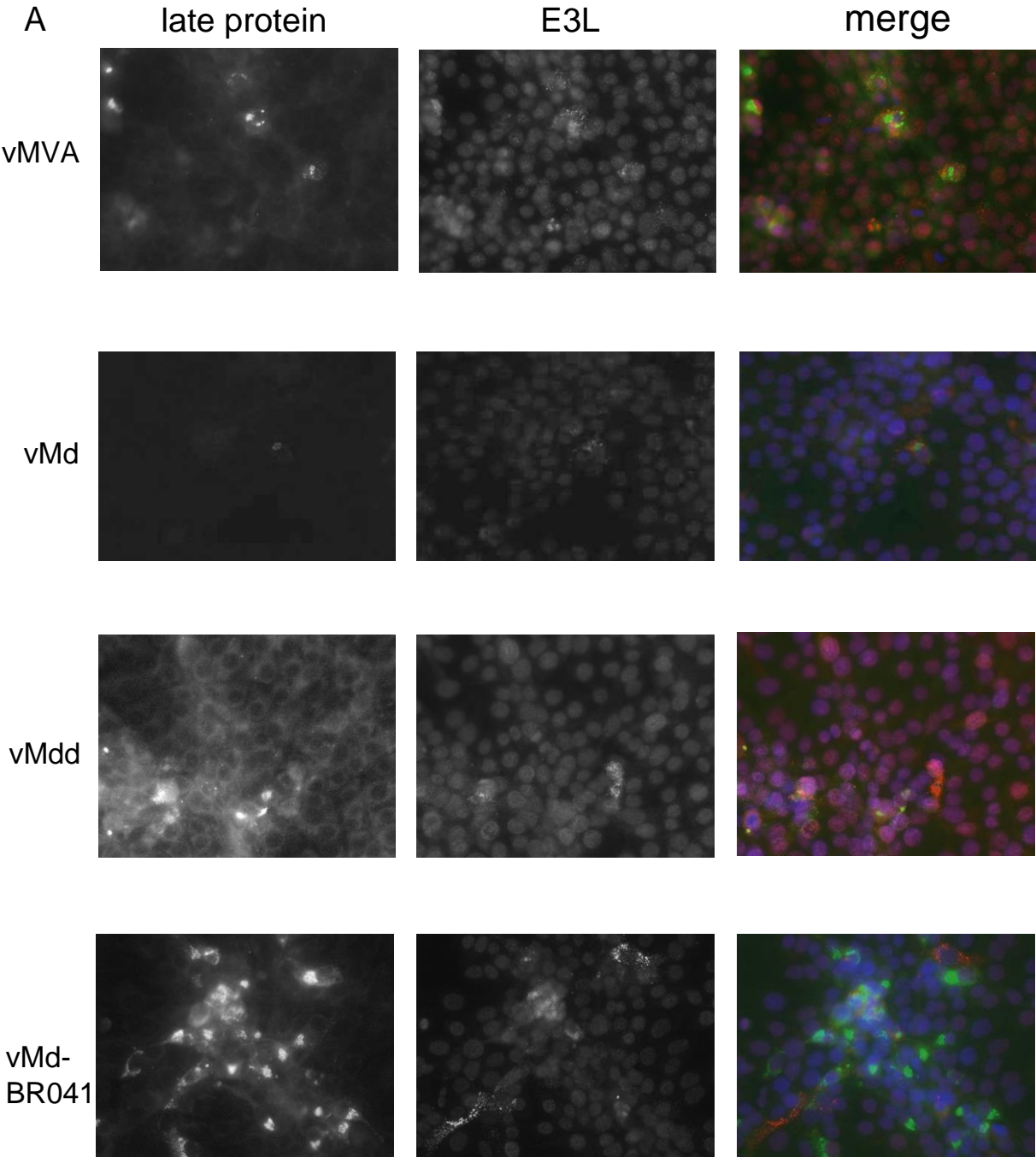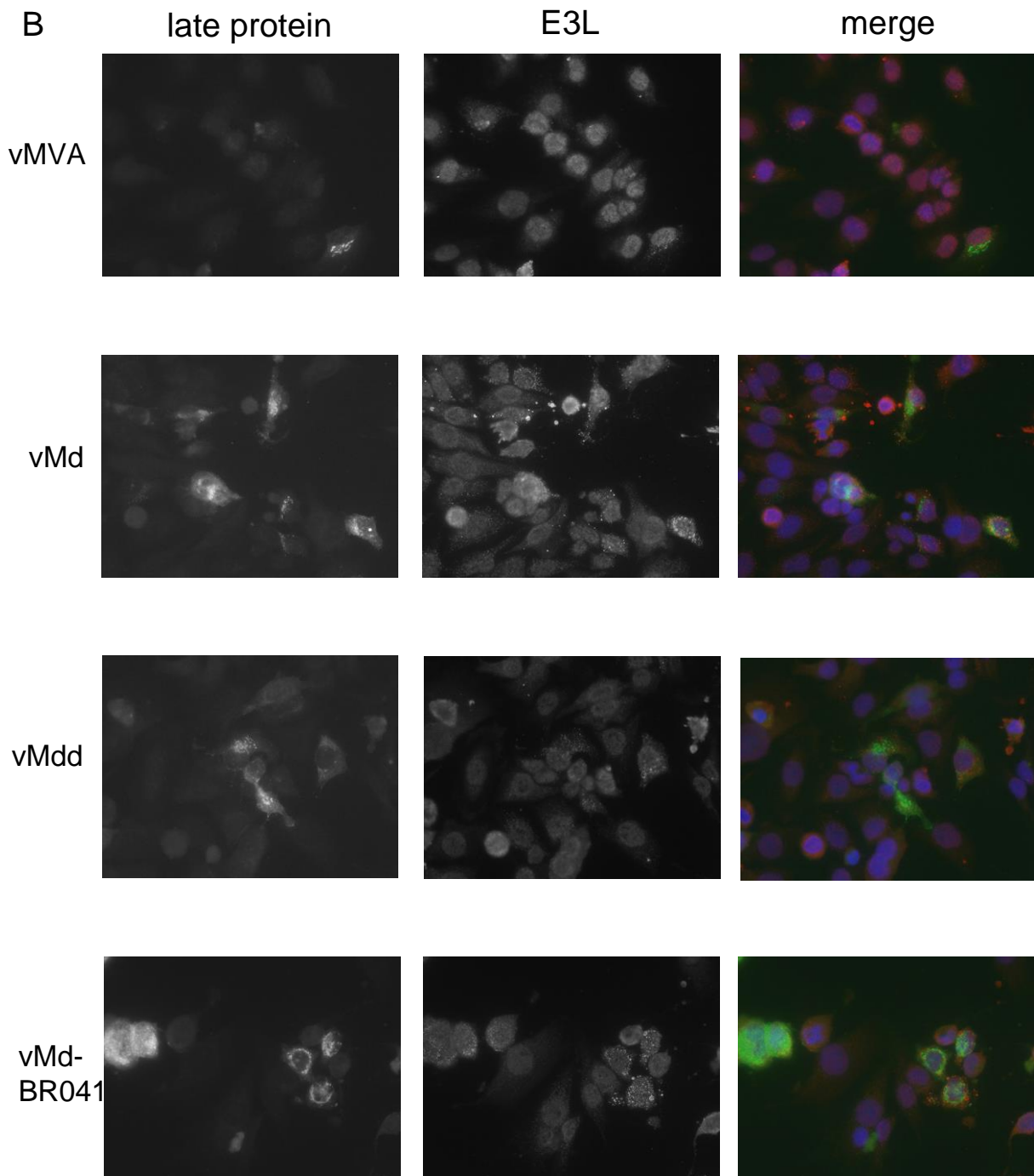
vMdd

vMd-BR041

Fig. 26 RK13 cells (A) and HeLa cells (B) were infected with vMVA, vMd, vMdd, vMd-BR-041 at an MOI of 0.01. At 48 h post infection cells were fixed and stained against late vaccinia virus protein and the early expressed protein E3L. DAPI was used for nuclear staining.

Fig. 26 depicts clearly enhanced late virus protein expression in vMd-BR-041 infected RK13 cells. Additionally, they show plaque formation caused by viral cell to cell spread in vMd-BR-041 infected cells. For the indicated virus mutants, the expression of early proteins, as the detected E3L, seemed to be equal. In contrast to RK13 cells, HeLa cells infected with vMd-BR-041 did not show enhanced late virus protein expression as well as plaque formation. In addition, the expression of E3L and late vaccinia virus protein seemed to be comparable for all virus mutants tested on HeLa cells.

3.10.6 Influence on IκBα during MVA infection in RK13 cells

The NF-κB pathway is activated by several signals as UV light exposure, proinflammatory cytokines and pathogen-associated molecular patterns. The presence of any of those signals lead to the phosphorylation of IκBα by the IκB kinase, which is itself activated by phosphorylation by active cellular protein kinases. The phosphorylation of IκBα leads to its degradation and thereby to the release of NF-κB to which it is bound in the cytoplasm. NF-κB can then stimulate transcription of its target genes in the nucleus. It is potentially harmful to virus infected cells, as it induces the expression of host antiviral cytokines and inflammatory chemokines. Those chemokines are able to attract immune cells to the area of virus infection and thereby interfere with the survival of the virus. Thus, viruses are interested to inhibit IκBα degradation. It was published from Shisler and Jin, that an MVA mutant expressing the VACV K1L protein inhibits IκBα degradation during MVA infection in RK13 cells (Shisler and Jin, 2004). As a consequence, the generated vMd-BR041 and vMdd-BR041 mutants were tested concerning their influence on IκBα in infected RK13 cells. Cell monolayers were infected with vMVA, vMd, vMdd, vMd-BR041 and vMdd-BR041 at an MOI of 3 for 8 h. Cytoplasmic extracts were prepared from virus infected cells as well as from control non-infected cells. As an additional control for IκBα degradation ability, mock infected cells were treated with 10 ng/ml TNF-α or left untreated 30 min before harvest (Fig.27).
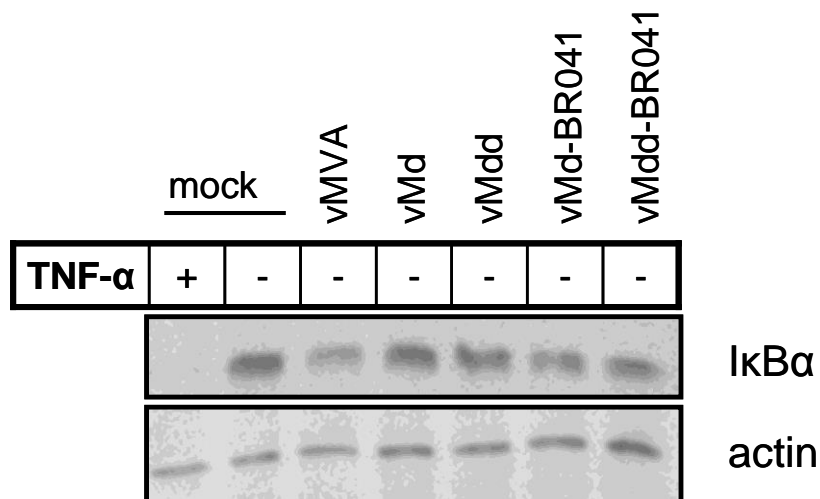
Fig. 27: Influence on IκBα in virus infected RK13 cells. RK13 cells were infected with vMVA, vMd, vMdd, vMd-BR041 and vMdd-BR041 with a MOI of 3. Cytoplasmic extracts were prepared 8 h post infection. Mock infected cells served as a control and were left untreated or treated with 10 ng/ml TNF-α for 30 min before harvest.

The cytoplasmic cell extracts from infected RK13 cells were used for the detection of IκBα and actin. The BR041 knock-in mutants as well as the parental virus and the deletions mutants show comparable IκBα protein levels after 8 h post infection. Cell extracts from infected cells which were treated with 10 ng/ml TNF-α (lane 1) or left untreated (lane 2)

served as controls. The induction with TNF-α showed clearly the decreased protein level of IκBα, ensuring the inducibility of the cell line with TNF-α. This result is in contrast to the data published from Shisler and Jin (Shisler and Jin, 2004). They propose that the degradation of IκBα in RK13 can be inhibited by infection with MVA/K1L mutant.

3.11 Characterization of eIF2α phosphorylation during MVA infection

Viruses are known to induce stress signals during infection. One of the main actors in the stress pathway is the protein kinase R. Its activation results in the phosphorylation and therefore inactivation of eIF2α (eukaryotic initiation factor 2α). EIF2α inactivation led to arrest of both viral and cellular mRNAs and therefore mediates viral replication inhibition. Viruses developed several strategies to circumvent the complete translation inhibition in the host either by direct modulation of eIF2α or by acting upon PKR. The ARP protein and host range factor for CHO cells CP77 was ascertained for the ability to inhibit the phosphorylation of eIF2α in HeLa cells after 4 h of infection (Hsiao et al., 2004), indicating a possible interplay between the presence of viral ARPs and translation inhibition. Owing to those reports, the effect on phosphorylation of eIF2α in RK13 cells was tested for the identified RK13 host range factor BR041 and BR027. RK13 cell monolayers were infected with vMVA, vMd, vMdd, vMd-BR041, vMdd-BR041 and vMd-BR027 at an MOI of 3. After 2 h and 4 h, whole cell lysates were prepared and analyzed by Western blotting (Fig. 28).
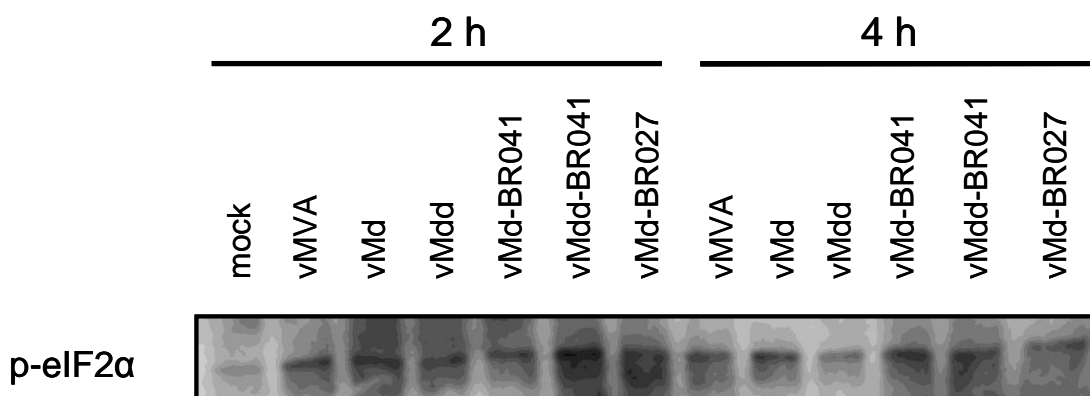
Fig. 28: Characterization of phosphorylation of eIF2α. RK13 cell were infected with vMVA, vMd, vMdd, vMd-BR041, vMdd-BR041 and vMd-BR027 at an MOI of 3. Cells were harvested 2 and 4 h post infection and analyzed by Western blotting.

The detection of phosphorylated eIF2α protein levels showed comparable amounts at 2 h and 4 h after infection. Additionally, the levels did not vary between the different generated virus mutant strains used for infection. This led to the conclusion, that neither the vMVA nor any of the virus mutants had an effect on the phosphorylation of eIF2α in RK13 cells.

3.12 Influence of ARPs on the NF-κB pathway

Effective viruses as well as bacterial pathogens have evolved intriguing strategies to circumvent innate and adaptive immune response mechanisms. For both microbial pathogens, NF-κB is an abundant target for manipulation. This transcription factor plays a pivotal role in establishment and maintenance of inflammation. In response to viral infection, the NF-κB pathway is often activated by viral products which occur during the process of viral replication, e.g. by dsRNA. Influencing the activation of NF-κB is therefore a remarkable strategy for viruses to affect several immune response processes by targeting a single regulatory pathway in the host. Interaction of the CPXV ARP BR006 with NF-κB *in vitro* was shown by Mohamed et al. (Mohamed et al., 2009a). Furthermore, they showed that a CPXV-BR006 deletion mutant failed to inhibit virus induced NF-κB regulated gene expression (Mohamed et al., 2009b). Therefore, the question arose if the newly invented host range mutants vMd-BR041 and vMd-BR041 or the insertion of another single ARP has an influence on NF-κB induction. To evaluate the impact of several CPXV ARPs on NF-κB activation during virus infection, reporter cell lines which stably express firefly luciferase under an NF-κB inducible promoter and constitutively express Renilla luciferase were infected with newly generated MVA mutants. Additionally, cells were treated with 10 ng/ml human TNF-α for 4 h, polyIC for 4 h or left untreated before cell lysis was performed. The immunostimulant polyIC is similar to double stranded RNA which is produced by some viruses during replication. It interacts with TLR3 which then leads to the activation of NF-κB. TNF-α, another immunostimulant, binds to ubiquitous TNF-α receptors and acts in a different signaling cascade but leading also to activation of NF-κB. Both reagents lead to the activation of the NF-κB pathway, but from different points of induction.

After luminescence measurement in Tristar LB941, the values determined by firefly luciferase were divided by the values given by Renilla detection. Subsequently values were normalized to untreated mock infected cells (Fig. 29).

infected reporter cells - / + TNF-α/polyIC induction
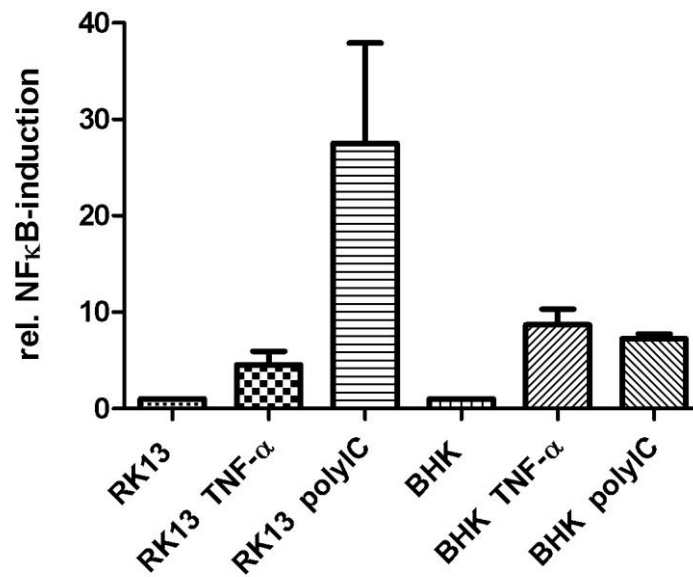
Fig. 29: Comparison of mock infected BHK or RK13 cells induced with TNF-α or polyIC. Mock infected cells were treated with TNF-α or polyIC. The bars indicate values normalized to untreated mock cells.

TNF-α treatment of mock infected RK13 cells resulted in a ~4.5-fold increase of firefly luciferase expression and a ~27.5 fold increase in polyIC induced cells. The expression of firefly luciferase rose in BHK cells ~8.6-fold after TNF-α induction and ~7.2-fold after polyIC treatment.

To monitor the influence of generated ARP mutants on the NF-κB pathway, BHK and RK13 reporter cell lines were infected for 8 h with various virus mutants with an MOI of 3 (Fig. 30). Additionally, cells were stimulated 4 h before harvest with TNF-α (Fig.29 A and C), polyIC (Fig. 30B and D) or left untreated. Differences in NF-κB-induction between various virus mutants could not be observed.

A)   infected RK13 reporter cells - / + TNF-α induction
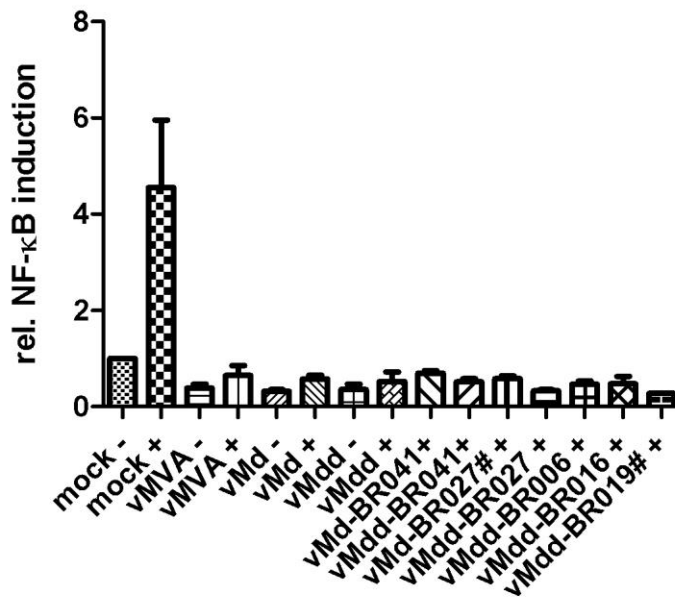
B)   infected RK13 reporter cells - / + polyIC induction
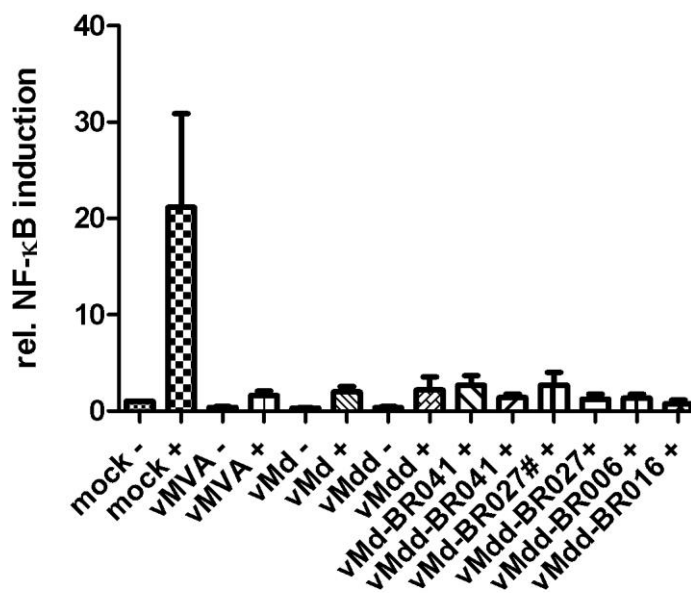
C) infected BHK reporter cells - / + TNF-α induction
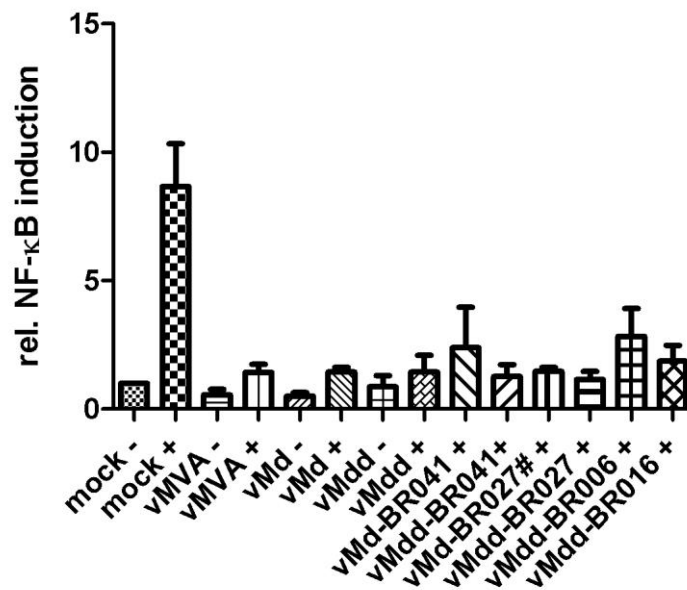
D) infected BHK reporter cells - / + polyIC induction
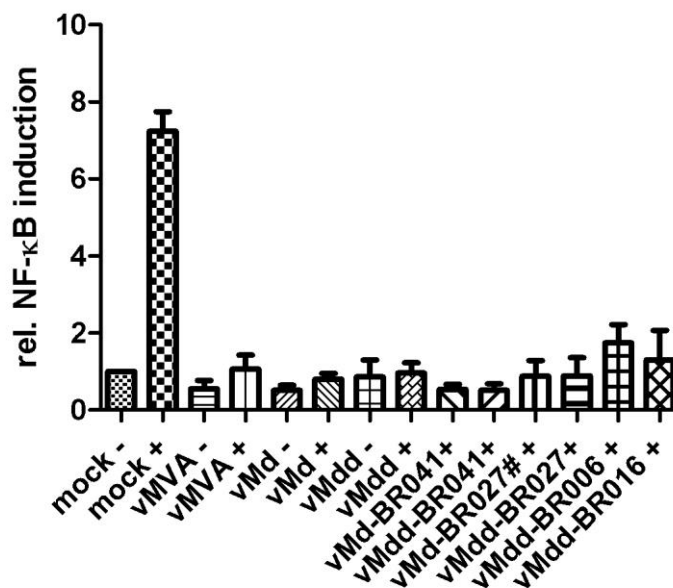
Fig. 30: Comparison of infected RK13 (A and B) and BHK (C and D) cells. Infected cells were treated with TNF-α (A and C) or polyIC (B and D). The bars indicate absolute values normalized to untreated mock cells. Statistical analysis was performed by one-way ANOVA, values are not not-normally distributed, data are representatives of at least three experiments with the exception of data marked with #, which represent data of two experiments only.

To determine if knock-in mutants differ from their parental virus in NF-κB response, determined mutant values were calculated relative to the respective determined parental values by dividing mutant values by parental virus values in RK13 cells. None of the generated mutants developed significant differences to its respective parental (Fig. 31A and B).

Additionally, values from induced infected RK13 cells were calculated relative to their respective untreated control. For this purpose values determined for induced samples were divided by values from respective non-induced RK13 cells (Fig. 31C and D).
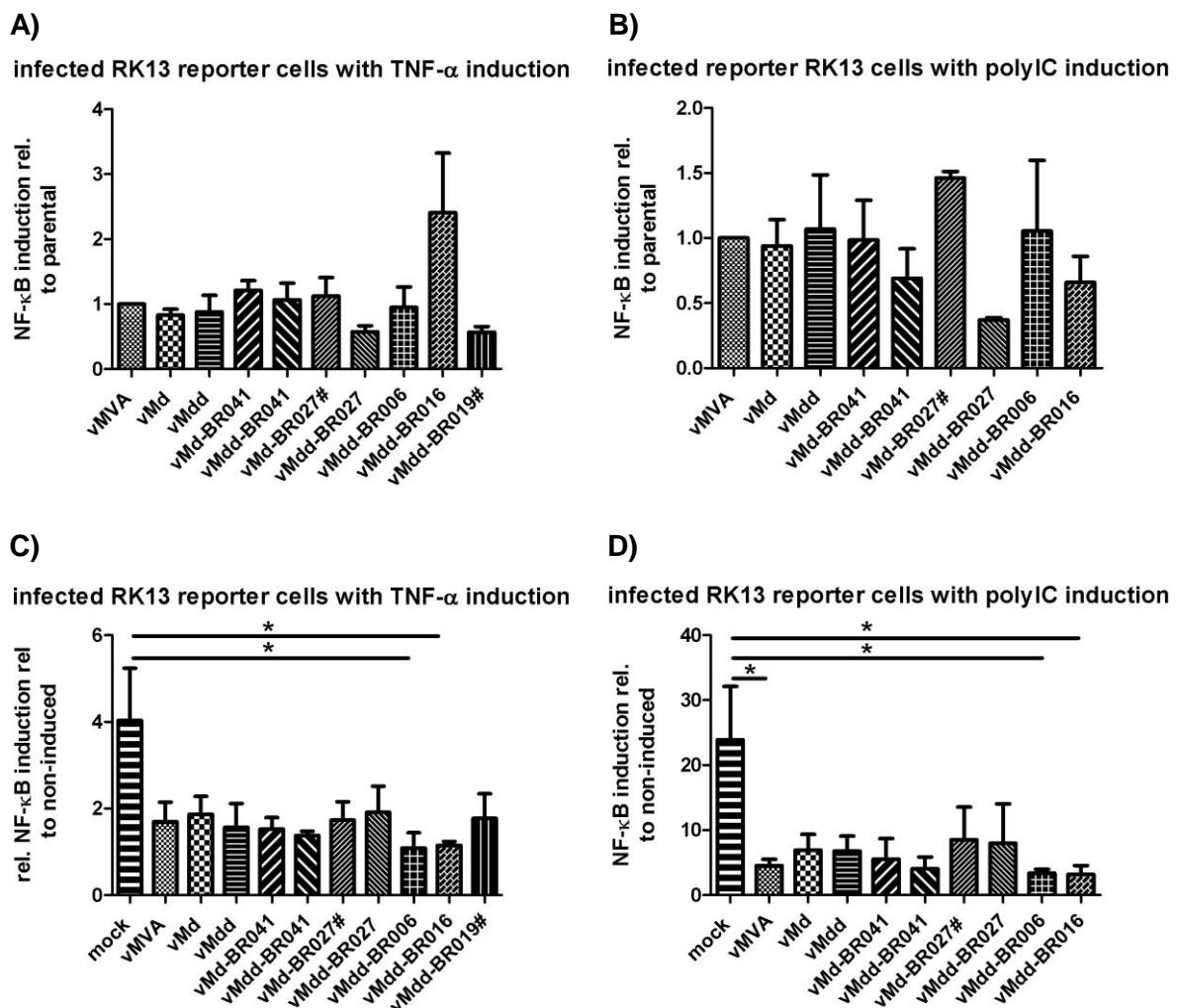
Fig. 31: Comparison of various mutants concerning NF-κB response in RK13 cells. RK13 cells were infected with the indicated viruses and induced with TNF-α (A and C) or pIC (B and D) for 30 min or 4 h or left untreated. The measurement results were calculated relative to mock (A and B) or to untreated respective virus mutant (C and D). Statistical analysis was performed by one-way ANOVA, values are not not-normal distributed, data are representatives of at least three experiments with the exception of # marked data, which represent data of two experiments only.

Significant differences could be shown for relative values for mock versus (vs.) vMdd-BR006 and mock vs. vMdd-BR016 after TNF-α treatment (Fig. 30C). Moreover, significant

differences could be found after polyIC induction for mock vs vMVA, mock vs. vMdd-BR006 and mock vs vMdd-BR016 (Fig. 31D).

The same experiment setting and calculation is shown for BHK cells in Fig.32. The calculation for NF-κB induction relative to parental virus aa well as induced samples was done as described above for RK13 cells. None of the MVA mutants showed significant differences to its parental after TNF-α or polyIC treatment (Fig. 32A and B). Despite from vMdd-BR019 infection, all viruses showed significant lower NF-κB induction after treatment with TNF-α (Fig. 32 C) compared mock. Moreover, induced virus infected cells showed significant lower results (P<0.05) compared to mock after polyIC induction (Fig. 32D).

A)

B)

C)

D)
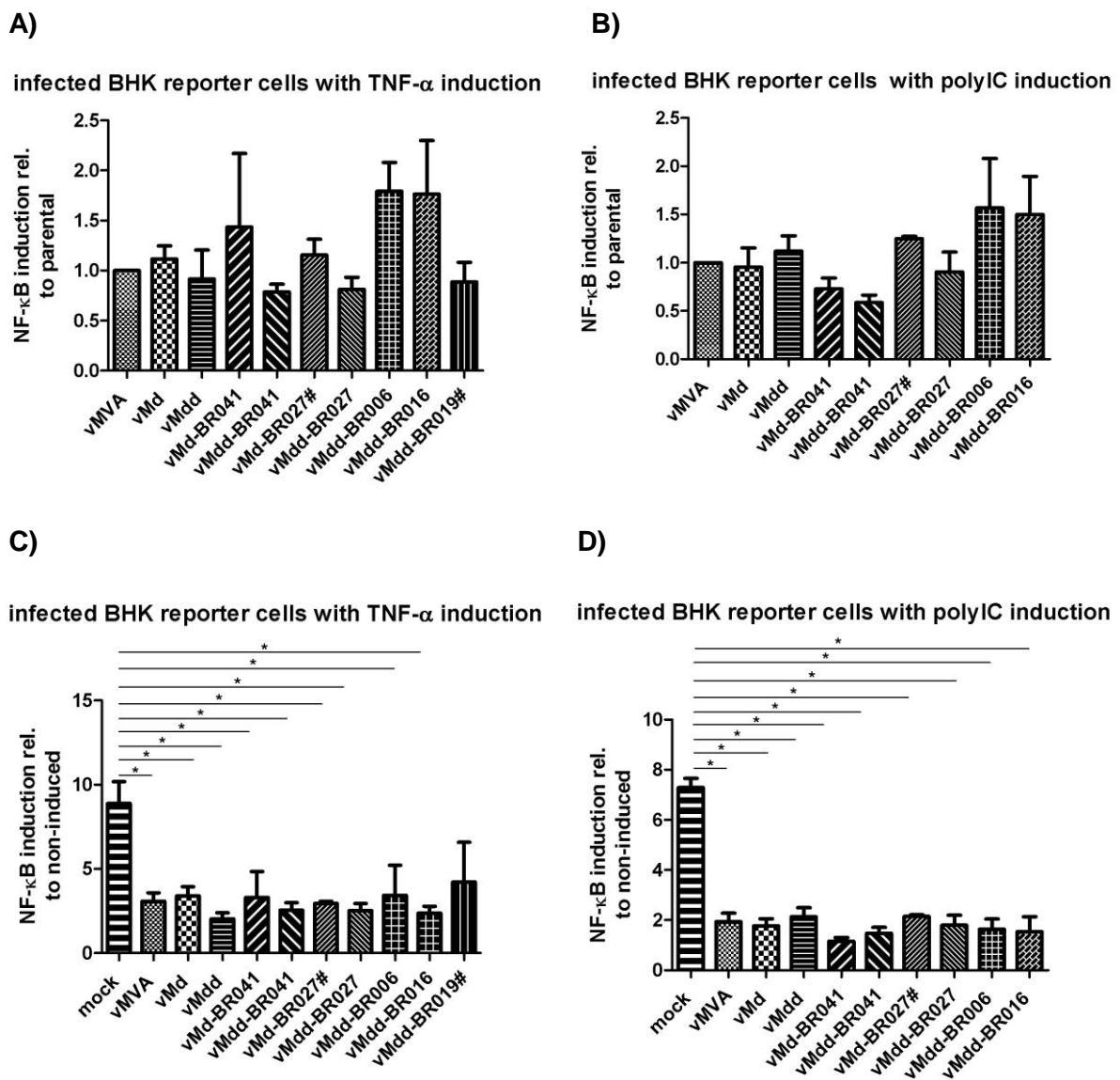
Fig. 32: Comparison of various mutants concerning NF-κB response in BHK cells. BHK cells were infected with the indicated viruses and left untreated or treated with TNF-α (A and C) or polyIC (B and D) for 4 h. The measurement results were calculated in relation to mock (A and B) or to untreated virus (C and D) infected cells. Statistical analysis was performed by one-way ANOVA, values are not not-normal distributed, data are representatives of at least three experiments with the exception of # marked data, which represent data of two experiments only.

3.13 PARP cleavage in HeLa cells following infection with various virus mutants

Several poxvirus proteins are known to modulate apoptosis in infected cells. Therefore, the effect of various ARP expressing virus mutants was tested concerning the ability to potentially circumvent the induction of apoptosis. HeLa cell monolayers were infected with vMVA, vMd, vMdd, vMd-BR041, vMdd-BR041, vMd-BR027, vMdd-BR027, vMdd-BR016 and vMdd-BR006 with an MOI of 3 for 24 h Fig. 33. Infected cells were treated with 1 µM staurosporine for 4 h or left untreated before whole cell lysates were prepared. Staurosporine is a known inducer of apoptosis and was used as a positive control for induced apoptosis in mock infected cells (lane 2).
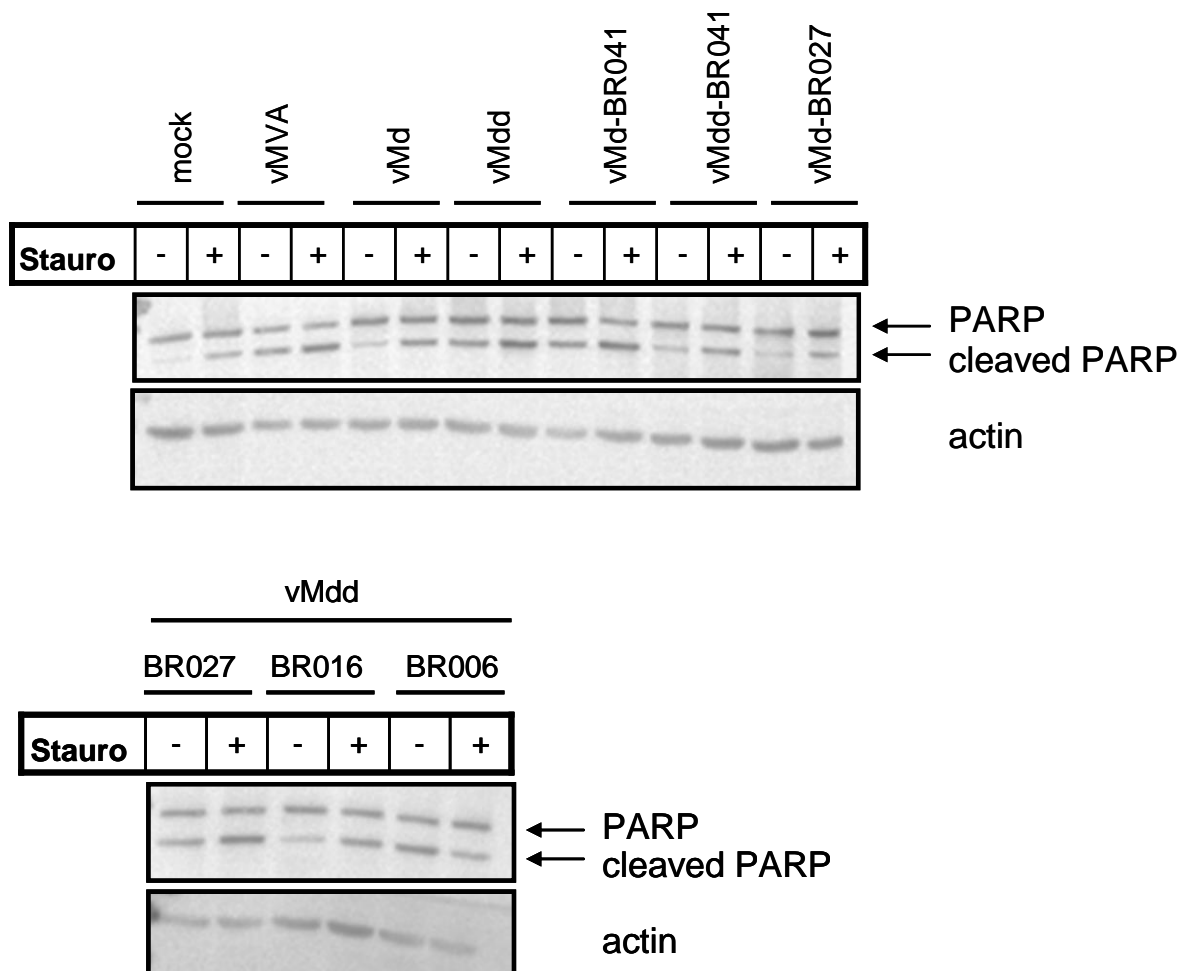
Fig. 33: PARP cleavage in HeLa cells following infection with various virus mutants. HeLa cells were infected with vMVA, vMd, vMdd, vMd-BR041, vMdd-BR041, vMd-BR027, vMdd-BR027, vMdd-BR016 and vMdd-BR006 with a MOI of 3 for 24 h. Cells were left untreated or treated with 1 µM staurosporine before whole cell lysates were prepared. Detection was performed with antibodies recognizing the full length PARP, the cleaved form of PARP and actin. Stauro: staurosporine.

All tested virus mutants induced apoptosis in HeLa cells. Nevertheless, even after 24 h of infection the PARP cleavage was not complete. However, it could not be shown that one of

the generated virus mutants had an avoiding function in apoptosis induction. This is more clearly shown in the samples which were treated with staurosporine.

In summary, several ARP mutants were analyzed in order to determine a role of ARPs in virus replication, plaque formation, pocks induction, cell tropism and cell signaling.

4. Discussion

4.1 Characterization of vMd and vMdd

The MVA mutant MVA-Δ68-kDa lacking the *ORF186* was generated with the K1L-specific growth selection method by Sperling et al. (Sperling et al., 2009). To their knowledge, the *ORF186* encodes for the only ARP left in MVA. However, to our knowledge the MVA genome harbours an additional ARP encoding ORF on position 171. We generated a recombinant virus mutant vMd which is genetically equal to the published MVA-Δ68-kDa and in addition a complete ankyrin ORF free virus, vMdd in which both, *ORF171* and *ORF186* are deleted.

4.1.1 Multiple-step growth analysis

To compare the replication capacity of vMVA, vMd and vMdd multiple-step growth analysis in BHK cells was performed. It could be shown that all three viruses replicate in comparable extent to each other. This is in line with the data published by Sperling et al.. They found that the replication efficiency of MVA-Δ68-kDa is similar to the parental virus in CEF cells (Sperling et al., 2009). Due to the fact that BHK cells and CEF cells are both permissive for MVA this result might by expected for vMd. Furthermore, for the first time it could be shown that a complete ankyrin free MVA virus, vMdd, replicated with the same capacity as parental vMd and the parental vMVA in permissive BHK cells. This result indicates that neither the expression of *ORF186* nor of *ORF171* has an essential function for MVA in completing its replication cycle in BHK cells. One might conclude that ARP deletion in MVA does not cause an effect on viral replication capacity in permissive cell lines in general. This might also lead to the assumption that the ARPs left are mainly responsible for the fact that a few cell lines are still considered as permissive for MVA.

4.1.2 Early virus protein expression in BHK, HaCaT and NIH 3T3 cells

The viruses vMVA, vMd and vMdd were characterized concerning their early protein expression levels. It could be shown that the expression of VACV early protein E3L is similar for all three viruses in BHK cells as well as in HaCaT cells. In addition, E3L protein levels were compared at 2 h and 4 h in NIH 3T3 cells after infection with vMVA, vMd and vMdd. At both points of time early protein expression did not differ among the three viruses tested. The same result was also shown for BHK and HaCaT cells and indicated that the expression of early phase proteins was unaffected by the deletion of ARPs. Therefore, the protein levels

detected in these three lines can be determined as comparable within one cell line. This result was expected for BHK cells, because the three viruses did not show differences in their replication capacity in this cell line. These findings underline the data given by the growth kinetic experiment. As in MVA, the entire gene expression cascade is necessary for completing the virus life cycle. Therefore, the similarity in early protein levels is in line with the data coming from the growth kinetic experiments.

4.1.3 Late virus protein expression in BHK, HaCaT and NIH 3T3 cells

The expression of L1R, a protein expressed in late phase of infection, was detected 24 h post infection in BHK and HaCaT cells. It could be clearly shown that the L1R level of vMd in BHK and HaCaT cells was not significantly weaker than that detected in the parental vMVA. The total amount of detected L1R protein in BHK cells could not be described as comparable to the level detected in non-permissive HaCaT cells. Additionally, in non-permissive NIH 3T3 cells late L1R protein levels at 6 h post infection were faintly detectable. At later points of time, after 24h, L1R was detectable to a convincing amount. Nevertheless, the L1R level for vMVA, vMd and vMdd were comparable to each other. This is not in accordance with the findings published by Sperling et al. (Sperling et al., 2009). They claimed less late protein amounts for MVA-Δ68-kDa 24 h after infection in NIH 3T3 cells. The contrasting results could be explained by the fact that the cell lines used were different due to less or extensive passaging. Although, the cell lines used in this thesis were certified.

An additional explanation might be the different methods of mutant generation. The mutant MVA-Δ68-kDa was generated by usage of the K1L-based host range selection protocol, whereas, vMd was generated through BAC-based *en passant* mutagenesis. But the parental MVA BAC was sequenced and characterized by growth kinetics by Cottingham et al. and claimed to be comparable to the virus MVA (Cottingham et al., 2008). To exclude differences in the genome sequence, derived deletion mutants were confirmed by RFLP analysis. Furthermore, the deleted area in the generated ARP deletion BAC pMd was sequenced and did not show unwanted mutations. Thus, the pMd sequence can be considered as relatively verified. The mutated area was also confirmed by sequencing and RFLP in reconstituted vMd and did not show any variations in comparison to BAC DNA.

Moreover, it should be possible to monitor a high amount of infected HaCaT and NIH 3T3 cells after infection with high MOIs of 3 for example. In our case, HaCaT and NIH 3T3 cells were hard to infect by vMVA, vMd and vMdd with an MOI of 3 as the GFP expression was only barely observable in a very few number of single cells. Despite from the explanations

above this issue might also be a result of different 4b fowlpox GFP promoter activity in HaCaT and NIH 3T3 cells compared to BHK cells.

An additional reason why the block in late virus gene expression could not be confirmed might be due to the choice of different late proteins for detection. Both L1R and B5R are listed as late expressed poxvirus proteins. L1R is essential for formation of infectious intracellular mature virions, whereas, B5R is a component of the extracellular-cell-associated enveloped virions. Therefore, B5R might be translated later in the late phase than L1R or it is present to a less extent. Unfortunately an antibody against B5R was not available in this study. Another option to confirm the findings would be Northern blot or quantitative reverse transcriptase real-time analyses which were not performed yet. Sperling et al. found less amounts of intermediate and late (047R) transcripts in Northern blot analysis in NIH 3T3 and HaCaT cells (Sperling et al., 2009). All in all, the published result that the deletion of the ARP encoded by the *ORF186* leads to a decrease in late protein levels could not be confirmed in this thesis by the experimental set-up and methods used.

4.1.4 Macroscopic description of infected CAMs

Poxvirus proteins are known to modify the structure of pocks developed on infected CAMs. In contrast to red pocks found after infection with CPXV on CAMs or greyish-white pocks found after infection with camelpox, the pocks shown by MVA are completely white and do not show any occurrence of hemorrhagic signs. CAM infection with vMVA exhibits a number of smaller, secondary pocks next to a prominent primary pock. In comparison, infection with vMd and vMdd displayed a couple of smaller pocks in the size comparable to the secondary pocks developed by vMVA. This effect could be explained by deficient cell-to-cell spread of vMd and vMdd. The effect was detectable in CAMs infected with very low amounts of virus notably PFU 10 (not shown) and PFU 25. The condition of less virus particles for detectable effects might explain why this aspect could not be observed in performed growth kinetics. In growth kinetic experiments the applied amount of viral particles lead to the fact that after one cycle of efficient virus replication the number of virus particles might be too high to make such an observation. To our knowledge, it was the first time that CAMs were infected with a complete ARP free mutant as well as a mutant which is genetically comparable to MVA-Δ68-kDa.

4.2 Generation of knock-in mutants

Inserted CPXV encoding ARPs were fused to an N-terminal Flag-tag. Unfortunately, it was not possible to detect the proteins via tag by western blot in virus infected cells. One explanation might be that ARPs are degraded in the host cell, maybe by host cell proteins, which bind to translated proteins followed by destabilisation and degradation in the proteasome. The regulation could also be already at the mRNA level. Host cell RNA binding proteins (RBP) could destabilize ARP mRNA by facilitating deadenylation and thus degradation of the mRNA. Another possible regulatory mechanism for ARP mRNAs could also be host cell miRNAs, which bind and mediate deadenylation or decapping what then lead to mRNA degradation in p-bodies or the exosome. Additionally, the detection via immunofluorescence in transiently transfected HeLa cells was not possible. For this purpose, cells were transfected with pcDNA3.1 and pcDNA3.1/V5-His-Topo harbouring ARP encoding sequences fused with Flag-tag sequences. An additional reason for the lack of detection could also be the protein folding, resulting in a no longer accessible tag for detection. Nevertheless, the expression or ARPs could be clearly confirmed by generating the revertant virus of vMd-BR041. Without CPXV ORF BR041 the revertant virus mutant was not able to sustain the host range function in RK13 cells.

4.3 Host range determination

MVA is described as replication deficient in various mammalian cell lines, in particular in those of human origin. This means the virus cannot complete its full replication cycle supposed to block in the late phase of morphogenesis. However, it is able to finish the entire cascade of viral early, intermediate and late protein expression. To investigate if the knock-out or knock-in of ARP encoding ORFs has an effect on the host range function of MVA, 15 different cell lines were tested in an endpoint titration experiment with low MOI infection. Until now, the effect of MVA was tested on CEF, BHK, DF-1 (permissive), CHO, HeLa, MDBK, RK13, HaCaT, NIH 3T3, A549 and CRFK (non-permissive) and Vero (semi-permissive) cells (Carroll and Moss, 1997; Meyer et al., 1991). In this study, Nie168, Ken-R and NRB cells could be newly determined as non-permissive for MVA as the virus did not reveal replication ability higher than 1-fold by dividing output titer by input titer. Interestingly, in comparison to the other non-permissive cell lines the titer determined on HeLa cells was the highest by far. Besides vMVA, the set of generated MVA knock-out and knock-in viruses was also tested. HeLa cells showed borderline values towards semi-permissive after infection with vMdd-BR027 and vMd-BR213. This was also the case for RK13 cells after vMdd-BR027 infection. The CPXV-BR041 could be clearly defined as host range factor for RK13 cells. The claimed replication factor of 25-fold to consider a cell line as permissive was markedly higher for both,

vMdd-BR041 and vMdd-BR041. In this experiment, the host range expansion of CPXV-BR041 to RK13 cells was shown for the first time. Unfortunately, both vMd-BR041 and vMdd-BR041 were not able to extend the host range effect in any other cell line tested. This led to the conclusion that at the one hand the host range function of CPXV-BR041 could indeed be limited to RK13 cells or at the other hand more cell lines coming from a broader variety of hosts have to be tested.

The african green monkey cell line Vero could be confirmed as semi-permissive for MVA. From the set of virus mutants tested, Vero cells showed only borderline results to semi-permissive after infection with vMdd-BR019.

Besides DF-1 and CEF cells, which were already described as permissive for MVA, the equine cell line NBL-6 could be discovered as permissive for recombinant MVA infections. In DF-1, CEF and NBL-6 cells, vMdd-BR019 showed less replication capacity compared to the other knock-in mutants as the determined virus titers were at the lower end of the range. Interestingly, homologs of BR019 are not found in any other poxvirus family. One possible explanation could be that it does not contribute to the broad host range of CPXV.

4.4 Characterization of vMd-BR041 and vMdd-BR041 on RK13 cells

The CPXV-BR041 protein is the homolog of VACV K1L (identity value 95.77 %, similarity value 97.18 % (alignment poxvirus.org)). An alignment is shown in Fig. 34. It underlines the percentages given by the alignment tool.

```
CPXV BR041   1    MDLSRINTWKSKQLKSFLSSKDAFKADVHGHSALYYAIADNNVRLVCTLLNAGALKNLLE    60
                  MDLSRINTWKSKQLKSFLSSKD FKADVHGHSALYYAIADNNVRLVCTLLNAGALKNLLE
VACV K1L     1    MDLSRINTWKSKQLKSFLSSKDTFKADVHGHSALYYAIADNNVRLVCTLLNAGALKNLLE    60

CPXV BR041   61   NEFPLHQAATLEDTKIAKILLFSGMDDSQFDDKGNTALYYAVDSGNMQTVKLFVKKNWRL   120
                  NEFPLHQAATLEDTKI KILLFSGMDDSQFDDKGNTALYYAVDSGNMQTVKLFVKKNWRL
VACV K1L     61   NEFPLHQAATLEDTKIVKILLFSGMDDSQFDDKGNTALYYAVDSGNMQTVKLFVKKNWRL   120

CPXV BR041   121  MFYGKTGWKTSFYHAVMLNDVSIVSYFLSEIPSTFDLAILYSCIHDSIKNGNVDMMILLL   180
                  MFYGKTGWKTSFYHAVMLNDVSIVSYFLSEIPSTFDLAIL SCIH +IKNG+VDMMILLL
VACV K1L     121  MFYGKTGWKTSFYHAVMLNDVSIVSYFLSEIPSTFDLAILLSCIHTTIKNGHVDMMILLL   180

CPXV BR041   181  DYMESTNTNNSLLFIPDIKLAIDNKDLEMLQALFKYDINIYSVNLENVLLDDAEIAKMII   240
                  DYM STNTNNSLLFIPDIKLAIDNKD+EMLQALFKYDINIYSVNLENVLLDDAEI KMII
VACV K1L     181  DYMTSTNTNNSLLFIPDIKLAIDNKDIEMLQALFKYDINIYSVNLENVLLDDAEITKMII   240

CPXV BR041   241  EKHVEYKSDSYTKDLDIVKNNKLDEIISKNKELRLMYVNYARKN    284
                  EKHVEYKSDSYTKDLDIVKNNKLDEIISKNKELRLMYVN  +KN
VACV K1L     241  EKHVEYKSDSYTKDLDIVKNNKLDEIISKNKELRLMYVNCVKKN    284
```

Fig. 34. Alignment of CPXV-BR041 and VACV K1L. The alignment shows the amino acids of CPXV-BR041 and VACV K1L in comparison. + indicates amino acids which are not identical but belong to the same chemical amino acid group.

The alignment of CPXV-BR041 and VACV K1L depicts different amino acid substitutions. Amino acid exchanges on position 77, 167, 208, 281 and 282 are exchanges within the same

amino acid group. Those substitutions are predicted to cause minor changes in protein folding. Changes from polar to non-polar or vice versa are found on position 23,161 and 236. If those amino acids are localized at the surface of the folded protein, they could influence the final conformation, because of altered interaction with the surrounding environment. A substitution from acid to polar is found on amino acid position 166 and 284. This might also have an effect. If the altered amino acids are on the protein surface, it could affect protein structure and thus its function.

There are also some changes found which involve serine or threonine (position 12, 166, 167, 184 and 236). Those amino acids are known to be phosphorylated by casein kinase II (CKII). But potential phosphorylation sites are not affected because three residues C-terminal of the potential phosphate acceptor sites acidic residues (either aspartic acid or glutamic acid) are not found. On position 184 glutamic acid is altered to threonine, but three residues N-terminal a serine or threonine for potential phosphorylation is missing. Motif scans also suggest the amino acids on position 167 to 169 as possible phosphorylation sites for CKII. Under comparable conditions serine is favoured over threonine. If this site cannot be determined as phosphorylated by CKII in VACV, it would be interesting to know if the change from threonine to serine on position 167 lead to phosphorylation in CPXV.

4.4.1 Monitoring of virus encoded GFP expression in RK13 cells

RK13 cells infected with parental and BR041 knock-in mutant viruses were infected for 1 h before cells were overlayed with methocel. As the appropriate viruses express GFP under the late 4b fowlpox promotor, the viral protein expression can be easily monitored via fluorescence. Plaque formation mediated from cell-to-cell spread could be shown for vMd-BR041 and vMdd-BR041 in infected RK13 cells. In contrast, single cell infection only was monitored for vMVA, vMd, vMdd and vMd-BR041-rev. Detectable single cell infection by GFP fluorescence indicates late virus gene expression. This difference may us conclude that BR041 affects viral morphogenesis or virus release or the survival of cells until release can be accomplished. The fact that the vMd-BR041-rev did not show plaque formation maintains the finding for BR041 as host range factor for RK13 cells. Likewise, this result underlined the expression and functionality of CPXV-BR041 in the MVA background, as vMd-BR041 and vMdd-BR041 were able to circumvent the block of late morphogenesis in normally non-permissive RK13 cells. The virus mutant completed the full life cycle in RK13 cells leading to the ability of cell-to-cell spread.

4.4.2 Low multiplicity growth kinetics on RK13 cells

In this experiment, for the first time, the replication of ARP deletion MVA mutants expressing or lacking CPXV-BR041 was compared directly on RK13 cells. The infection with vMd-BR041 and vMdd-BR041 resulted in an increase of extracellular virus titer of two orders of magnitude at 24 h post infection, up to nearly three orders of magnitude at 48 h respectively 72 h post infection. This effect is found in the same manner for intracellular virus titer but starts early at 12 h post infection. Interestingly, in the first 12 h post infection, the titer of vMVA, vMd, vMdd and vMd-BR041-rev dropped down but increased in the following 12 h before the virus developed a steady state. A reason for the lacking detectable drop in virus titer for vMd-BR041 and vMdd-BR041 could be that on the one hand the drop occurs in earlier points of time during virus replication or is shorter and could therefore not be detected. On the other hand it may be that the drop does simply not exist in RK13 cells because they are permissive for those virus mutants. The initial decrease in titer was also described for MVA/K1L on RK13 cells but to an earlier starting point directly after infection before replication went on progressively (Sutter et al., 1994). But in the data from Sutter et al. extracellular and intracellular viruses were not considered separately (Sutter et al., 1994).

In this study the infection with vMVA, vMd, vMdd and vMd-BR041-rev showed similar intracellular and extracellular virus titer. The titer determination of vMd-BR041-rev in comparison to vMd-BR041 and vMdd-BR041 underlines clearly the function of CPXV-BR041 as host range factor for RK13 cells.

4.4.3 RK13 endpoint titrations

To characterize the effect of CPXV-BR041 on RK13 cells more closely, endpoint titrations with different MOIs were performed. In vMd-BR041 and vMdd-BR041 infections with MOI 0.1, 0.5 and 1.0 the increase of viral titer up to two orders of magnitude in comparison to parental viruses could be confirmed. The total viral titer of vMd-BR041 and vMdd-BR041 were comparable to each other. The determined titer for MOI 0.1, 0.5 and 1.0 were slightly higher in comparison of those from infections with MOI 5. This is mainly due to the fact that the titers of vMVA and vMdd increased, whereby the titers of vMd-BR041 and vMdd-BR041 decreased. The decrease could be explained by the virus overload and therefore strong damage to cells as well as less intact cells available for new infection with vMd-BR041 and vMdd-BR041.

4.4.4 Comparison of virus genome copy numbers and Immunofluorescence of early and late virus proteins in RK13 cells and HeLa cells

Genome levels were determined in RK13 cells infected with vMVA, vMd, vMdd, vMd-BR041, vMdd-BR041 and vMdd-BR027 at 8 h post infection. The ratios were calculated relative to the parental vMVA. It could be shown that the levels for vMd-BR041 and vMdd-BR041 were significant higher in comparison to their parental viruses vMd and vMdd. This result substantiates the findings for BR041 as a host range factor on RK13. Additionally, it is clear now that the genome replication of mutants which harbour BR041 in their genome proceeds to a measurable difference at 8 h. Additionally, vMdd-BR027 did not give significant results on genome level determination. This shows that CPXV ARPs are not randomly exchangeable and by that leading to enhanced genome replication in RK13 cells. In poxviruses, genome replication is a requirement for late protein expression. Therefore, it should be proven if late protein synthesis is blocked in infected RK13 and HeLa cells.

RK13 cells and Hela cells were infected with vMVA, vMd, vMdd and vMd-BR041. The cells were overlayed with methocel after 1 h before cells were fixed at 48 h post infection. For detection, specific antibodies recognizing the early expressed E3L protein and late VACV proteins were used. It could be pointed out that in vMVA, vMd and vMdd infected RK13 and HeLa cells, the detection of early and late proteins was comparable. Additionally, only single cells could be detected, which is the result of the lack in cell-to-cell spread for those viruses. Thus underlines that MVA was able to finish the cascade of early, intermediate and late protein expression in RK13 as well as in HeLa cells but was not able to complete its full life cycle. On the contrary, vMd-BR041 evolved stronger expression of early and especially late proteins in RK13 cells. This was not only detectable in single cells but also in cells, which showed infection through cell-to-cell spread. Since the cells were overlayed with semisolid medium before late gene expression started, this effect can only be due to direct spread outgoing from one cell to the neighbouring cell. This effect for vMd-BR041 could not be observed in HeLa cells. The genome copy number determination together with the immunofluorescence data might lead to the result that BR041 affects virus DNA-replication and as a consequence vMd-BR041 can overcome the block in late morphogenesis in RK13 cells. It could also be shown that this feature cannot be transferred to other cell lines, such as HeLa cells for instance. Further, both the results from immunofluorescence and genome copy number determination are in line with the data derived by growth kinetics analysis.

4.4.5 Influence on IκBα during MVA infection in RK13 cells

IκBα as a key modulator in immune responses is often considered in viral infection experiments. Also the influence of the homolog of BR041 K1L was observed to force IκBα degradation. Consequently, RK13 cells were infected with vMVA, vMd, vMdd, vMd-BR041 and vMdd-BR041 with a MOI of 3. At 8 h post infection the cells were harvested and cytoplasmic extracts were prepared. For IκBα detection mock infected cells treated with 10 ng/ml TNF-α at 30 min before harvest served as controls. The controls showed clearly that in the cell line used TNF-α induction led to IκBα degradation. It was published that the expression of VAVC K1L in MVA lead to the absence of IκBα degradation in RK13 cells at 4 h post infection (Shisler and Jin, 2004). Additionally, they showed that IκBα levels did not recover at 8 h post infection and that this effect is based on poxvirus inhibition of host cell protein synthesis. In contrast to the results of Shishler and Jin, the expected phenotype for the virus mutants harbouring the homolog of VACV K1L, could not be confirmed. This might be due to the fact that CPXV-BR041 is indeed more different from K1L than expected by comparison in alignment tools. Another possible explanation for contrasting results could be the usage of varying virus populations in prepared stocks. This means viruses derived from several passaging events versus high clonal prepared virus stocks. Nevertheless, vMd-BR041 and vMdd-BR041 did not show any influence on IκBα degradation.

4.4.6 Characterization of eIF2α phosphorylation

Hsiao et al. detected a reduced phosphorylation level of eukaryotic translation initiation factor 2A (eIF2α) in HeLa cells infected with a VACV deletion mutant (VV-hr) harbouring the CPXV protein CP77 (VV-36hr). CP77 is known as host range factor for CHO cells. The level of phosphorylated eIF2α was published as a hallmark for stress response in virus infected cells. The correlation between eIF2α phosphorylation and stress response comes from the fact that translation initiation is blocked in virus infected cells (Clemens, 2001; Gale et al., 2000; Kawagishi-Kobayashi et al., 1997; Yan et al., 2002). The eIF2α phosphorylation in RK13 cells infected with vMVA, vMd, vMdd, vMd-BR041, vMdd-BR041 and vMd-BR027 with a MOI of 3 was investigated. At 2 h and 4 h post infection whole cell lysates were prepared. It turned out that the phosphorylation of eIF2α did not differ between 2 h and 4 h after infection and did also not differ among the different mutant viruses. From that it might be concluded that MVA, independently from the presence of considered ARPs, does not influence the phosphorylation of eIF2α in RK13 cells and that RK13 cells do not respond to viral infections by the inhibition of protein translation mediated by eIF2α. To investigate this in more detail one could determine the mRNA levels of eIF2α effector proteins in infected RK13 cells.

4.4.7 Influence of ARP knock-in mutants on NF-κB pathway

In order to prove the effect of inserted ARP encoding *ORF*s on the NF-κB pathway, the generated knock-in mutants were tested on cell lines which stably express firefly luciferase under control of an NF-κB inducible promoter. Mohamed et al. reported an effect for a CPXV-BR006 deletion mutant (Mohamed et al., 2009b). HeLa cells infected with CPXV deletion mutant vCpx-006KO induced a significant higher level of NF-κB regulated luciferase expression in the absence of TNF-α compared to mock infected cells, cells infected with parental virus and GFP expressing control virus infected cells. In cells infected with vCpx-006KO and treated with TNF-α, the level of luciferase was also higher in comparison to untreated vCpx-006KO infected cells or TNF-α treated cells infected with control viruses. They conclude that in absence of CPXV-BR006 the TNF-α induced NF-κB activation cannot be blocked completely. From this assumption, it follows the expectation that the vMdd-BR006 virus mutant should lead to a decrease of NF-κB regulated luciferase expression. Interestingly, in this study the effect could not be observed as well as none of the other ankyrin mutants showed effects in that manner on BHK or RK13 cells. This goes in line with results from an other CPXV deletion mutant in the lab, where this thesis was performed (personal communication B.K. Tischer). Additionally, the virus mutants tested did not develop any effect when treated with polyIC in comparison to their respective parental virus. One exception was vMdd-BR041. It showed significant lower NF-κB regulated luciferase expression compared to its parental in BHK cells. However, the absolute levels of NF-κB regulated luciferase expression in MVA infected and TNF-α or polyIC treated cells were significantly lower than the levels observed in mock infected and treated cells. This could be shown for both RK13 and BHK cells. This result confirmed that indeed MVA expresses NF-κB inhibitors in permissive BHK and non-permissive RK13 cells, which act in another pathway independently from the IκBα degradation pathway. It also showed that vMVA and the generated mutants were able to attenuate the effect provoked by induction with immunostimulants like TNF-α and polyIC. This effect relative to mock could still be observed after calculation of the induced values to the respective untreated controls for all viruses for polyIC and TNF-α treated BHK cells. But in RK13 cells this could be found only for vMVA, vMdd-BR006 and vMdd-BR016 after polyIC treatment and, with the exception of vMVA, after TNF-α induction.

Interestingly, for both vMd-BR041 and vMdd-BR041 an effect concerning NF-κB response could not be observed on RK13 cells since an effect was not observed in untreated as well as in TNF-α or polyIC treated cells. This is surprising and it contrasts to Lynch et al.. They

published that MVA harbouring K1L lack the ability of IκBα degradation compared to parental MVA in HEK (Lynch et al., 2009) 293T cells. IκBα degradation releases the transcription factor NF-κB which than initiates the transcription of target genes (Lynch et al., 2009).

One could conclude that the host range function of BR041 does not stand in relation to the NF-κB mediated immune response in RK13 cells. But as mentioned above, one exception is the vMdd-BR041 mutant which shows significant lower NF-κB mediated luciferase expression relative to its parental vMdd on BHK cells.

Summarized, the characterization of vMdd-BR041 and vMdd-BR014 shows clearly the potential of CPXV-BR041 to enhance genome replication and virus morphogenesis of MVA in RK13 cells.

4.5 Determination of plaques areas in BHK cells

The determination of plaques areas gives information about the ability of a virus to spread from cell-to-cell. A significant plaque size reduction compared to vMVA was found for both vMd and vMdd and suggests a defect in cell-to-cell spread on BHK cells for these viruses. Interestingly, vMd and vMdd did not differ from each other significantly. Those findings underline the data determined by CAM infection experiments, as both mutants showed smaller pock formation in comparison to their parental vMVA. It seems as decreased virus spread might lead to smaller pock formation. One explanation, why this effect could not be found in growth kinetic analysis might be related to the low virus inoculation in plaque size experiments and CAM infection experiments. Taken together, the observation derived from plaque size and CAM infection experiments show that vMd and vMdd have a defect in cell-to-cell spread on BHK cells and in pock formation on the CAM of embryonated chicken eggs. Further, the results described show that the ARP encoded by *ORF186* indeed seems to have a function on cell-to-cell spread on CAMs and permissive BHK cells. The observations made, could mainly be attributed to the deletion of *ORF186*, as the further deletion of *ORF171* did not enhance the effect.

The comparison of vMd-BR027, vMd-BR041 and vMd-BR213 with their parental vMd did not lead to a significant change in plaque size. From this, it could be concluded that BR027, BR041 and BR213 are not able to restore the impairment provoked by the deletion of *ORF186*. From this could be further concluded that the poxvirus ARPs cannot be changed randomly to rescue the attenuation in cell-to-cell spread caused by deletion of one special ARP encoding ORF.

In addition, when vMdd-BR006, vMdd-BR016, vMdd-BR019, vMdd-BR041 and vMdd-BR213 were compared to their parental vMdd they showed an additional reduction in plaque size.

The tendencies of vMdd mutants for developing smaller plaques could already be observed when vMd was compared to vMdd, but the difference was not significant. Possibly, the weak disadvantage in spreading is enhanced by the expression of inappropriate CPXV-ARPs. Those findings also go in line with observation made for CPXV deletion mutants. The deletion of special CPXV-ARPs lead to larger plaque sizes on RK13 cells, whereas, the infection with other CPXV ARP deletion mutants lead do smaller plaques on RK13 cells (personal communication B.K. Tischer). Moreover, those cell specific properties were also found for a CPXV ARP negative mutant in which all 14 ARPs were deleted. It occupies up to double plaque size areas compared to plaques developed by the parental virus on BHK cells (personal communication B.K. Tischer).

It would be interesting to know how the situation for BR006, BR016 and BR019 inserted in vMd would be. Surprisingly, BR027 inserted in vMd and vMdd did not change the occupied area in any direction and behaved like its parental. These data may suggest an ARP-self-dependent acting, as ARPs might be regulated by members of their own virus protein family by mechanisms which are incompletely understood so far.

4.6 PARP cleavage in HeLa cells after infection with various virus mutants

It was published that CP77 expressed in VV-hr, a VACV deletion mutant, significantly lowers the caspase 3 activity in HeLa cells. Caspase 3 inactivates PARP by its cleavage. This cleavage is an intermediate step in apoptosis. Therefore, a lower caspase 3 activity should prevent cells from going into apoptosis.

In contrast to Hsiao et al. who proposed CP77 to be able to enhance the host range of a VACV deletion mutant to HeLa cells, this could not be confirmed by Schuenadel et al. (Schuenadel personal communication). They generated a recombinant CPXV CP77 deletion mutant, which does not show any replication deficiency despite from CHO cells (Schuenadel et al., 2012). Moreover, the effect of CP77 on apoptosis could not be confirmed (Schuenadel personal communication). It is still unknown, if apoptosis plays a key role in the establishment of expanded host tropism in virus infection and those controversies disapprove a clear connection between host range and apoptosis.

In the performed PARP assay for this study, it turned out that vMVA as well as the ARP deletion mutants and the ARP knock-in mutants are all able to induce apoptosis in HeLa cells. More clearly seen is this aspect in the samples treated with the apoptosis inducer staurosporine It could be shown that the tested virus mutants do not prevent PARP from being cleaved. Therefore, none of the inserted ARPs had the ability to prevent PARP from

being cleaved and from that it could be supposed that caspase 3 together with the upstream pathway are not affected by examined ARPs.

4.7 Histologic characterization of infected CAMs

The histologic investigation of HE stained CAMs showed for the non-recombinant MVA a stronger extent of autolysis and necrosis compared to the other virus mutants used for infection. This could be the case because this virus was more aggressive in infection capacity on CAMs than the recombinant viruses. In infections with non-recombinant MVA, vMVA, vMd171, vMd-BR041 and vMd-BR027 a higher presence of heterophile granulocytes than macrophages was found in the area of infiltration. Possibly, this was due to different cytokine sekretion in response to the viral infection by those mutants. The cornification observed for vMVA, vMdd, vMd171, vMdd-BR006 and vMd-BR027 infected CAMs was the consequence of very strong cell proliferation. With progressive cornification the permeability of tissue decreases in a proportional manner, from which also diminished tissue establishment resulted. Additionally, it could be used as prevention of mechanical disruption caused by friction of the membrane on the egg shell, as the pocks showed macroscopical cell structures of 0.7 cm in height. Most vessels were hyperaemic, which was a clear sign of inflammatory processes in the area of infection. The increased proliferation and infiltration in those areas results in a higher metabolic activity which therefore, required a greater blood flow. But in contrast to CPXV infection the endothelia cells, which coat blood vessels, were not infected by any MVA virus mutant.

Balloon cells as a sign of inflammation response were found in vMdd, vMd-BR027 and vMd-BR041. They appeared at the area where the pock proliferation ends, on the chorion membrane. For some human diseases, for example malignant melanoma and focal cortical dysplasia, the development of balloon cells is characteristic. If the presence of this cell type in infections with the mentioned viruses has a special function, has to be elucidated.

In this study experiments on cell tropism, with parental MVA and generated ARP knock-in mutants, identified the equine cell line NBL-6 as permissive for recombinant MVA infections. Published data for Δ68k-ank could not be confirmed with the generated genetically identical vMd virus mutant. But the deletion ARP virus mutants vMd and vMdd showed impaired cell-to-cell spread on BHK cell and smaller pock formation on CAMs. Additionally, the insertion of ARPs BR006, BR016, BR019, BR041 and BR 213 in vMdd led to further impaired virus spreading. Data about BR041 MVA mutants showed the ability of BR041 to expand the

replication efficiency of MVA to RK13 cells. One fact which could contribute to this phenotype might be increased level of genome replication in RK13 cells. A reason could also be improved virus morphogenesis or viral release. BR041 could also support cell survival until virus replication was completed. Both vMd-BR041 and vMdd-BR041 will help to identify involvement and influence of BR041 on signaling pathways concerning apoptosis, immunmodulation and cell signaling in the future. The set of generated ARP knock-in virus mutants will help to investigate the role of poxvirus ankyrin repeat proteins in virus tropism, viral immune response and apoptosis after poxvirus infection.

5. Abstract

In mammalian the ankyrin motif is one of the most common motifs which functions in protein protein interactions. Ankyrin repeat proteins (ARPs) are known as adaptors between the spectrin skeleton and integral membrane proteins. They are also known to be able to bind to proteins involved in apoptosis. However, within viruses ARPs are rather rare. One exception is the family of poxviruses. Proteins, which harbour an ankyrin motif encoded by poxviruses, were identified to influence the immune response via the NF-κB pathway, to play a role in apoptosis and serve as host range factors.

The aim of this thesis was the characterization of cowpox (CPXV) ARPs in a complete ARP free virus environment.

The poxvirus modified *vaccinia virus* Ankara (MVA) is well known as the prime vaccine against smallpox and was used in Germany in the 70´s. The virus is highly attenuated since it lost about 15 % of its parental genome in the process of passaging on chicken embryo fibroblasts (CEFs). Therefore, only one published ARP is left in its genome. The attenuation comes along with the description of MVA as host restricted to baby hamster kidney (BHK) cells and CEFs. Consequently, this virus is a convenient model to study the host range function of proteins.

We identified an additional still unknown ARP encoding open reading frame (ORF) in MVA. One after the other the ORFs were deleted in a bacterial artificial chromosome (BAC) of the MVA genome via *en passant* mutagenesis, thus allowing the generation of a complete ARP free virus. After virus reconstitution, the generated deletion viruses were characterized in terms of their growth properties and ability to spread from cell-to-cell. It could be shown that the deletion lead to a defect in cell-to-cell spread but virus replication does not seem to be affected.

Using the deletion mutants as a backbone various ARP encoding ORFs from CPXV were inserted. The generated knock-in mutants were tested on a representative number of different cell lines. Thereby, three new cell lines come to be known as non-permissive for MVA. Furthermore, a host range factor for RK13 cells could be identified and characterized concerning growth properties and cell-to-cell spread ability. Additionally, a selection of knock-in mutants was examined regarding the influence in apoptosis and in the NF-κB pathway.

It was published that poxvirus proteins are able to change the formation of pocks on chorion allantoic membranes (CAMs). Hence, the development of pocks on the CAM of embryonated chicken eggs was also monitored.

The results of this work contribute to of the potential application of MVA for the development of new vaccines and to a better understanding of poxvirus ARPs concerning host range and virus behaviour in general.

5. Zusammenfassung

Im Säuger ist das Ankyrin-Motiv eines der häufigsten Motive, das Protein-Protein Interaktionen vermittelt. Ankyrin-Repeat-Proteine (ARPs) sind bekannt als Adaptoren zwischen dem Spektrin Zytoskelett und integralen Membranproteinen und binden ebenfalls an Proteine, die in der Apoptose involviert sind. In Viren sind ARPs eher selten. Eine Ausnahme stellt die Familie der Pockenviren dar. Für Proteine, die das Ankyrin-Motiv enthalten und von Pockenviren kodiert werden, wurde gezeigt, dass sie die Immunantwort über den NF-κB Weg beeinflussen, eine Rolle in der Apoptose spielen und als host range Faktoren fungieren.

Das Ziel dieser Arbeit war die Charakterisierung von Kuhpocken ARPs in einem komplett ARP freien Virus Umfeld.

Das modifizierte Vaccinia Virus Ankara (MVA), bekannt als Prime-Vaccine gegen die Pockenerkrankung, wurde in Deutschland in den späten 70igern benutzt. Das Virus ist stark geschwächt, da es ungefähr 15 % seines Ursprungsgenoms bei der Passagierung auf Hühnerembryofibroblasten (CEFs) verloren hat. Daher ist nur ein ARP in seinem Genom übriggeblieben und veröffentlicht. Die Abschwächung geht einher mit der Beschreibung von MVA als wirtseingeschränkt auf Baby-Hamster-Nieren (BHK) Zellen und CEFs. Folglich ist dieses Virus ein geeignetes Modell, um die Wirtsspezifität von Proteinen zu untersuchen.

Wir identifizierten einen weiteren noch unbekannten ARP kodierenden offenen Leserahmen (ORF). Ein ORF nach dem anderen wurde in einem künstlichen bakteriellen Chromosom (BAC) des MVA Genoms mittels *en passant* Mutagenese deletiert, um ein komplett ARP freies Virus zu generieren. Nach der Rekonstitution der Viren wurden die generierten Deletionsmutanten bezüglich ihrer Wachstumseigenschaften und der Fähigkeit sich von Zelle zu Zelle auszubreiten untersucht. Es konnte gezeigt werden, dass die Deletion zu einem Defekt in der Ausbreitung von Zelle zu Zelle führt, wohingegen die Virusreplikation nicht beeinträchtigt zu sein scheint.

In die Deletionsmutanten wurden unterschiedliche Kuhpocken ARP kodierende ORFs insertiert. Die generierten knock-in Mutanten wurden auf einer representativen Anzahl unterschiedlicher Zelllinien getestet. Dadurch konnten drei neue Zelllinien als nicht-permissiv für MVA identifiziert werden. Außerdem wurde ein host range Faktor für RK13 Zellen identifiziert und bezüglich der Wachstumsfähigkeiten und der Ausbreitung von Zelle zu Zelle charakterisiert. Zusätzlich wurde eine Auswahl von knock-in Mutanten betreffend des Einflusses auf Apoptose und des NF-κB Weges charakterisiert.

Es ist publiziert worden, dass Pockenvirenproteine in der Lage sind die Ausbildung von Pocken auf der Chorion-Allantois-Membran (CAM) zu verändern. Infolgedessen wurde die Entwicklung von Pocken auf CAMs von embryonierten Hühnereiern überprüft.

Die Ergebnisse dieser Arbeit tragen zur möglichen Nutzung von MVA zur Entwicklung neuer Impfstoffe und zum besseren Verständnis von Pockenvirus ARPs bezüglich Wirtsspezifität und Virusverhalten im Allgemeinen bei.

6. List of literature

Adrain, C., and Martin, S. J. (2001). The mitochondrial apoptosome: a killer unleashed by the cytochrome seas. *Trends Biochem Sci* **26,** 390-7.

Al-Khodor, S., Price, C. T., Kalia, A., and Abu Kwaik, Y. (2010). Functional diversity of ankyrin repeats in microbial proteins. *Trends Microbiol* **18,** 132-9.

Almazan, F., Dediego, M. L., Galan, C., Escors, D., Alvarez, E., Ortego, J., Sola, I., Zuniga, S., Alonso, S., Moreno, J. L., Nogales, A., Capiscol, C., and Enjuanes, L. (2006). Construction of a severe acute respiratory syndrome coronavirus infectious cDNA clone and a replicon to study coronavirus RNA synthesis. *J Virol* **80,** 10900-6.

Andrei, G., and Snoeck, R. (2010). Cidofovir Activity against Poxvirus Infections. *Viruses* **2,** 2803-30.

Babkin, I. V., and Babkina, I. N. (2011). Molecular dating in the evolution of vertebrate poxviruses. *Intervirology* **54,** 253-60.

Bai, C., Sen, P., Hofmann, K., Ma, L., Goebl, M., Harper, J. W., and Elledge, S. J. (1996). SKP1 connects cell cycle regulators to the ubiquitin proteolysis machinery through a novel motif, the F-box. *Cell* **86,** 263-74.

Basu, M. K., Carmel, L., Rogozin, I. B., and Koonin, E. V. (2008). Evolution of protein domain promiscuity in eukaryotes. *Genome Res* **18,** 449-61.

Becerra, C., Jahrmann, T., Puigdomenech, P., and Vicient, C. M. (2004). Ankyrin repeat-containing proteins in Arabidopsis: characterization of a novel and abundant group of genes coding ankyrin-transmembrane proteins. *Gene* **340,** 111-21.

Beinke, S., and Ley, S. C. (2004). Functions of NF-kappaB1 and NF-kappaB2 in immune cell biology. *Biochem J* **382,** 393-409.

Blanchard, T. J., Alcami, A., Andrea, P., and Smith, G. L. (1998). Modified vaccinia virus Ankara undergoes limited replication in human cells and lacks several immunomodulatory proteins: implications for use as a human vaccine. *J Gen Virol* **79 (Pt 5),** 1159-67.

Blasco, R., and Moss, B. (1992). Role of cell-associated enveloped vaccinia virus in cell-to-cell spread. *J Virol* **66,** 4170-9.

Block, W., Upton, C., and McFadden, G. (1985). Tumorigenic poxviruses: genomic organization of malignant rabbit virus, a recombinant between Shope fibroma virus and myxoma virus. *Virology* **140,** 113-24.

Bork, P. (1993). Hundreds of ankyrin-like repeats in functionally diverse proteins: mobile modules that cross phyla horizontally? *Proteins* **17,** 363-74.

Borst, E. M., Hahn, G., Koszinowski, U. H., and Messerle, M. (1999). Cloning of the human cytomegalovirus (HCMV) genome as an infectious bacterial artificial chromosome in Escherichia coli: a new approach for construction of HCMV mutants. *J Virol* **73,** 8320-9.

Breeden, L., and Nasmyth, K. (1987). Similarity between cell-cycle genes of budding yeast and fission yeast and the Notch gene of Drosophila. *Nature* **329,** 651-4.

Brune, W., Messerle, M., and Koszinowski, U. H. (2000). Forward with BACs: new tools for herpesvirus genomics. *Trends Genet* **16,** 254-9.

Camus-Bouclainville, C., Fiette, L., Bouchiha, S., Pignolet, B., Counor, D., Filipe, C., Gelfi, J., and Messud-Petit, F. (2004). A virulence factor of myxoma virus colocalizes with NF-kappaB in the nucleus and interferes with inflammation. *J Virol* **78,** 2510-6.

Carroll, M. W., and Moss, B. (1997). Host range and cytopathogenicity of the highly attenuated MVA strain of vaccinia virus: propagation and generation of recombinant viruses in a nonhuman mammalian cell line. *Virology* **238,** 198-211.

Chang, S. J., Hsiao, J. C., Sonnberg, S., Chiang, C. T., Yang, M. H., Tzou, D. L., Mercer, A. A., and Chang, W. (2009). Poxvirus host range protein CP77 contains an F-box-like domain that is necessary to suppress NF-kappaB activation by tumor necrosis factor alpha but is independent of its host range function. *J Virol* **83,** 4140-52.

Chantrey, J., Meyer, H., Baxby, D., Begon, M., Bown, K. J., Hazel, S. M., Jones, T., Montgomery, W. I., and Bennett, M. (1999). Cowpox: reservoir hosts and geographic range. *Epidemiol Infect* **122,** 455-60.

Chen, W., Drillien, R., Spehner, D., and Buller, R. M. (1992). Restricted replication of ectromelia virus in cell culture correlates with mutations in virus-encoded host range gene. *Virology* **187,** 433-42.

Chichon, F. J., Rodriguez, M. J., Pereiro, E., Chiappi, M., Perdiguero, B., Guttmann, P., Werner, S., Rehbein, S., Schneider, G., Esteban, M., and Carrascosa, J. L. (2012). Cryo X-ray nano-tomography of vaccinia virus infected cells. *J Struct Biol* **177,** 202-11.

Chiu, W. L., Lin, C. L., Yang, M. H., Tzou, D. L., and Chang, W. (2007). Vaccinia virus 4c (A26L) protein on intracellular mature virus binds to the extracellular cellular matrix laminin. *J Virol* **81,** 2149-57.

Chlanda, P., Carbajal, M. A., Cyrklaff, M., Griffiths, G., and Krijnse-Locker, J. (2009). Membrane rupture generates single open membrane sheets during vaccinia virus assembly. *Cell Host Microbe* **6,** 81-90.

Chung, C. S., Hsiao, J. C., Chang, Y. S., and Chang, W. (1998). A27L protein mediates vaccinia virus interaction with cell surface heparan sulfate. *J Virol* **72,** 1577-85.

Chung, C. S., Vasilevskaya, I. A., Wang, S. C., Bair, C. H., and Chang, W. (1997). Apoptosis and host restriction of vaccinia virus in RK13 cells. *Virus Res* **52,** 121-32.

Clemens, M. J. (2001). Initiation factor eIF2 alpha phosphorylation in stress responses and apoptosis. *Prog Mol Subcell Biol* **27,** 57-89.

Cottingham, M. G., Andersen, R. F., Spencer, A. J., Saurya, S., Furze, J., Hill, A. V., and Gilbert, S. C. (2008). Recombination-mediated genetic engineering of a bacterial artificial chromosome clone of modified vaccinia virus Ankara (MVA). *PLoS One* **3,** e1638.

Delecluse, H. J., Hilsendegen, T., Pich, D., Zeidler, R., and Hammerschmidt, W. (1998). Propagation and recovery of intact, infectious Epstein-Barr virus from prokaryotic to human cells. *Proc Natl Acad Sci U S A* **95,** 8245-50.

Domi, A., and Moss, B. (2002). Cloning the vaccinia virus genome as a bacterial artificial chromosome in Escherichia coli and recovery of infectious virus in mammalian cells. *Proc Natl Acad Sci U S A* **99,** 12415-20.

Drexler, I., Heller, K., Wahren, B., Erfle, V., and Sutter, G. (1998). Highly attenuated modified vaccinia virus Ankara replicates in baby hamster kidney cells, a potential host for virus propagation, but not in various human transformed and primary cells. *J Gen Virol* **79 (Pt 2),** 347-52.

Drillien, R., Koehren, F., and Kirn, A. (1981). Host range deletion mutant of vaccinia virus defective in human cells. *Virology* **111,** 488-99.

Earl, P. L., Americo, J. L., Wyatt, L. S., Eller, L. A., Whitbeck, J. C., Cohen, G. H., Eisenberg, R. J., Hartmann, C. J., Jackson, D. L., Kulesh, D. A., Martinez, M. J., Miller, D. M., Mucker, E. M., Shamblin, J. D., Zwiers, S. H., Huggins, J. W., Jahrling, P. B., and Moss, B. (2004). Immunogenicity of a highly attenuated MVA smallpox vaccine and protection against monkeypox. *Nature* **428,** 182-5.

Fang, Q., Yang, L., Zhu, W., Liu, L., Wang, H., Yu, W., Xiao, G., Tien, P., Zhang, L., and Chen, Z. (2005). Host range, growth property, and virulence of the smallpox vaccine: vaccinia virus Tian Tan strain. *Virology* **335,** 242-51.

Flint, S. J., Enquist, L. W., Racaniello, V. R., and Skalka, A. M. (2004), Principles of virology, molecular biology, pathogenesis, and control of animal viuses. *ASM press*. **second edition**.

Gale, M., Jr., Tan, S. L., and Katze, M. G. (2000). Translational control of viral gene expression in eukaryotes. *Microbiol Mol Biol Rev* **64,** 239-80.

Gillard, S., Spehner, D., and Drillien, R. (1985). Mapping of a vaccinia host range sequence by insertion into the viral thymidine kinase gene. *J Virol* **53,** 316-8.

Gillard, S., Spehner, D., Drillien, R., and Kirn, A. (1986). Localization and sequence of a vaccinia virus gene required for multiplication in human cells. *Proc Natl Acad Sci U S A* **83,** 5573-7.

Guo, C. J., Chen, W. J., Yuan, L. Q., Yang, L. S., Weng, S. P., Yu, X. Q., and He, J. G. (2011). The viral ankyrin repeat protein (ORF124L) from infectious spleen and kidney necrosis virus attenuates nuclear factor-kappaB activation and interacts with IkappaB kinase beta. *J Gen Virol* **92,** 1561-70.

Hayden, M. S., and Ghosh, S. (2008). Shared principles in NF-kappaB signaling. *Cell* **132,** 344-62.

Hendrickson, R. C., Wang, C., Hatcher, E. L., and Lefkowitz, E. J. (2010). Orthopoxvirus genome evolution: the role of gene loss. *Viruses* **2,** 1933-67.

Hollinshead, M., Rodger, G., Van Eijl, H., Law, M., Hollinshead, R., Vaux, D. J., and Smith, G. L. (2001). Vaccinia virus utilizes microtubules for movement to the cell surface. *J Cell Biol* **154,** 389-402.

Hsiao, J. C., Chung, C. S., and Chang, W. (1999). Vaccinia virus envelope D8L protein binds to cell surface chondroitin sulfate and mediates the adsorption of intracellular mature virions to cells. *J Virol* **73,** 8750-61.

Hsiao, J. C., Chung, C. S., Drillien, R., and Chang, W. (2004). The cowpox virus host range gene, CP77, affects phosphorylation of eIF2 alpha and vaccinia viral translation in apoptotic HeLa cells. *Virology* **329,** 199-212.

Jamsai, D., Orford, M., Nefedov, M., Fucharoen, S., Williamson, R., and Ioannou, P. A. (2003). Targeted modification of a human beta-globin locus BAC clone using GET Recombination and an I-Scei counterselection cassette. *Genomics* **82,** 68-77.

Johnson, R. F., Yellayi, S., Cann, J. A., Johnson, A., Smith, A. L., Paragas, J., Jahrling, P. B., and Blaney, J. E. (2011). Cowpox virus infection of cynomolgus macaques as a model of hemorrhagic smallpox. *Virology* **418,** 102-12.

Jones, E. V., and Moss, B. (1985). Transcriptional mapping of the vaccinia virus DNA polymerase gene. *J Virol* **53,** 312-5.

Jones, E. V., Puckett, C., and Moss, B. (1987). DNA-dependent RNA polymerase subunits encoded within the vaccinia virus genome. *J Virol* **61,** 1765-71.

Kates, J. R., and McAuslan, B. R. (1967). Poxvirus DNA-dependent RNA polymerase. *Proc Natl Acad Sci U S A* **58,** 134-41.

Kawagishi-Kobayashi, M., Silverman, J. B., Ung, T. L., and Dever, T. E. (1997). Regulation of the protein kinase PKR by the vaccinia virus pseudosubstrate inhibitor K3L is dependent on residues conserved between the K3L protein and the PKR substrate eIF2alpha. *Mol Cell Biol* **17,** 4146-58.

Kennedy, R. B., Ovsyannikova, I. G., Jacobson, R. M., and Poland, G. A. (2009). The immunology of smallpox vaccines. *Curr Opin Immunol* **21,** 314-20.

Kerr, J. F., Wyllie, A. H., and Currie, A. R. (1972). Apoptosis: a basic biological phenomenon with wide-ranging implications in tissue kinetics. *Br J Cancer* **26,** 239-57.

Kotwal, G. J., Hugin, A. W., and Moss, B. (1989). Mapping and insertional mutagenesis of a vaccinia virus gene encoding a 13,800-Da secreted protein. *Virology* **171,** 579-87.

Kurth, A., Wibbelt, G., Gerber, H. P., Petschaelis, A., Pauli, G., and Nitsche, A. (2008). Rat-to-elephant-to-human transmission of cowpox virus. *Emerg Infect Dis* **14,** 670-1.

Lee, G., Abdi, K., Jiang, Y., Michaely, P., Bennett, V., and Marszalek, P. E. (2006). Nanospring behaviour of ankyrin repeats. *Nature* **440,** 246-9.

Letai, A., Bassik, M. C., Walensky, L. D., Sorcinelli, M. D., Weiler, S., and Korsmeyer, S. J. (2002). Distinct BH3 domains either sensitize or activate mitochondrial apoptosis, serving as prototype cancer therapeutics. *Cancer Cell* **2,** 183-92.

Luckow, V. A., Lee, S. C., Barry, G. F., and Olins, P. O. (1993). Efficient generation of infectious recombinant baculoviruses by site-specific transposon-mediated insertion of foreign genes into a baculovirus genome propagated in Escherichia coli. *J Virol* **67,** 4566-79.

Lux, S. E., John, K. M., and Bennett, V. (1990). Analysis of cDNA for human erythrocyte ankyrin indicates a repeated structure with homology to tissue-differentiation and cell-cycle control proteins. *Nature* **344,** 36-42.

Lynch, H. E., Ray, C. A., Oie, K. L., Pollara, J. J., Petty, I. T., Sadler, A. J., Williams, B. R., and Pickup, D. J. (2009). Modified vaccinia virus Ankara can activate NF-kappaB

transcription factors through a double-stranded RNA-activated protein kinase (PKR)-dependent pathway during the early phase of virus replication. *Virology* **391,** 177-86.

Mayr, A., and Munz, E. (1964). [Changes in the vaccinia virus through continuing passages in chick embryo fibroblast cultures]. *Zentralbl Bakteriol Orig* **195,** 24-35.

McCurdy, L. H., Larkin, B. D., Martin, J. E., and Graham, B. S. (2004). Modified vaccinia Ankara: potential as an alternative smallpox vaccine. *Clin Infect Dis* **38,** 1749-53.

McFadden, G. (2005). Poxvirus tropism. *Nat Rev Microbiol* **3,** 201-13.

McFadden, G., Mohamed, M. R., Rahman, M. M., and Bartee, E. (2009). Cytokine determinants of viral tropism. *Nat Rev Immunol* **9,** 645-55.

Meisinger-Henschel, C., Spath, M., Lukassen, S., Wolferstatter, M., Kachelriess, H., Baur, K., Dirmeier, U., Wagner, M., Chaplin, P., Suter, M., and Hausmann, J. (2010). Introduction of the six major genomic deletions of modified vaccinia virus Ankara (MVA) into the parental vaccinia virus is not sufficient to reproduce an MVA-like phenotype in cell culture and in mice. *J Virol* **84,** 9907-19.

Messerle, M., Crnkovic, I., Hammerschmidt, W., Ziegler, H., and Koszinowski, U. H. (1997). Cloning and mutagenesis of a herpesvirus genome as an infectious bacterial artificial chromosome. *Proc Natl Acad Sci U S A* **94,** 14759-63.

Meyer, H., Sutter, G., and Mayr, A. (1991). Mapping of deletions in the genome of the highly attenuated vaccinia virus MVA and their influence on virulence. *J Gen Virol* **72 (Pt 5),** 1031-8.

Michaely, P., and Bennett, V. (1992). The ANK repeat: a ubiquitous motif involved in macromolecular recognition. *Trends Cell Biol* **2,** 127-9.

Michaely, P., Kamal, A., Anderson, R. G., and Bennett, V. (1999). A requirement for ankyrin binding to clathrin during coated pit budding. *J Biol Chem* **274,** 35908-13.

Michaely, P., Tomchick, D. R., Machius, M., and Anderson, R. G. (2002). Crystal structure of a 12 ANK repeat stack from human ankyrinR. *EMBO J* **21,** 6387-96.

Minnigan, H., and Moyer, R. W. (1985). Intracellular location of rabbit poxvirus nucleic acid within infected cells as determined by in situ hybridization. *J Virol* **55,** 634-43.

Modrow, S., Falke, D., and Truyen, U. (2003). Molekulare Virologie, *Spektrum Akademischer Verlag*. **second edition**.

Mohamed, M. R., and McFadden, G. (2009). NFkB inhibitors: strategies from poxviruses. *Cell Cycle* **8,** 3125-32.

Mohamed, M. R., Rahman, M. M., Lanchbury, J. S., Shattuck, D., Neff, C., Dufford, M., van Buuren, N., Fagan, K., Barry, M., Smith, S., Damon, I., and McFadden, G. (2009a). Proteomic screening of variola virus reveals a unique NF-kappaB inhibitor that is highly conserved among pathogenic orthopoxviruses. *Proc Natl Acad Sci U S A* **106,** 9045-50.

Mohamed, M. R., Rahman, M. M., Rice, A., Moyer, R. W., Werden, S. J., and McFadden, G. (2009b). Cowpox virus expresses a novel ankyrin repeat NF-kappaB inhibitor that controls inflammatory cell influx into virus-infected tissues and is critical for virus pathogenesis. *J Virol* **83,** 9223-36.

Mohler, P. J., Gramolini, A. O., and Bennett, V. (2002). Ankyrins. *J Cell Sci* **115,** 1565-6.

Mosavi, L. K., Cammett, T. J., Desrosiers, D. C., and Peng, Z. Y. (2004). The ankyrin repeat as molecular architecture for protein recognition. *Protein Sci* **13,** 1435-48.

Moss, B. (2012). Poxvirus Cell Entry: How Many Proteins Does it Take? *Viruses* **4,** 688-707.

Munyon, W., Paoletti, E., and Grace, J. T., Jr. (1967). RNA polymerase activity in purified infectious vaccinia virus. *Proc Natl Acad Sci U S A* **58,** 2280-7.

Nicholson, D. W. (1999). Caspase structure, proteolytic substrates, and function during apoptotic cell death. *Cell Death Differ* **6,** 1028-42.

Parato, K. A., Breitbach, C. J., Le Boeuf, F., Wang, J., Storbeck, C., Ilkow, C., Diallo, J. S., Falls, T., Burns, J., Garcia, V., Kanji, F., Evgin, L., Hu, K., Paradis, F., Knowles, S., Hwang, T. H., Vanderhyden, B. C., Auer, R., Kirn, D. H., and Bell, J. C. (2012). The oncolytic poxvirus JX-594 selectively replicates in and destroys cancer cells driven by genetic pathways commonly activated in cancers. *Mol Ther* **20,** 749-58.

Park, B. H., Hwang, T., Liu, T. C., Sze, D. Y., Kim, J. S., Kwon, H. C., Oh, S. Y., Han, S. Y., Yoon, J. H., Hong, S. H., Moon, A., Speth, K., Park, C., Ahn, Y. J., Daneshmand, M.,

Rhee, B. G., Pinedo, H. M., Bell, J. C., and Kirn, D. H. (2008). Use of a targeted oncolytic poxvirus, JX-594, in patients with refractory primary or metastatic liver cancer: a phase I trial. *Lancet Oncol* **9,** 533-42.

Parrino, J., and Graham, B. S. (2006). Smallpox vaccines: Past, present, and future. *J Allergy Clin Immunol* **118,** 1320-6.

Perkus, M. E., Goebel, S. J., Davis, S. W., Johnson, G. P., Limbach, K., Norton, E. K., and Paoletti, E. (1990). Vaccinia virus host range genes. *Virology* **179,** 276-86.

Pickup, D. J., Bastia, D., Stone, H. O., and Joklik, W. K. (1982). Sequence of terminal regions of cowpox virus DNA: arrangement of repeated and unique sequence elements. *Proc Natl Acad Sci U S A* **79,** 7112-6.

Ramsey-Ewing, A., and Moss, B. (1995). Restriction of vaccinia virus replication in CHO cells occurs at the stage of viral intermediate protein synthesis. *Virology* **206,** 984-93.

Ramsey-Ewing, A. L., and Moss, B. (1996). Complementation of a vaccinia virus host-range K1L gene deletion by the nonhomologous CP77 gene. *Virology* **222,** 75-86.

Ray, C. A., Black, R. A., Kronheim, S. R., Greenstreet, T. A., Sleath, P. R., Salvesen, G. S., and Pickup, D. J. (1992). Viral inhibition of inflammation: cowpox virus encodes an inhibitor of the interleukin-1 beta converting enzyme. *Cell* **69,** 597-604.

Rice, C. M., Grakoui, A., Galler, R., and Chambers, T. J. (1989). Transcription of infectious yellow fever RNA from full-length cDNA templates produced by in vitro ligation. *New Biol* **1,** 285-96.

Riedel, S. (2005). Edward Jenner and the history of smallpox and vaccination. *Proc (Bayl Univ Med Cent)* **18,** 21-5.

Roper, R. L., Wolffe, E. J., Weisberg, A., and Moss, B. (1998). The envelope protein encoded by the A33R gene is required for formation of actin-containing microvilli and efficient cell-to-cell spread of vaccinia virus. *J Virol* **72,** 4192-204.

Rosel, J., and Moss, B. (1985). Transcriptional and translational mapping and nucleotide sequence analysis of a vaccinia virus gene encoding the precursor of the major core polypeptide 4b. *J Virol* **56,** 830-8.

Roth, S. J., Hoper, D., Beer, M., Feineis, S., Tischer, B. K., and Osterrieder, N. (2011). Recovery of infectious virus from full-length cowpox virus (CPXV) DNA cloned as a bacterial artificial chromosome (BAC). *Vet Res* **42,** 3.

Schuenadel, L., Tischer, B. K., and Nitsche, A. (2012). Generation and characterization of a Cowpox virus mutant lacking host range factor CP77. *Virus Res* **168,** 23-32.

Sedgwick, S. G., and Smerdon, S. J. (1999). The ankyrin repeat: a diversity of interactions on a common structural framework. *Trends Biochem Sci* **24,** 311-6.

Shisler, J. L., and Jin, X. L. (2004). The vaccinia virus K1L gene product inhibits host NF-kappaB activation by preventing IkappaBalpha degradation. *J Virol* **78,** 3553-60.

Shizuya, H., Birren, B., Kim, U. J., Mancino, V., Slepak, T., Tachiiri, Y., and Simon, M. (1992). Cloning and stable maintenance of 300-kilobase-pair fragments of human DNA in Escherichia coli using an F-factor-based vector. *Proc Natl Acad Sci U S A* **89,** 8794-7.

Shope, R. E. (1932). A Transmissible Tumor-Like Condition in Rabbits. *J Exp Med* **56,** 793-802.

Smith, G. L., and Law, M. (2004). The exit of vaccinia virus from infected cells. *Virus Res* **106,** 189-97.

Smith, G. L., and McFadden, G. (2002). Smallpox: anything to declare? *Nat Rev Immunol* **2,** 521-7.

Song, W. Y., Pi, L. Y., Wang, G. L., Gardner, J., Holsten, T., and Ronald, P. C. (1997). Evolution of the rice Xa21 disease resistance gene family. *Plant Cell* **9,** 1279-87.

Sonnberg, S., Fleming, S. B., and Mercer, A. A. (2011). Phylogenetic analysis of the large family of poxvirus ankyrin-repeat proteins reveals orthologue groups within and across chordopoxvirus genera. *J Gen Virol* **92,** 2596-607.

Sonnberg, S., Seet, B. T., Pawson, T., Fleming, S. B., and Mercer, A. A. (2008). Poxvirus ankyrin repeat proteins are a unique class of F-box proteins that associate with cellular SCF1 ubiquitin ligase complexes. *Proc Natl Acad Sci U S A* **105,** 10955-60.

Spehner, D., Gillard, S., Drillien, R., and Kirn, A. (1988). A cowpox virus gene required for multiplication in Chinese hamster ovary cells. *J Virol* **62,** 1297-304.

Sperling, K. M., Schwantes, A., Staib, C., Schnierle, B. S., and Sutter, G. (2009). The orthopoxvirus 68-kilodalton ankyrin-like protein is essential for DNA replication and complete gene expression of modified vaccinia virus Ankara in nonpermissive human and murine cells. *J Virol* **83,** 6029-38.

Stickl, H., Hochstein-Mintzel, V., Mayr, A., Huber, H. C., Schafer, H., and Holzner, A. (1974). [MVA vaccination against smallpox: clinical tests with an attenuated live vaccinia virus strain (MVA) (author's transl)]. *Dtsch Med Wochenschr* **99,** 2386-92.

Suter, M., Meisinger-Henschel, C., Tzatzaris, M., Hulsemann, V., Lukassen, S., Wulff, N. H., Hausmann, J., Howley, P., and Chaplin, P. (2009). Modified vaccinia Ankara strains with identical coding sequences actually represent complex mixtures of viruses that determine the biological properties of each strain. *Vaccine* **27,** 7442-50.

Sutter, G., and Moss, B. (1992). Nonreplicating vaccinia vector efficiently expresses recombinant genes. *Proc Natl Acad Sci U S A* **89,** 10847-51.

Sutter, G., Ramsey-Ewing, A., Rosales, R., and Moss, B. (1994). Stable expression of the vaccinia virus K1L gene in rabbit cells complements the host range defect of a vaccinia virus mutant. *J Virol* **68,** 4109-16.

Taylor, J. M., Quilty, D., Banadyga, L., and Barry, M. (2006). The vaccinia virus protein F1L interacts with Bim and inhibits activation of the pro-apoptotic protein Bax. *J Biol Chem* **281,** 39728-39.

Taylor, R. C., Cullen, S. P., and Martin, S. J. (2008). Apoptosis: controlled demolition at the cellular level. *Nat Rev Mol Cell Biol* **9,** 231-41.

Tischer, B. K., Kaufer, B. B., Sommer, M., Wussow, F., Arvin, A. M., and Osterrieder, N. (2007). A self-excisable infectious bacterial artificial chromosome clone of varicella-zoster virus allows analysis of the essential tegument protein encoded by ORF9. *J Virol* **81,** 13200-8.

Tischer, B. K., Smith, G. A., and Osterrieder, N. (2010). En passant mutagenesis: a two step markerless red recombination system. *Methods Mol Biol* **634,** 421-30.

Tulman, E. R., Afonso, C. L., Lu, Z., Zsak, L., Kutish, G. F., and Rock, D. L. (2004). The genome of canarypox virus. *J Virol* **78,** 353-66.

Voronin, D. A., and Kiseleva, E. V. (2007). [Functional role of proteins containing ankyrin repeats]. *Tsitologiia* **49,** 989-99.

Vos, J. C., and Stunnenberg, H. G. (1988). Derepression of a novel class of vaccinia virus genes upon DNA replication. *EMBO J* **7,** 3487-92.

Wasilenko, S. T., Banadyga, L., Bond, D., and Barry, M. (2005). The vaccinia virus F1L protein interacts with the proapoptotic protein Bak and inhibits Bak activation. *J Virol* **79,** 14031-43.

Weaver, J. R., Shamim, M., Alexander, E., Davies, D. H., Felgner, P. L., and Isaacs, S. N. (2007). The identification and characterization of a monoclonal antibody to the vaccinia virus E3 protein. *Virus Res* **130,** 269-74.

Willer, D. O., McFadden, G., and Evans, D. H. (1999). The complete genome sequence of shope (rabbit) fibroma virus. *Virology* **264,** 319-43.

Wittek, R., and Moss, B. (1980). Tandem repeats within the inverted terminal repetition of vaccinia virus DNA. *Cell* **21,** 277-84.

Wyatt, L. S., Carroll, M. W., Czerny, C. P., Merchlinsky, M., Sisler, J. R., and Moss, B. (1998). Marker rescue of the host range restriction defects of modified vaccinia virus Ankara. *Virology* **251,** 334-42.

Xu, Y., Rodriguez-Huete, A., and Pari, G. S. (2006). Evaluation of the lytic origins of replication of Kaposi's sarcoma-associated virus/human herpesvirus 8 in the context of the viral genome. *J Virol* **80,** 9905-9.

Yan, W., Frank, C. L., Korth, M. J., Sopher, B. L., Novoa, I., Ron, D., and Katze, M. G. (2002). Control of PERK eIF2alpha kinase activity by the endoplasmic reticulum stress-induced molecular chaperone P58IPK. *Proc Natl Acad Sci U S A* **99,** 15920-5.

7. Appendix

7.1 List of abbreviations

µ	mikro
µF	microfarad
aa	amino acid
AIDS	acquired immunodeficiency syndrome
AMP	adenosine monophosphate
APS	ammonium persulfate
ARP	ankyrin repeat protein
B.C.	before Christ
BAC	bacterial artificial chromosome
BHK	baby hamster kidney
bp	base pair
BR	Brighton Red
BSA	bovine serum albumin
CAM	chorion allantois membrane
cDNA	complementary DNA
CE	cytoplasmic extract
CEF	chicken embryo fibroblast
CEV	cell-associated enveloped virus
CHO	chinese hamster ovary
CPXV	cowpox virus
CTL	cytotoxic T lymphocytes
CVA	vaccinia virus Ankara
DMSO	dimethyl sulfoxide
DNA	deoxyribonucleic acid
dNTP	deoxyribonucleotide
dsDNA	double stranded DNA
DTT	dithiothreitol
E.coli	Escherichia coli
EBV	epstein barr virus
EDTA	ethylenediaminetetraacetic acid
EEV	external enveloped virus
EGTA	ethylene glycol tetraacetic acid
eIF2α	eukaryotic initiation factor 2 alpha
EV	enveloped virus
FCS	fetal calf serum
FIBV	Hare fibroma virus
g	gramm
GFP	green fluorescent protein
h	hour
HCMV	human cytomegalovirus
HEPES	N-(2-hydroxyethyl)-piperazine-N'-2-ethanesulfonic acid
HGP	Human Genome Program

HHV-8	human herpesvirus-8
IEV	internal enveloped virus
IKK	IκB kinase complex
IMV	internal mature virus
ISKNV	infectious spleen and kidney necrosis virus
ITR	inverted terminal repeat
IV	immature virus
IκBα	inhibitor of NF-κB
l	litre
LB	lysogeny broth
m	milli
M	molar
mA	milliampere
MCMV	mouse cytomegalovirus
min	minute
MNF	myxoma nuclear factor
MOI	multiplicity of infection
mRNA	messenger RNA
MRV	malignat rabbit fibroma virus
MV	mature virus
MVA	modified vaccina virus Ankara
MYXV	Myxoma virus
NF-κB	nuclear factor-κB
NK	natural killer
nm	nanometer
OD	optical density
OPV	orthopoxvirus
ORF	open reading frame
PAGE	polyacrylamide gel electrophoresis
PARP	poly (ADP-ribose) polymerase
PBS	posphate buffered saline
PBS-T	PBS Tween
PCR	polymerase chain reaction
p-eIF2α	phosphorylated eIF2α
PFU	plaque forming unit
polyIC	polyinosinic:polycytidylic acid
Ppi	pyrophosphate
PRANC	pox protein repeat of ankyrin C-terminus
PVDF	polyvinylidenfluoride
rATP	ribonucleotide adenine ribose triphosphate nucleotide
RFLP	restriction fragment length polymorphism
RFV	Rabbit fibroma virus
RNA	riboncleic acid
rpm	rounds per minute
SCF	skp-, cullin-, F-box
SDS	sodium dodecyl sulfate
sec	second

SFV	Shope fibroma virus
SOCS	suppressor of cytokine signaling
SQFV	Squirrel fibroma virus
TAE	Tris base, acetic acid EDTA
TBS	Tris-buffered saline
TE	Tris base, EDTA
TMV	tobacco mosaic virus
TNF-α	tumour necrosis factor alpha
UV	ultraviolet
V	volt
v/v	volume/volume
VACV	vaccinia virus
VAV	variola virus
vs.	versus
w/v	mass/volume
WHO	world health organisation
WV	wrapped virus
YAC	yeast artificial chromosome
zf-DHHC	Zn-finger domain
zn	zinc
Ω	ohm

8. Danksagung

Ich danke Herrn Prof. Dr. Nikolaus Osterrieder für die Möglichkeit diese Arbeit in seinem Institut anfertigen zu dürfen.

Herrn Prof. Dr. Markus Wahl danke ich für die Übernahme des Referats herzlich.

Ich danke Herrn Dr. B. Karsten Tischer, der mir ein stets hilfsbereiter Betreuer war.

Ich danke meinen Kollegen in der Arbeitsgruppe Tischer, die unermüdlich für eine entpannte und gute Atmosphäre im Labor gesorgt haben. Desweiteren danke ich den Kollegen im gesamten Institut von Prof. Osterrieder für ihre Hilfsbereitschaft.

Meiner Familie und meinen Freunden, besonders Cathleen Thomas, Jan-Henrik Baumgarten und Stephan Schröder danke ich für Unterstützung, Vertrauen und Zuspruch.

8. Danksagung

9. Erklärung

Hiermit erkläre ich, Imme Sakwa, die vorliegende Arbeit selbstständig unter Anleitung meiner akademischen Lehrer angefertigt und verfasst zu haben. Es wurden keine anderen als die angegebenen Hilfsmittel und Quellen verwendet. Diese Arbeit wurde an keiner anderen Fakultät zur Begutachtung vorgelegt.

Ich erkläre hiermit zusätzlich, dass keine Aberkennung eines bereits erworbenen Doktorgrades vorliegt.

Berlin, 2013

Imme Sakwa

10. Curriculum Vitae

Curriculum Vitae

For reasons of data protection,
the curriculum vitae is not included in the online version